Characteristics of Equipment Components, Equipment Cooling System Design, and Temperature Control System Design

AIR1168/6

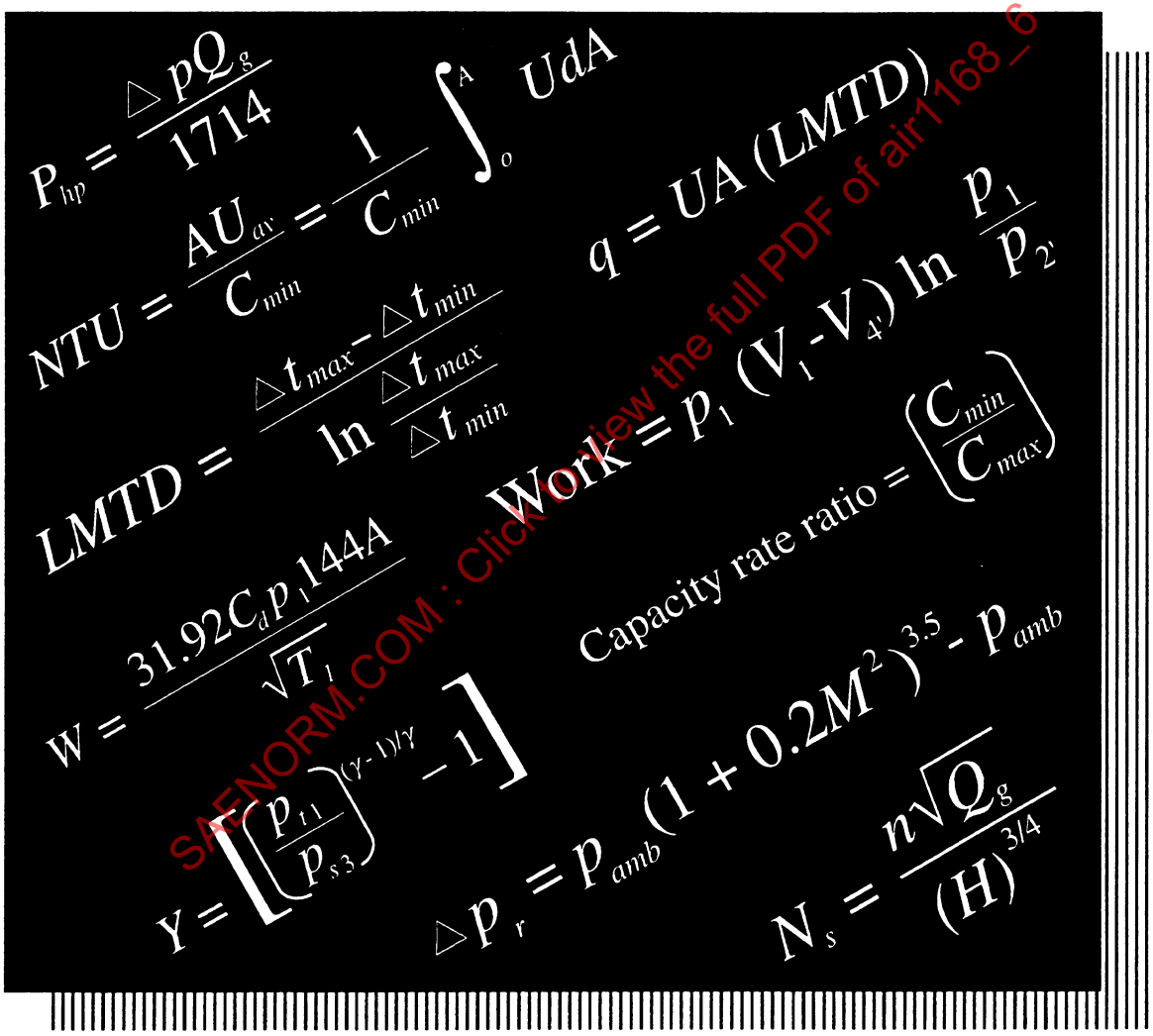

SAE Aerospace Applied Thermodynamics Manual

SAE INTERNATIONAL
The Engineering Society For Advancing Mobility Land Sea Air and Space®

SAE Aerospace
An SAE International Group

AEROSPACE INFORMATION REPORT

SAE AIR1168/6

Issued 1994-04
Reaffirmed 2004-06

Characteristics of Equipment Components,
Equipment Cooling System Design, and
Temperature Control System Design

PREFACE

This document is one of 14 Aerospace Information Reports (AIR) of the Third Edition of the SAE Aerospace Applied Thermodynamics Manual. The manual provides a reference source for thermodynamics, aerodynamics, fluid dynamics, heat transfer, and properties of materials for the aerospace industry. Procedures and equations commonly used for aerospace applications of these technologies are included.

In the Third Edition, no attempt was made to update material from the Second Edition nor were SI units added. However, all identified errata were corrected and incorporated and original figure numbering was retained, insofar as possible.

The SAE AC-9B Subcommittee originally created the SAE Aerospace Applied Thermodynamics Manual and, for the Third Edition, used a new format consisting of AIR1168/1 through AIR1168/10. AIR1168/11 through AIR1168/14 were created by the SAE SC-9 Committee.

The AIRs comprising the Third Edition are shown below. Applicable sections of the Second Edition are shown parenthetically in the third column.

AIR1168/1	Thermodynamics of Incompressible and Compressible Fluid Flow	(1A,1B)
AIR1168/2	Heat and Mass Transfer and Air-Water Mixtures	(1C,1D,1E)
AIR1168/3	Aerothermodynamic Systems Engineering and Design	(3A,3B,3C,3D)
AIR1168/4	Ice, Rain, Fog, and Frost Protection	(3F)

TO PLACE A DOCUMENT ORDER:
Tel: 877-606-7323 (inside USA and Canada)
Tel: 724-776-4970 (outside USA)
Fax: 724-776-0790
Email: custsvc@sae.org
SAE WEB ADDRESS: **http://www.sae.org**

AIR1168/5	Aerothermodynamic Test Instrumentation and Measurement	(3G)
AIR1168/6	Characteristics of Equipment Components, Equipment Cooling System Design, and Temperature Control System Design	(3H,3J,3K)
AIR1168/7	Aerospace Pressurization System Design	(3E)
AIR1168/8	Aircraft Fuel Weight Penalty Due to Air Conditioning	(3I)
AIR1168/9	Thermophysical Properties of the Natural Environment, Gases, Liquids, and Solids	(2A,2B,2C,2D)
AIR1168/10	Thermophysical Characteristics of Working Fluids and Heat Transfer Fluids	(2E,2F)
AIR1168/11	Spacecraft Boost and Entry Heat Transfer	(4A,4B)
AIR1168/12	Spacecraft Thermal Balance	(4C)
AIR1168/13	Spacecraft Equipment Environmental Control	(4D)
AIR1168/14	Spacecraft Life Support Systems	(4E)

F.R. Weiner, formerly of Rockwell International and past chairman of the SAE AC-9B Subcommittee, is commended for his dedication and effort in preparing the errata lists that were used in creating the Third Edition.

Table of Contents

List of Figures

List of Tables

COMMON ABBREVIATIONS

A	— Amperes
abs.(ABS.)	— Absolute
AC	— Alternating Current
ad	— Adiabatic
Aeronaut.	— Aeronautical
AIR	— Aeronautical Information Report (SAE)
amb	— Ambient
ARP	— Aerospace Recommended Practice (SAE)
ASG	— Aerospace Ground Support
ASME	— American Society of Mechanical Engineers
ASTIA	— Armed Services Technical Information Agency (Now Defense Documentation Center)
av	— Average
BTU	— British Thermal Units
BWD	— Backward
Calif.	— California
cfm	— Cubic feet per minute
Co.	— Company
const.	— Constant
Cont.	— Continuous
Corp.	— Corporation
cos	— Cosine
cps	— Cycles per second
db	— Decibels
DC	— Direct Current
deg(DEG)	— Degrees
dia(DIA)	— Diameter
dis	— Discharge
ed.	— Edition
emf	— Electromotive force
ELEC.	— Electrical
Eng.	— Engineering
Eq(Eqs.)	— Equation(s)
EXCHG.	— Exchanger
f ( )	— Function of quantity in parenthesis
^{o}F	— Degrees Fahrenheit
Fig.(Figs)	— Figure(s)
ft	— Feet

ft/min(fpm)	— Feet per minute
ft/sec(fps)	— Feet per second
FWD	— Forward
gal	— Gallon
GALCIT	— Guggenheim Aeronautical Laboratory, California Institute of Technology
gpm	— Gallons per minute
HG	— Mercury
hp	— Horsepower
hr	— Hour
H_2O	— Water
ID	— Inside Diameter
in	— Input
in.(IN.)	— Inch
Inc.	— Incorporated
iso	— Isothermal
J.	— Journal
Jan.	— January
kW	— Kilowatts
lb	— Pounds
LMTD	— Logarithmic Mean Temperature Difference
ln	— Natural logarithm to the base e
log	— Logarithm to the base 10
L/D	— Lift - drag ratio
m	— Meters
ma	— Milliamperes
Mach	— Mach Number
max(MAX)	— Maximum
Memo	— Memorandum
min	— Minute(s)
min(MIN)	— Minimum
mV	— Millivolt
NACA	— National Advisory Committee for Aeronautics
NASA	— National Aeronautics and Space Administration
NAVWEPS	— Naval Weapons Systems
no.(NO.)	— Number
nos.	— Numbers
NTU	— Number of Transfer Units
OD	— Outside Diameter
ov	— Overall
p.	— Page
Par.	— Paragraph

psf — Pounds per square foot
psi — Pounds per square inch
psia — Pounds per square inch absolute
psig — Pounds per square inch gage
R — Resistance
^{o}R — Degrees Rankine
rad — Radian(s)
ref — Reference (referring to a base or known value)
Ref.(Refs.) — Reference(s)(referring to a publication)
rev(REV) — Revolution
rpm(RPM) — Revolutions per minute
SAE — Society of Automotive Engineers, Inc.
sec — Second
Servo — Servomechanism
SFC — Specific fuel consumption
SI — Système Internationale(French)
The International System of modern Metric Units
sin — Sine
S.L. — Sea Level
st — Static
SUS — Saybolt Universal Seconds
tank — Hyperbolic tangent
Tech. — Technical
Temp(TEMP.) — Temperature
TN — Technical Note
T/O — Takeoff
tot — Total
TR — Technical Report
Trans. — Transactions
TURB — Turbine
Δt — Temperature difference, ^{o}F
V — Volts
Vol. — Volume
W — Watts
WADC — Wright Air Development Center
% — Percent
μ — Microns ($1\mu = 10^{-6}$ m)

SECTION 3H - CHARACTERISTICS OF EQUIPMENT COMPONENTS

1. INTRODUCTION

1.1 Scope

This section relates the engineering fundamentals and thermophysical property material of the previous sections to the airborne equipment for which thermodynamic considerations apply. For each generic classification of equipment, information is presented for the types of equipment included in these categories, and the thermodynamic design considerations with respect to performance, sizing, and selection of this equipment.

1.2 Nomenclature

In this section, a nomenclature list is provided for each classification of equipment. Each list contains symbols which are used in each paragraph. There are additional commonly accepted standard symbols which are used in each paragraph of this section and are defined as follows:

A = Area, in.^{2}, ft^2
c_p = Specific heat capacity, constant pressure, Btu/lb-^{o}F
c_v = Specific heat capacity, constant volume, Btu/lb-^{o}F
D = Diameter, in., ft
g = Gravitational acceleration, ft/sec^2
J = Mechanical equivalent of heat, 778 ft-lb/Btu
n = Angular velocity, rpm, rad/sec
N_{Re} = Reynolds No., dimensionless
N_s = Specific speed, dimensionless
t = Temperature, ^{o}F
T = Temperature, ^{o}R
γ = Ratio of specific heats, c_p/c_v, dimensionless
ρg = Specific weight (density), lb/ft^3
η = Efficiency or effectiveness, dimensionless

2. PUMPS

2.1 Nomenclature

c = Absolute velocity, ft/sec
c_m = Meridional velocity, ft/sec
D = Characterization dimension, impeller diameter, ft
H = Pressure head, ft
H_{sv} = Pressure head above vapor pressure at pump inlet, ft

Δp = Pressure loss, lb/in.^{2}
P_{hp} = Horsepower
Q = Volume flow rate, ft^3/min.
Q_g = Volume flow rate, gal/min
N_s = Suction specific speed, dimensionless
u = Impeller velocity, ft/sec
V_{dis} = Theoretical displacement per revolution, ft^3/rev
w = Fluid relative velocity, ft/sec
β = Vane angle, deg
η_v = Volumetric efficiency, dimensionless
λ = Experimental cavitation coefficient, dimensionless
ϕ = Flow coefficient, dimensionless
ψ = Head coefficient, dimensionless

Subscripts

1 = Inlet
2 = Outlet
id = Ideal
in = Input
ov = Overall

2.2 General Considerations

Pumps are considered here to be used with thin fluids that have no appreciable volume change with reasonable changes in temperature and pressure, and as such are considered to act as incompressible fluids.

2.3 Types of Pumps

2.3.1 Dynamic Machines

Dynamic machines depend on the change of the angular momentum of the fluid. The various types include:

1. Centrifugal - The volute type is shown in Fig. 3H-1 and the diffuser type in Fig. 3H-2.
2. Mixed.
3. Axial.

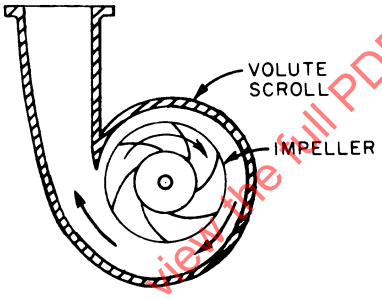

Figure 3H-1 - Volute Pump

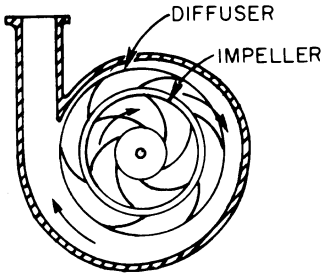

Figure 3H-2 - Diffuser Pump

2.3.2 Positive Displacement Machines

The relative motion between the fluid and the rotor or piston is not essential in this type of pump. Typical types with reciprocating motion are the piston, the plunger, and the diaphragm.

Typical types with rotary motion are the screw (Fig. 3H-3), the gear (Fig. 3H-4), the vane (Fig. 3H-5) and the lobe (Fig. 3H-6).

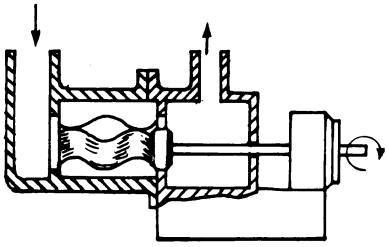

Figure 3H-3 - Single Screw Pump

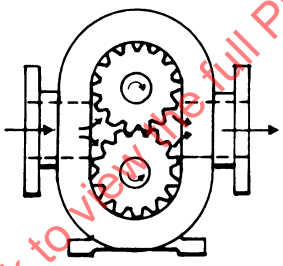

Figure 3H-4 - External Gear Pump

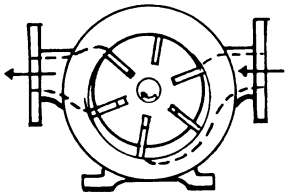

Figure 3H-5 - Sliding Vane Pump

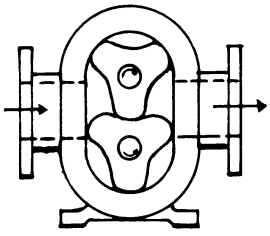

Figure 3H-6 - Three Lobe Pump

2.4 Fundamental Considerations

Characteristics of the types just described are discussed below.

2.4.1 Dynamic Machines

2.4.1.1 Flow Rate

In a dynamic pump, the pressure developed can be expressed by the time rate of change of angular momentum of the mass of fluid passing through the impeller passages. A form of Euler's equation conveniently expresses the various processes in the ideal head developed by a dynamic pump, as depicted by the velocity triangles of Fig. 3H-7.

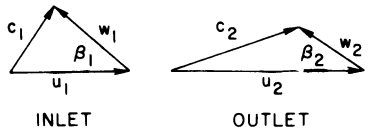

Figure 3H-7 - Impeller Velocity Triangles

$$H_{id} = \frac{u_2^2 - u_1^2}{2g} + \frac{c_2^2 - c_1^2}{2g} + \frac{w_2^2 - w_1^2}{2g} \qquad (3H\text{-}1)$$

The first term expresses the head rise due to centrifugal force; the second, head rise due to kinetic energy; the third term, head rise due to relative velocity change in the impeller.

The flow of a dynamic pump is determined by the impeller geometry and speed. Examples of varying impeller geometry are shown in Fig. 3H-8.

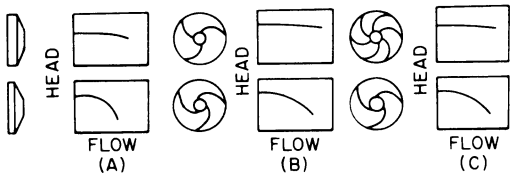

Figure 3H-8 - Effect of Changes in Impeller Geometry: (a) impeller width; (b) blade angle; (c) number of blades

2.4.1.2 Overall Efficiency

In a dynamic pump, the major loss is associated with fluid friction. The fluid velocities in a pump are relatively high, and extreme care is required in the design of the pump inlet, impeller, diffuser, and scroll to realize good efficiencies. Mechanical friction and fluid leakage losses in a dynamic pump are small.

2.4.1.3 Similarity Considerations

The laws of similarity for pumps are based on the assumption that: inertia forces are the only forces acting on the fluid, geometric similarity relationships are preserved, the fluid is incompressible, and the degree of change of physical properties is negligible. The computations involve the following equations:

$$\text{Capacity} = \frac{Q_{g1}}{Q_{g2}} = \left(\frac{D_1}{D_2}\right)^3 \frac{n_1}{n_2} \tag{3H-2}$$

$$\text{Head} = \frac{H_1}{H_2} = \left(\frac{D_1 n_1}{D_2 n_2}\right)^2 \tag{3H-3}$$

$$\text{Power} = \frac{P_{hp,1}}{P_{hp,2}} = \frac{H_1 Q_{g1}}{H_2 Q_{g2}} = \left(\frac{D_1}{D_2}\right)^5 \left(\frac{n_1}{n_2}\right)^3 \tag{3H-4}$$

$$\text{Specific speed} = N_s = \frac{n\sqrt{Q_g}}{(H)^{3/4}} \tag{3H-5}$$

In the consideration of pump performance, sizing, and the correlation of significant pump design constants, the specific speed criterion is to pump design as the Reynolds number criterion is to pipe flow. As a basic pump comparison, the specific speed at peak efficiency is utilized.

These relationships are useful when establishing the size of a pump from a previous design, but extreme care must be exercised when they are used with small pumps or with a very viscous working fluid.

2.4.1.4 Cavitation

Cavitation is the local vaporization of a fluid when the static pressure falls below the vapor pressure because of high local velocities (dynamic pressure). The inlet conditions to a pump are usually associated with low absolute total pressures and are subject to cavitational erosion as well as to a performance reduction if the system is improperly designed. Because of the dynamic flow condition at the impeller inlet, each pump design will have different suction requirements, which must be considered in light of the vapor pressure characteristics of the fluid being pumped.

Cavitation will therefore exist when

$$H_{vapor} = H_{total\ suction} = \frac{c_1^2}{2g} + \lambda \frac{w_1^2}{2g} \quad \text{(3H-6)}$$

As a guide when first considering a pump installation, it is possible to evaluate suction specific speed N_s:

$$N_s = \frac{n\sqrt{Q_g}}{(H_{sv})^{3/4}} \quad \text{(3H-7)}$$

By careful pump design, an upper limit of suction specific speed of 15,000 is possible, but for most centrifugal designs a value of 7000-10,000 is common.

2.4.2 Positive Displacement Machine

2.4.2.1 Flow Rate

A positive displacement machine induces fluid motion by taking a finite portion of the fluid and forcing it into the system against the system pressure. Consequently (neglecting leakage) the flow rate of a positive displacement machine is the displacement volume times the revolutions or strokes per unit time.

2.4.2.2 Volumetric Efficiency

The volumetric efficiency of a positive displacement pump is expressed as the ratio of the actual flow to the theoretical displacement volume per unit time. The volumetric efficiency is a function of leakage, delay in closing of valves, and the compressibility of the fluid, which can be of consequence when dealing with liquids over a wide range in pressure.

The leakage rate for any pump is a function of discharge pressure and speed, which is shown in Fig. 3H-9 as the difference between actual and theoretical flows.

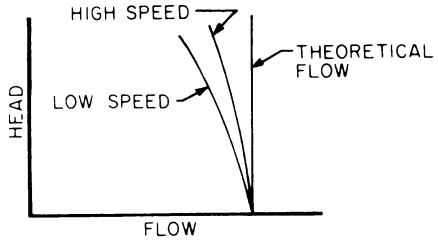

Figure 3H-9 - Effect of Speed on Pump Flow

2.4.2.3 Hydraulic Efficiency

Friction flow losses through a positive displacement machine are very small and usually are included in the mechanical efficiency.

2.4.2.4 Overall Efficiency

The overall efficiency of a pump includes the mechanical losses from friction, the fluid losses from friction, and the loss associated with work done on any fluid that leaks back to the inlet. The overall efficiency is given by

$$\eta_{ov} = \frac{Hydraulic\ power\ out}{Shaft\ power\ in} \tag{3H-8}$$

2.4.2.5 Flow Rate

The flow rate is defined as

$$Q = V_{dis}\, n\, \eta_v \tag{3H-9}$$

2.4.2.6 Hydraulic Power and Input Power

The hydraulic power can be defined as

$$P_{hp} = \frac{\Delta p Q_g}{1714} \tag{3H-10}$$

and input power as

$$P_{hp,in} = \frac{\Delta p Q_g}{1714 \eta_{ov}} \tag{3H-11}$$

2.5 Performance of Pumps

2.5.1 Dynamic Machines

2.5.1.1 Specific Speed and Efficiency

The specific speed parameter is a convenient presentation of the various pump configurations when plotted against "best efficiency." The specific speed parameter is derived without consideration for Reynolds number or changes in fluid property. Fig. 3H-10 presents a typical specific speed plot where the Reynolds numbers are in the order of 1×10^5 to 1×10^6 (where the characteristic dimension is the impeller tip diameter and the characteristic velocity is the impeller tip velocity).

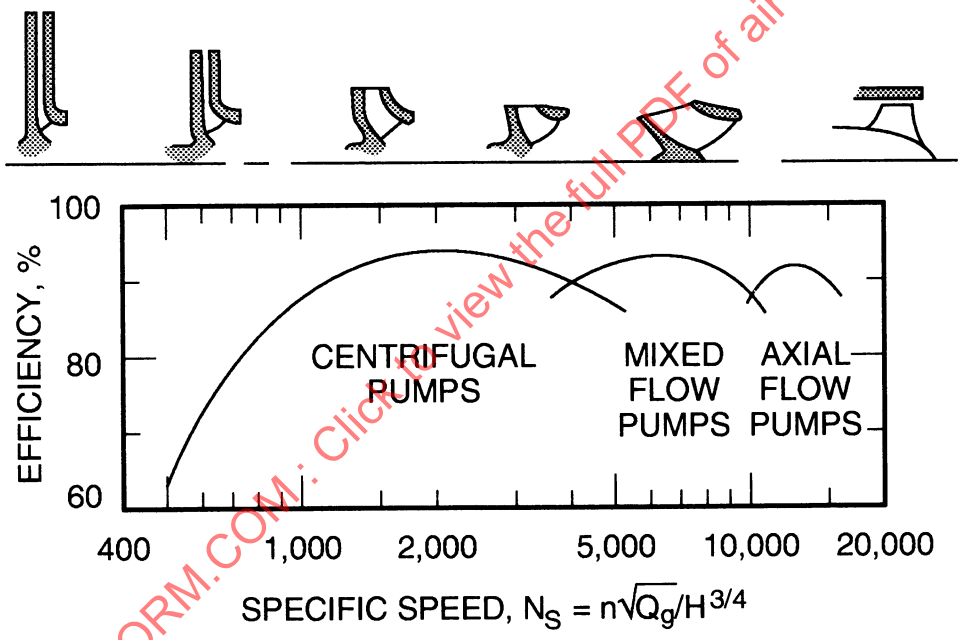

Figure 3H-10 - Pump Specific Speed

2.5.1.2 Reynolds Number and Efficiency

As the Reynolds number decreases proportionally with the increased viscosity of a fluid or in a machine of small diameter, there will be, in general, a reduction in pump efficiency. Fig. 3H-11 presents a plot of Reynolds number as a function of efficiency correction η/η_o, where η_o is efficiency at a Reynolds number of 1×10^6.

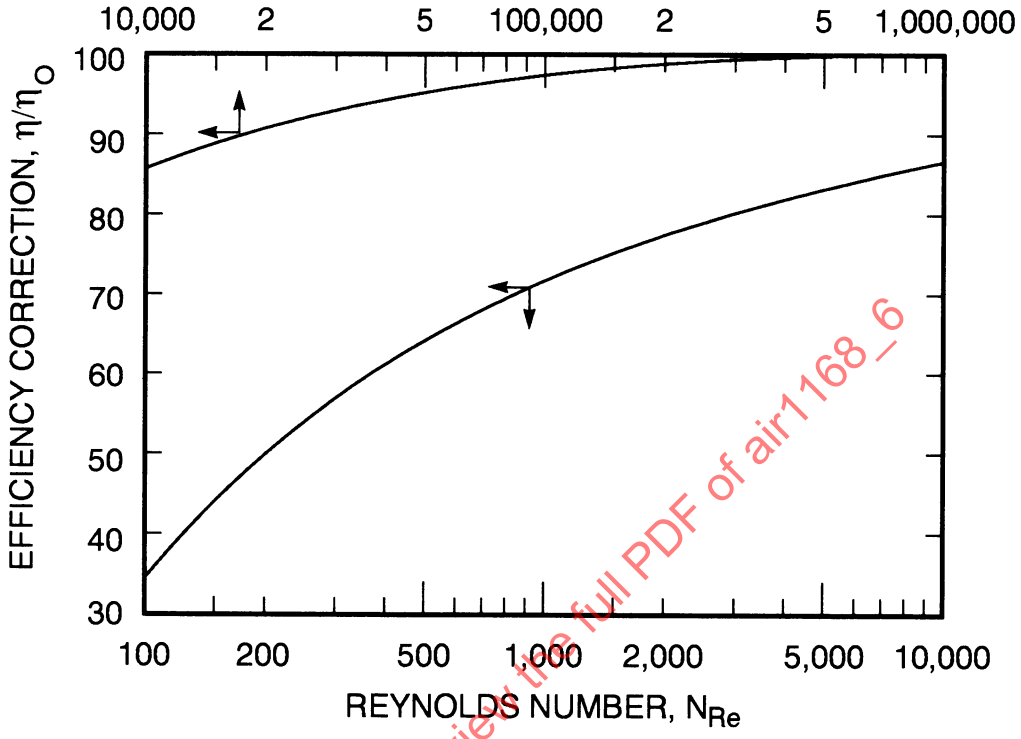

Figure 3H-11 - Effects of Reynolds Number on Pump Efficiency

2.5.1.3 Impeller Characteristics as a Function of Specific Speed

It is possible to relate the dimensionless flow coefficient ϕ and the head coefficient ψ to specific speed. These two parameters, as well as the inlet to outlet diameter ratio, D_1/D_2, are presented in Fig. 3H-12 for a vane discharge angle β_2 of 22.5 deg. The flow coefficient is defined as

$$\phi = \frac{c_{m2}}{u_2} \tag{3H-12}$$

and the head coefficient as

$$\psi = \frac{H}{(u_2^2/2g)} \tag{3H-13}$$

In general, the design values of β_2 will fall between 17.5 and 27.5 deg. For preliminary one-dimensional considerations, the values given in Fig. 3H-12 will give reasonable pump size and performance. Refinements required for a final pump design should be based on a more comprehensive analysis of the fluid flow, such as that presented in Refs. 1 and 2.

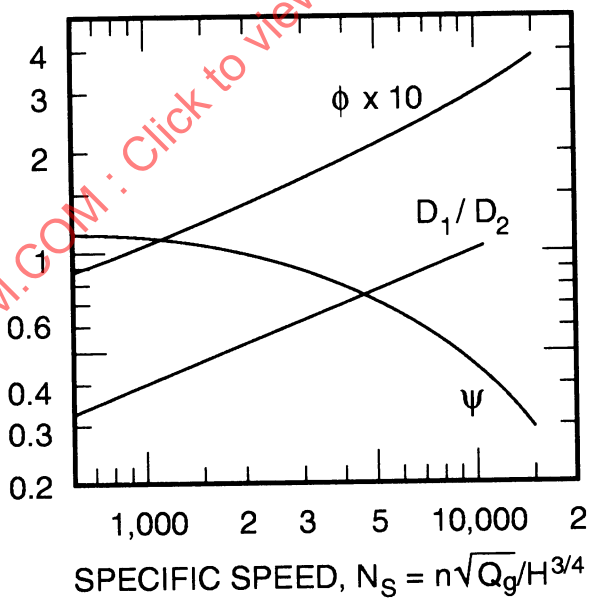

Figure 3H-12 - Typical Values of Flow and Pressure Coefficients for Dynamic Pumps, Where $\beta_2 = 22.5$ deg

2.5.2 Positive Displacement Machines

2.5.2.1 Pump Efficiencies

Fig. 3H-13 presents a range of typical volumetric and overall efficiencies for piston, gear, and vane pumps. This figure indicates the efficiencies that can be expected from available equipment.

In general, the upper values of both volumetric and overall efficiency are more easily obtained with a piston pump. Gear pumps can have high volumetric efficiencies, but will have overall efficiencies near the lower line. Vane pumps are more limited in discharge pressure and are mainly considered for pressures below 1000 psia, since leakage can become significant.

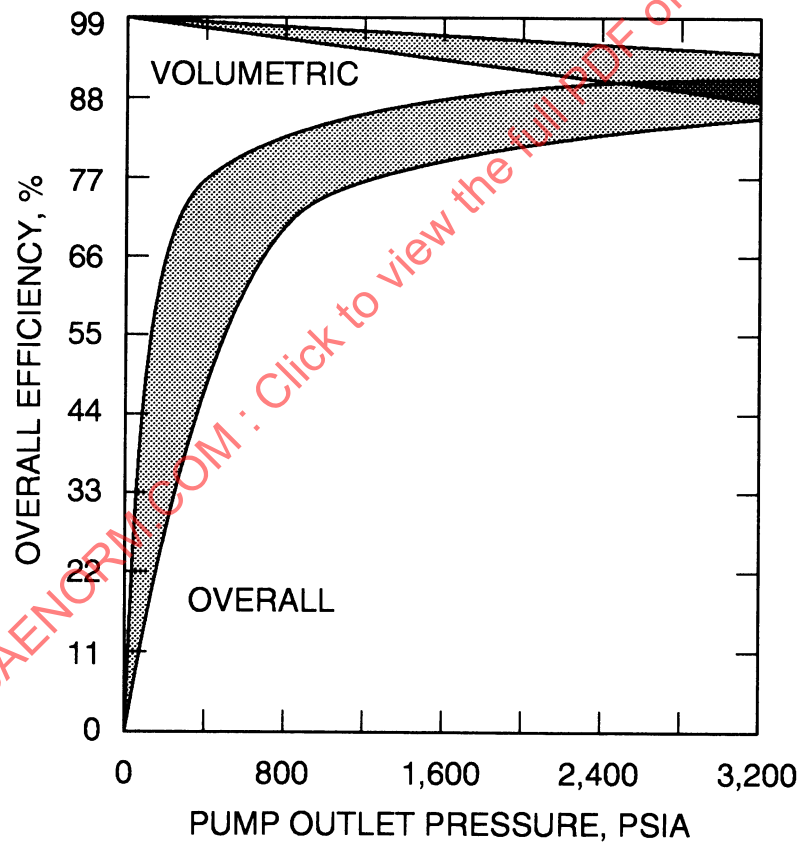

Figure 3H-13 - Positive Displacement Pump Efficiencies for Piston, Gear, and Vane Pumps

2.5.2.2 Displacement Volume and Speed

The displacement volume is an indication of pump size. The smaller displacement volume pump can operate at higher speeds. Typical values of pump speed and displacement volume per revolution are shown in Fig. 3H-14 for piston, gear, and vane pumps.

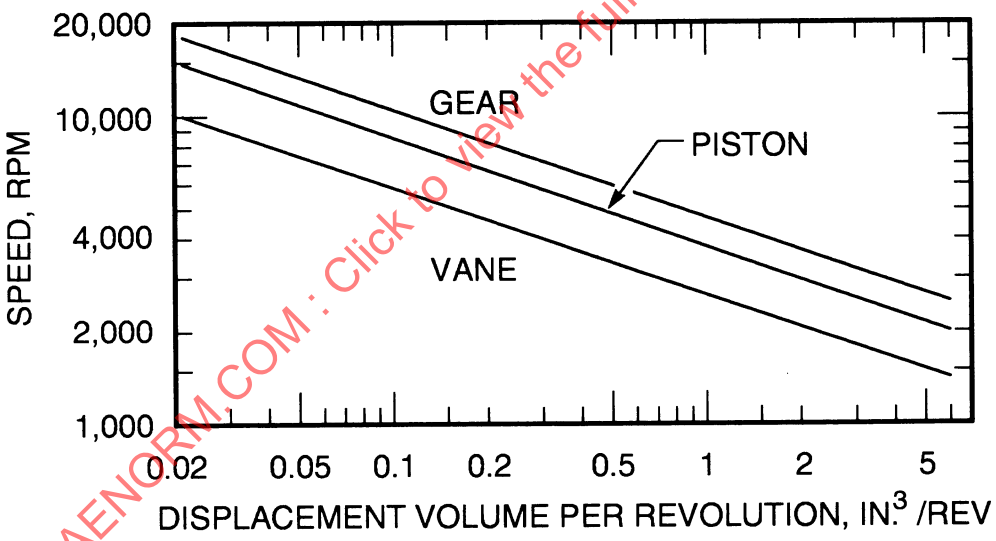

Figure 3H-14 - Typical Continuous Speeds for Piston, Gear, and Vane Pumps

2.5.2.3 Displacement Volume and Pump Weight

A range of pump weights as a function of displacement volume is presented in Fig. 3H-15. The pump weights are exclusive of the power source and are representative of available equipment. For a specific application, it is possible to have higher or lower values than those shown in the figure.

The upper line of values will be more typical of a piston pump while the lower line is more typical of a light-weight vane pump. At the lower displacement volumes, the gear pump will compare with the vane pump, but at displacements in the order of 0.2 in.^{3}/rev, it can be as heavy as a lightweight piston pump.

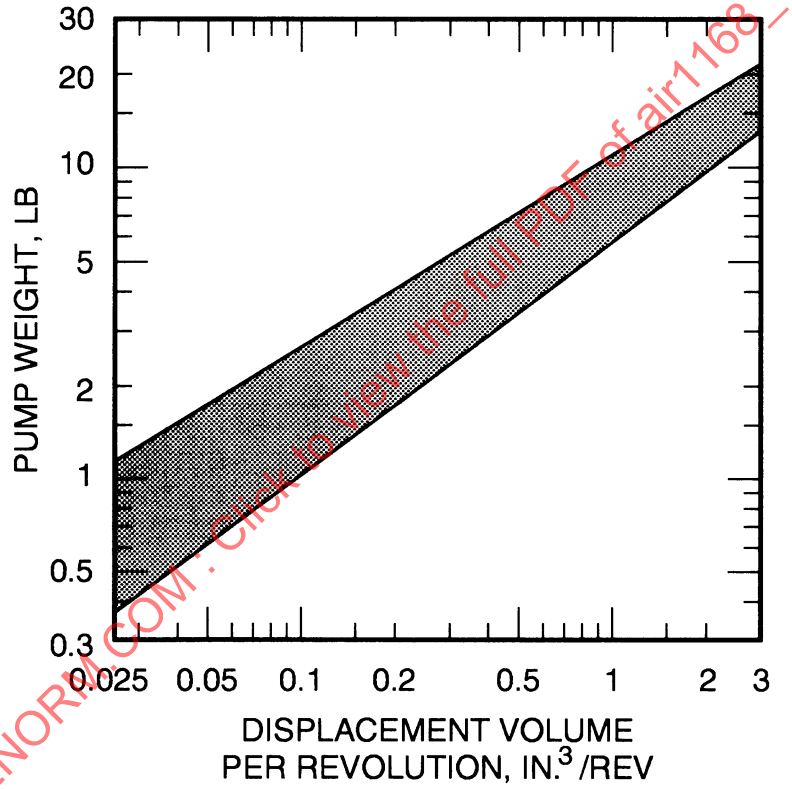

Figure 3H-15 - Approximate Weights for Piston, Gear, and Vane Pumps (Less Motor)

2.6 Sizing Techniques

The performance information presented in paragraph 2.5 is intended to serve as a guide in developing approximate equipment sizes when conducting a preliminary design of a system incorporating a pump. This information should be considered for first approximations only, since a final design will require considerations and refinements far beyond the scope of this presentation.

2.6.1 Sizing of a Dynamic Machine

Listed below is a procedure that can be used in arriving at an approximate size and performance of a dynamic pump when the flow and head are given. The procedure involves seven steps, as follows.

(1) Select a pump speed consistent with the available drive speed (the reader is cautioned against selecting excessive wheel speeds because of cavitation; see paragraph 2.4.1.4) and determine a specific speed. From Fig. 3H-12, ϕ, ψ, and D_1/D_2 can be selected.

(2) Impeller tip speed:

$$u_2 = \sqrt{\frac{2gH}{\psi}} \tag{3H-14}$$

(3) Impeller tip diameter:

$$D_2 = \frac{60u_2}{\pi n} \tag{3H-15}$$

(4) Inlet eye diameter:

$$D_1 = \left(\frac{D_1}{D_2}\right) D_2 \tag{3H-16}$$

(5) Outlet area (disregarding vane thickness):

$$A_2 = \frac{Q}{60\phi u_2} \tag{3H-17}$$

(6) The casing dimensions can be approximated by assuming that the casing shape is a logarithmic spiral.

(7) From Fig. 3H-10 the ''best possible'' pump efficiency for the specific speed under consideration is selected. A Reynolds number correction can be applied from Fig. 3H-11.

2.6.2 Sizing a Positive Displacement Machine

The following procedure is suggested for sizing a positive displacement pump when the flow and head are known:

(1) From Fig. 3H-14 a speed and displacement can be uniquely selected to satisfy the flow.

(2) Fig. 3H-13 can be used for both volumetric and overall efficiency.

(3) Approximate weight can be determined from Fig. 3H-15.

2.7 Selection of Pump Type

The selection of a pump type depends upon whether its advantages outweigh its disadvantages in the particular application.

2.7.1 Dynamic Machines

The advantages of these machines are large capacity, low cost, small size, and long life. Their disadvantages are that they have low head per stage and turbulence.

2.7.2 Positive Displacement Machines

Each of the three types are discussed below.

2.7.2.1 Reciprocating Piston

The advantages of this type are that it can develop high pressure and high efficiency, and it can handle high viscosity fluids.Its disadvantages are its large size, heavy weight, pulsating flow, and high cost.

2.7.2.2 Reciprocating Diaphragm

The particular advantage of this type is that it has no seals. However, limited pressures and pulsating flows are disadvantages.

2.7.2.3 Rotary

The advantages are low cost, small size, self priming, and a capability for handling high viscosity fluids. Disadvantages are its close clearances and lower efficiencies.

2.8 References

Elaboration of the material on pumps presented above can be found in Refs. 1-7, Par. 9.

3. FANS

3.1 Nomenclature

c = Absolute velocity, ft/sec
c_m = Meridional velocity, ft/sec
c_u = Tangential component of absolute velocity, ft/sec
D = Fan diameter, ft
db = Decibels
H_e = Euler's head, ft
H_{tot} = Total head, ft
K = Resistance constant, dimensionless
l = Chord length, ft
ΔP = Pressure rise, in. H_2O
P_{hp} = Horsepower
q = Dynamic pressure, in. H_2O
Q = Volume flow rate, ft^3/min
r = Radius of impeller, ft
Δr_c = Scroll discharge height at point c, ft
t = Blade pitch, ft
u = Wheel velocity, ft/sec
W = Flow, lb/min
w = Relative velocity, ft/sec
β = Blade angle, deg
η = efficiency, dimensionless
σ = Density ratio, dimensionless
ν = Diameter ratio, dimensionless
ϕ = Flow coefficient, dimensionless
ψ = Head coefficient, dimensionless

Subscripts

0 = Entrance
1 = Inlet
2 = Outlet
3 = Exit
ov = Overall
st = Static
tip = Tip
tot = Total

3.2 General Considerations

Fans are considered here to include any device that mechanically imparts energy to a compressible fluid and for which the compression ratio is less than 1.05:1. By considering limited fan compression ratios, it is possible to neglect density changes through the machine, and the flow can be treated as incompressible. As such, fans are dynamic machines that depend on the change of the angular momentum of the fluid.

3.3 Types of Fans

3.3.1 Centrifugal Fans

Three types are shown in Fig. 3H-16:

(1) Forward Curved - This type of centrifugal fan has a major portion of the impeller input energy in the form of kinetic energy, and requires more care in the design of the fan scroll.

(2) Backward Curved - In this fan, a large percentage of the input energy leaving the impeller is in the form of static pressure.

(3) Radial - This is the simplest type of centrifugal fan. A lesser portion of the input energy to the impeller is in the form of static pressure.

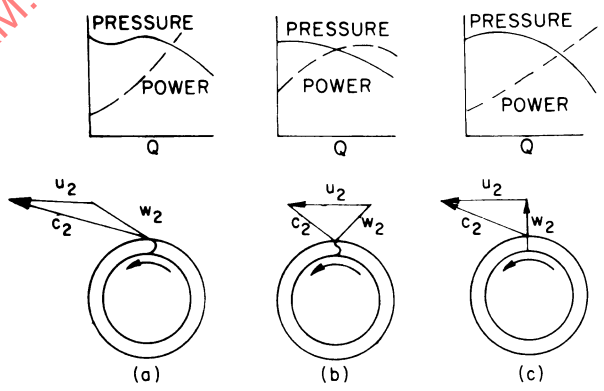

Figure 3H-16 - Centrifugal Fans: (a) forward curved; (b) backward curved; (c) radial

3.3.2 Axial Fans

Three types are shown in Fig. 3H-17:

(1) Propeller Fans - This fan is used mainly for moving large quantities of air at very low static pressures. It is often constructed from sheet metal.

(2) Tube Axial - The tube axial fan has an external housing and, commonly, a refined fan blading, but it does not have inlet or outlet guide vanes.

(3) Vane Axial - This fan represents the more refined axial machine and incorporates inlet or outlet guide vanes.

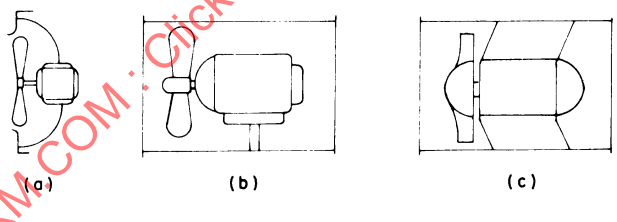

Figure 3H-17 - Axial Fans: (a) propeller; (b) tube axial; (c) vane axial

3.4 Fundamental Considerations

3.4.1 Centrifugal Fans

In general, centrifugal fans are simple machines composed of an inlet, impeller, and scroll, and is constructed of light sheet metal.

3.4.1.1 Centrifugal Fan Inlet

Most centrifugal fans have a rounded or bellmouth inlet to reduce the entrance losses to the impeller, as shown in Fig. 3H-18.

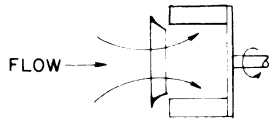

Figure 3H-18 - Centrifugal Fan Inlet

Where increased pressure is required, inlet guide vanes may be incorporated to provide prerotation against the direction of the impeller. Alternatively, by providing prerotation in the direction of impeller rotation, reduced pressure and capacity may be obtained.

3.4.1.2 Centrifugal Impellers

The ideal head that can be developed by the impeller is expressed by Euler's equation:

$$H_e = \frac{u_2 c_{u2} - u_1 c_{u1}}{g} \qquad \text{(3H-18)}$$

The velocity terms correspond to the velocity triangles shown in Fig. 3H-19.

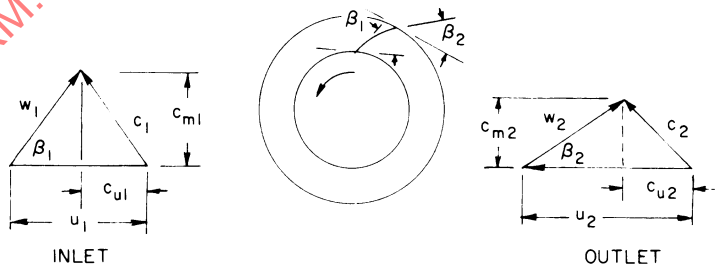

Figure 3H-19 - Euler's Velocity Triangles

With real machines, the fluid flow angles, β, will differ from the physical vane angles, β, and performance calculated from the physical vane angles will always result in a pressure rise considerably higher than that obtainable from the actual machine. This effect is associated with the aerodynamics of the impeller vane and is sometimes called the ''vane efficiency.'' An additional reduction in the head rise occurs because of impeller fluid friction losses.

3.4.1.3 Fan Scrolls

The scroll of a centrifugal fan converts high velocity pressures at the impeller discharge to static pressure. The performance of the scroll is more important in the case of a forwardly curved impeller because a greater portion of the input energy is in the form of kinetic energy leaving the impeller.

Optimum scroll conversion efficiency is obtained with a scroll designed for free vortex:

$$c_{u2}\, r_2 \;=\; c_{u1}\, r_1 \;=\; const. \tag{3H-19}$$

However, the physical size resulting from this approach is extremely large.

Most fan scrolls are designed by empirical methods and have a spiral shape and a discharge area consistent with the flow rate. One such method considers the scroll as a folded diffuser, as shown in Fig. 3H-20, where:

$$R \;=\; r_{impeller} + \Delta r_c \tag{3H-20}$$

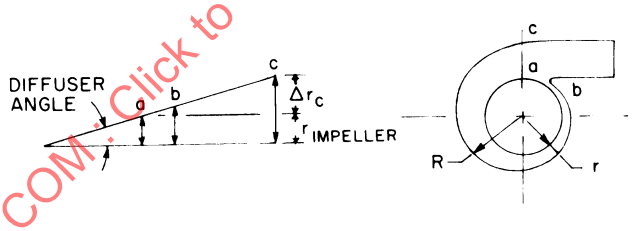

Figure 3H-20 - Scroll Design Procedure

3.4.2 Axial Fans

Axial fans cover the range from the relatively simple propeller fans made with formed sheet metal blading to the carefully designed vane axial machine that incorporates airfoil blade shapes and guide vanes.

In the case of sheet metal propeller fans, efficiency is sacrificed for low first costs. With refined blading, tube axial fans exhibit higher efficiencies. With the incorporation of inlet or outlet guide vanes or both, higher overall efficiencies are obtainable, since the kinetic energy associated with the discharge swirl is reduced.

3.4.2.1 Inlet Guide Vanes

When guide vanes are used ahead of the fan wheel, they usually are designed to impart swirl opposite to the direction of rotation. The amount of swirl is determined at the design point so that the flow leaving the fan is only axial; that is, there is no tangential component. This is illustrated in Fig. 3H-21.

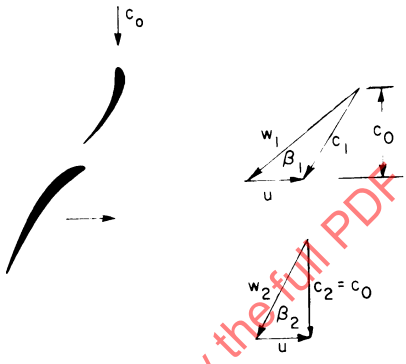

Figure 3H-21 - Velocity Triangles with Inlet Guide Vanes

A fan designed with preswirl and axial discharge will, in general, have higher overall efficiencies, since there is no loss of kinetic energy associated with swirl at the discharge.

The effects of prerotation of the fluid entering the fan wheel are shown in Fig. 3H-22.

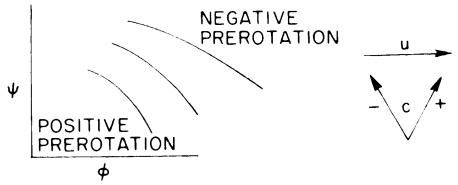

Figure 3H-22 - Effect of Prerotation

3.4.2.2 Axial Fan Wheels

The ideal head developed by an axial flow wheel can be expressed by Euler's equation for free vortex flow:

$$H_e = \frac{u\,(c_{u2} - c_{u1})}{g} \qquad \text{(3H-21)}$$

A typical velocity diagram is presented in Fig. 3H-23.

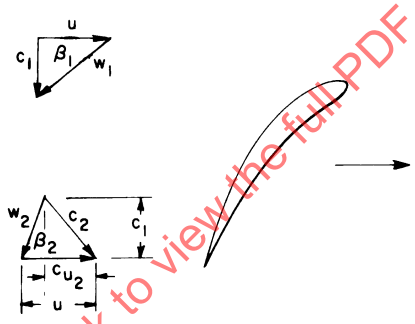

Figure 3H-23 - Euler's Velocity Triangles

The purpose of the blading is to impart a directional change to air such that the outlet angle β_2 is greater than β_1. The greater the average turn angle $(\beta_2 - \beta_1)$, the greater the required blade loading and static pressure rise.

A detailed aerodynamic design of fan blading is beyond the scope of this presentation, but the influences of some of its design variables are shown in Fig. 3H-24 as functions of dimensionless pressure coefficient ψ and flow coefficient ϕ. Fig. 3H-24(a) shows that by increasing the number of blades, the pressure coefficient increases without a change in flow coefficient. Fig. 3H-24(b) shows the effect of a variation in the hub - to - tip ratio. In Fig. 3H-24(c) it can be seen that as the pitch angle is increased, the flow coefficient increases without a change in pressure coefficient. Fig. 3H-24(d) shows the effect of blade chord length - to - blade spacing.

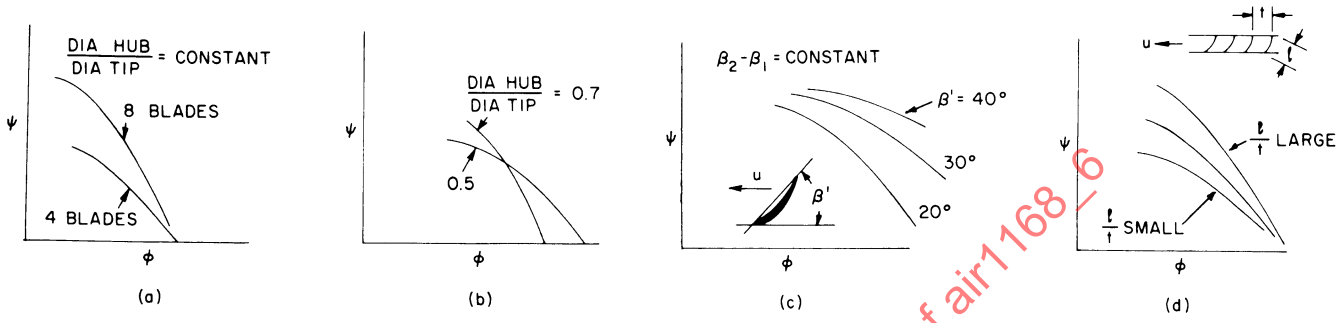

Figure 3H-24 - Influence of Design Variables: effects of (a) increasing blades, (b) increase in hub diameter, (c) blade pitch, and (d) chord length - to - blade spacing

3.4.2.3 Outlet Guide Vanes

The use of outlet guide vanes performs a function similar to inlet guide vanes except that in this case the swirl or tangential velocity component leaving the wheel is removed by the guide vanes. This is shown in Fig. 3H-25.

In addition, a divergent diffuser is sometimes used with very high performance fans to reduce the axial velocity component.

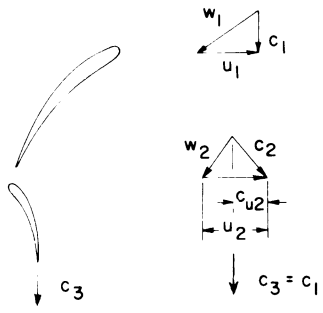

Figure 3H-25 - Velocity Triangles with Outlet Guide Vanes

3.4.3 Fan Efficiency

The overall fan efficiency is defined as

$$\eta_{ov} = \frac{\text{Fluid horsepower}}{\text{Shaft horsepower}} \qquad \text{(3H-22)}$$

The losses in a fan are mainly associated with fluid stream friction, disc friction, and mechanical losses. In general, the mechanical losses are very low.

The most common method of defining fan overall efficiency is by means of static pressure rise, where the fluid horsepower is determined by the difference between the static discharge pressure and the inlet total pressure. When defined this way, the overall efficiency is called static efficiency. Total efficiency is sometimes used where the pressure rise is defined as the difference between outlet total and inlet total pressure.

The pressure rise presented for most fans is the static pressure rise (outlet static minus inlet total) and has been determined under favorable conditions. The inlet flow condition permits a uniform velocity distribution, and the discharge static pressure is measured far enough downstream so that some kinetic energy recovery is realized from the higher velocities leaving the fan wheel annulus.

3.4.4 Fan Laws

The fan laws in their simplest form can be expressed in three relationships, which completely describe all the variables of similarity. The assumptions underlying the fan laws are that inertia forces are the only forces acting on the fluid, that the fluid is incompressible, and that viscous effects can be neglected. Within these limits for any machine, the following parameters can be assumed constant:

Flow:

$$\frac{Q}{nD^3} = \text{const.} \qquad \text{(3H-23)}$$

Pressure:

$$\frac{\Delta P_{st}}{\sigma n^2 D^2} = \text{const.} \qquad \text{(3H-24)}$$

where: ΔP_{st} = Static pressure rise across fan, in.H_2O

Power:

$$\frac{P_{hp}}{\sigma n^3 D^5} = \text{const.} \qquad \text{(3H-25)}$$

The flow and pressure parameters can be presented in another form, which is used in fan design, and are called the flow and pressure coefficients.

Flow coefficient:

$$\phi = \frac{c}{u} \approx \frac{Q}{nD^3(1-\nu^2)} \qquad \text{(3H-26)}$$

where ν = Dia hub/dia tip

Pressure coefficient:

$$\psi = \frac{H_{tot}}{u^2/2g} \approx \frac{\Delta P_{st} + q}{\sigma n^2 D^2} \qquad \text{(3H-27)}$$

noting that $u \approx nD_{tip}$ *and* $H_{tot} \approx \Delta P_{tot}/\rho g$ for incompressible flow.

3.4.5 Specific Speed

Specific speed is a useful parameter in the selection of the most efficient fan for a particular application. The restriction imposed on the use of the fan laws also applies to specific speed. For use in comparing fans, specific speed is often defined as

$$N_s = \frac{n\sqrt{Q}}{(\Delta P_{st}/\sigma)^{3/4}} \qquad \text{(3H-28)}$$

where ΔP_{st} = Static pressure rise across fan, in. H_2O

Specific speed is usually determined at the "best efficiency point" and is not necessarily an indication of the selection operating point for the fan.

3.5 Fan Performance

3.5.1 Specific Speed and Efficiency

Fig. 3H-26 presents specific speed as a function of static efficiency and shows the range of specific speeds for various types of fans. The efficiency values shown are an indication of the upper limits that can be obtained with the respective types of fans.

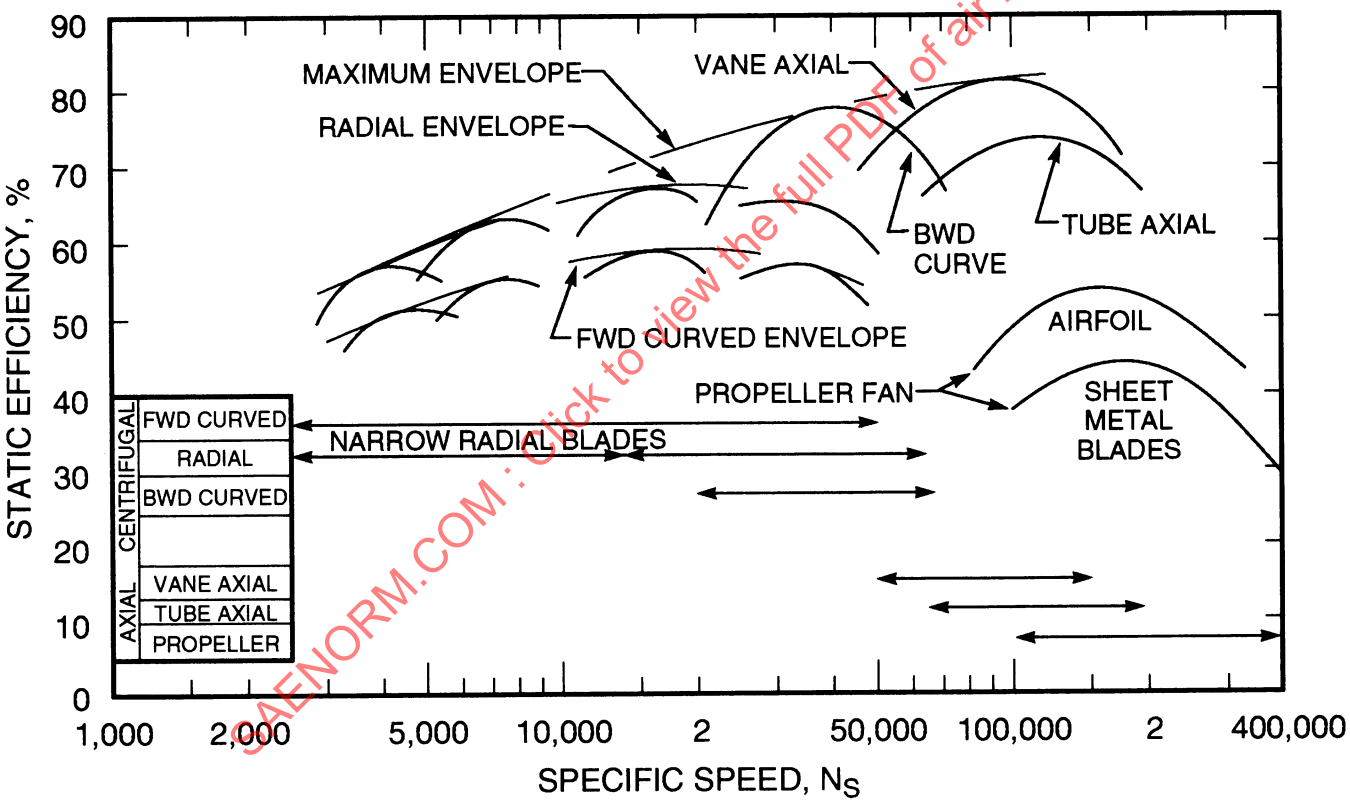

Figure 3H-26 - Fan Specific Speed

In practice, the efficiencies of most small commercial fans will not be as good as those shown in Fig. 3H-26, ranging 5-10% less, since design refinements are compromised in favor of lower first costs.

Most small centrifugal fans have either radial or forward curved blading, since for a given application where speed is fixed, these fans will be smaller than the inherently more efficient back-

ward curved fan. The use of a backward curved fan becomes significant only when operating efficiency is important and size is of lesser consequence.

The propeller fans, like the forward curved or radial fans, are inexpensive and inefficient. The design refinements necessary to achieve 70-80% efficiency in a tube or vane axial fan make it an expensive piece of equipment, limited to applications where input power and size are most important. As a consequence, these fans are used in a majority of the airborne applications where a significant air flow or pressure rise is required.

3.5.2 Centrifugal Fan Performance

Fig. 3H-27 shows typical centrifugal fan performance as a function specific flow, Q/nD^3, and specific pressure, $\Delta P_{st}/\sigma n^2 D^2$, for the three types of centrifugal fans. Because of the numerous design variables, the values shown in this figure are shown as typical of this type of equipment.

The specific flow in a centrifugal fan can be readily changed by increasing or decreasing the impeller and scroll width. As the impeller width approaches the impeller diameter, the flow in the impeller inlet begins to limit performance. In most centrifugal fans, the ratio of the wheel diameter to the wheel width can vary between 1 and 5. It should be noted that because of the simplified inlet, the impeller of most centrifugal fans is not completely full and the determination of the width is somewhat empirical.

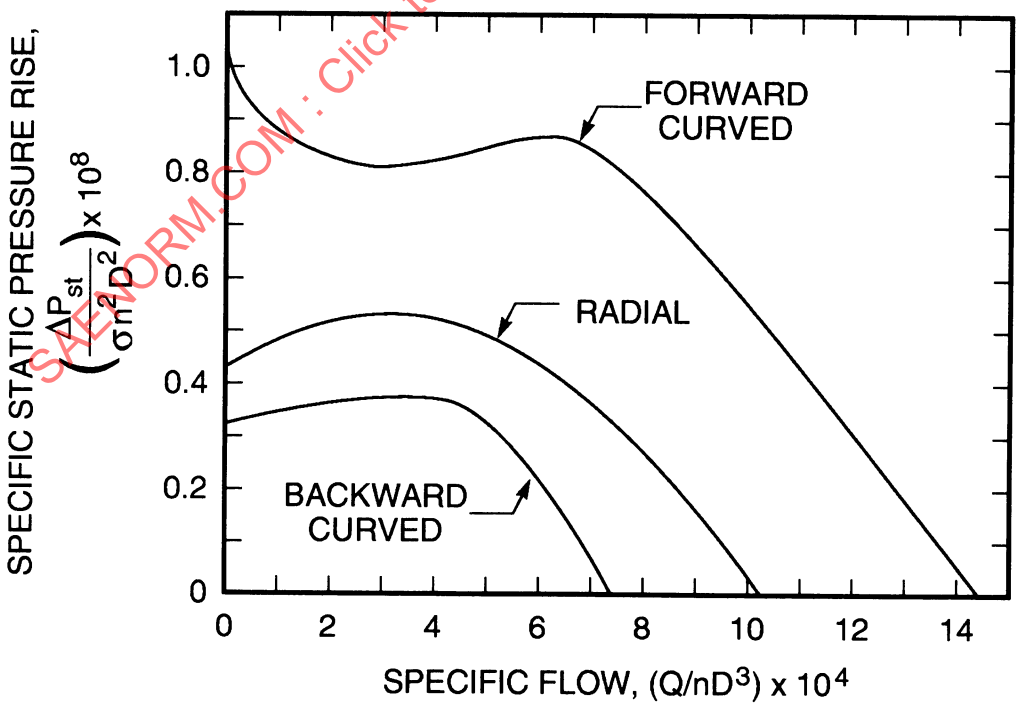

Figure 3H-27 - Typical Centrifugal Fan Performance

3.5.3 Axial Fan Performance

The performance of some typical axial fans is shown in Fig. 3H-28. Because of the several design variables (that is, number of blades, hub-to-tip ratio, blade length-to-blade spacing, blade pitch, and blade curvature), it is difficult to specify all the variables in a simple manner. Fig. 3H-28 is offered as a guide for approximating the speed and size of axial fan equipment.

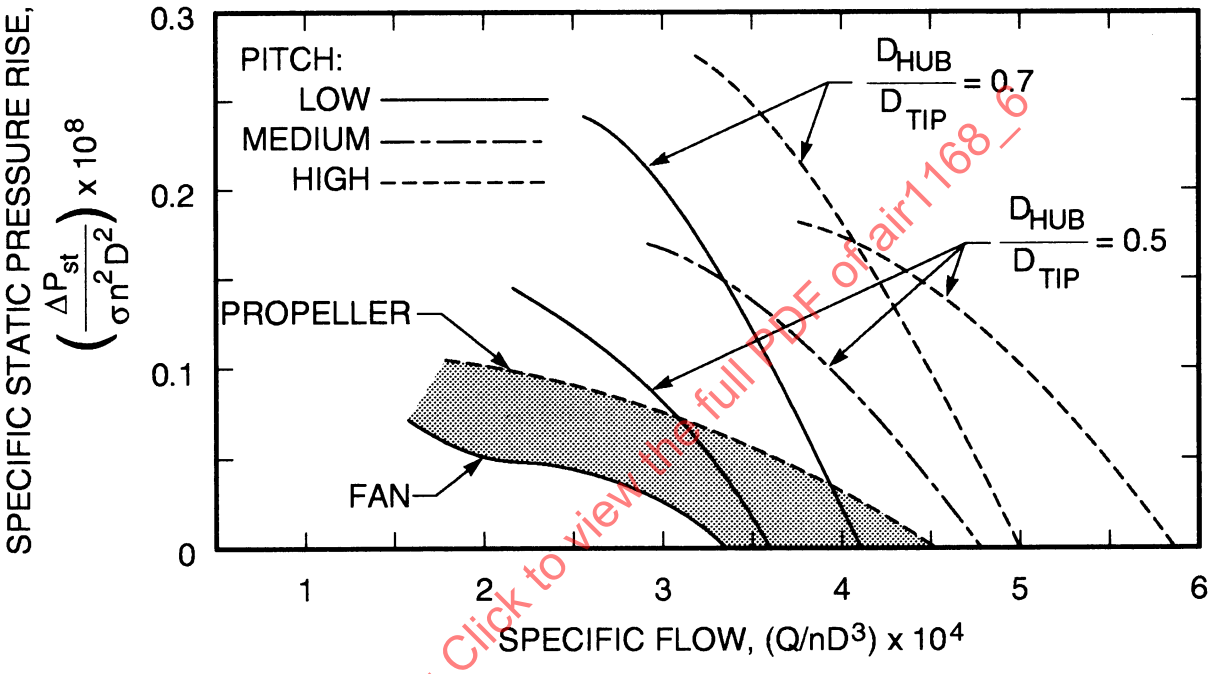

Figure 3H-28 - Typical Axial Flow Fan Performance

Propeller fans with sheet metal or airfoil blading will, in general, perform between the limits shown in Fig. 3H-28. Higher specific flows will occur with increased blade pitch. The more refined airfoil type of blading serves primarily to reduce blade losses, with a resultant increase in fan efficiency.

A tube axial fan can be designed with a specific static pressure rise approaching 0.2×10^{-8}. There are specialized vane axial fans that have exceeded this value. Examples of the effect of hub-to-tip ratio and blade pitch are shown in Fig. 3H-28 for well-designed vane and tube axial fans.

3.5.4 Fan Horsepower

The fluid horsepower can be approximated by the relationship

$$P_{hp\,(fluid)} = \frac{\Delta P Q}{6350} \qquad \text{(3H-29)}$$

The error in this approximation is 2.9% at a pressure ratio of 1.05.

$$\text{Shaft horsepower} = \frac{\Delta P_{st} Q}{6350 \eta_{st}} = \frac{\Delta P_{tot} Q}{6350 \eta_{tot}} \qquad \text{(3H-30)}$$

3.6 Selection and Sizing of a Fan

Knowing the required corrected static pressure rise ($\Delta P/\sigma$) and flow (Q), the following steps are suggested:

(1) Select a shaft speed consistent with that available from the planned fan drive unit.

(2) Determine the fan specific speed:

$$N_s = \frac{n\sqrt{Q}}{(\Delta P_{st}/\sigma)^{3/4}} \qquad \text{(3H-31)}$$

(3) Examine Fig. 3H-26 to determine the best type of fan for the application.

(4) From an evaluation of the application, based upon the importance of size and operational efficiency, select a specific static pressure rise from Fig. 3H-27 for centrifugal fans or from Fig. 3H-28 for axial fans. Next, solve for wheel diameter.

(5) Check specific flow to confirm the selection.

3.7 Fan Application

3.7.1 Fan Operating with Fixed Restriction

The operation of a fan in a system with a fixed restriction is shown by Fig. 3H-29. The performance of the system restriction is usually based on the relationship of $\sigma\Delta P$ versus weight flow; that is,

$$\sigma\Delta P = KW^a \qquad \text{(3H-32)}$$

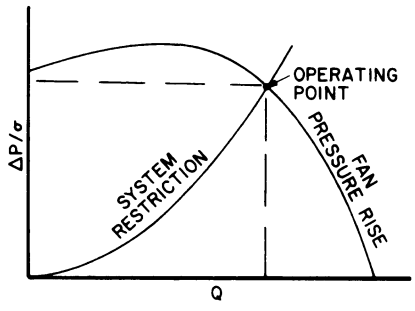

Figure 3H-29 - Fan System Characteristics

For the case where a = 2, it is possible to rearrange the pressure drop function so that it can be presented as

$$\frac{\Delta P}{\sigma} = K_2 Q^2 \tag{3H-33}$$

and when plotted against the fan performance, the intersection of the two curves will define the operating point. As long as the exponential value of Q remains equal to 2, the fan will operate at this point, delivering a constant airflow(cfm) and $\Delta P / \sigma$ regardless of the value of σ.

The preceding relationship is satisfactory when the system is operating in the turbulent region, but when in the laminar region and when the exponent of Q is less than 2, it is necessary to determine the operating point for each value of density. It should be noted that as density decreases, the system $\sigma \Delta P$ shifts toward the laminar region.

3.7.2 Sound Laws

Fan sound laws are helpful in evaluating the sound level of geometrically similar fans. Like fan laws, they apply to one particular operating point on the fan's dimensionless performance, and each operating point will have its own reference db level. The sound laws are based on the assumption that the relationship

$$db_2 - db_1 = 10 \log_{10} \left(\frac{D_2}{D_1}\right)^2 \left(\frac{u_2}{u_1}\right)^5 \tag{3H-34}$$

is true. Experimental evidence has supported this assumption.

The sound laws present the relationship of Eq. 3H-34 in a more convenient form, and the most useful relationships are

$$db_2 - db_1 = 10 \log_{10} \left(\frac{D_2}{D_1}\right)^2 \left(\frac{n_2}{n_1}\right)^5 \tag{3H-35}$$

$$db_2 - db_1 = 10 \log_{10} \left(\frac{D_2}{D_1}\right)^2 \left(\frac{\Delta P_2}{\Delta P_1}\right)^{5/2} \tag{3H-36}$$

$$db_2 - db_1 = 10 \log_{10} \left(\frac{Q_2}{Q_1}\right) \left(\frac{\Delta P_2}{\Delta P_1}\right)^2 \tag{3H-37}$$

3.8 References

Elaboration of the material presented above for fans can be found in Refs. 8-12.

4. COMPRESSORS

4.1 Nomenclature

c = Absolute velocity, ft/sec
D = Wheel tip diameter, ft
H = Pressure head, ft
Δh_{ad} = Isentropic enthalpy change, Btu/lb
K' = Pressure coefficient, dimensionless
M = Momentum, ft-lb/sec
p = Pressure, lb/in.^{2}
P_{hp} = Horsepower
P_t = Total pressure, lb/in.^{2}
Q = Volume flow rate, ft^3/min
r = Radius, ft
T_t = Total temperature, ^{o}R
u = Wheel speed, ft/sec
v = Velocity, ft/sec
V = Volume, ft^3
w = Weight flow rate, lb/sec
W = Weight of fluid, lb
Y = $[(P_{t2}/P_{t1})^{(\gamma-1)/\gamma}] - 1$
η = Efficiency, dimensionless
λ = K'/η_{ad}, dimensionless
δ = $P_{t1}/14.7$, dimensionless
θ = $T_{t1}/519$, dimensionless

Subscripts

ad = Adiabatic
c = Clearance
d = Displacement
e = Euler
iso = Isothermal
is = Isentropic
m = Mechanical
ov = Overall
st = Static
u = Tangential
v = Volume
1 = Compressor inlet
2 = Compressor discharge
0 = Initial

4.2 General Considerations

As defined in this manual, a compressor is a fluid-moving device used to pump a compressible gas to a pressure ratio of 1.05 or greater. As such, the gas undergoes a significant volume change with the changes in pressure and temperature of the compression process.

4.3 Types of Compressors

Compressors are classified by two fundamental types: positive displacement and dynamic.

4.3.1 Positive Displacement Compressors

Positive displacement compressors operate on the principle of isolating or capturing a small quantity of the gas to be compressed and then, by means of reciprocating or rotary action, reducing the volume of gas, thus raising its pressure and temperature.

4.3.1.1 Reciprocating Compressors

Two types, piston and diaphragm, are shown in Fig. 3H-30.

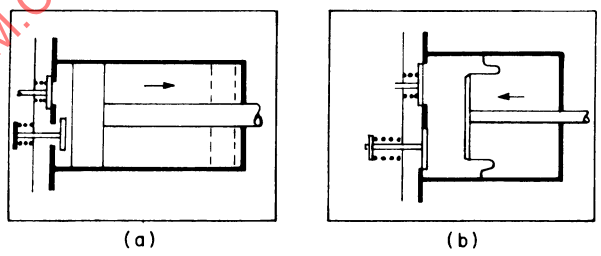

Figure 3H-30 - Reciprocating Compressors: (a) piston compressor; (b) diaphragm compressor

4.3.1.2 Rotary Compressors

Fig. 3H-31 illustrates three different designs: sliding vane, lobe (Roots), and axial flow helical lobe (Lysholm).

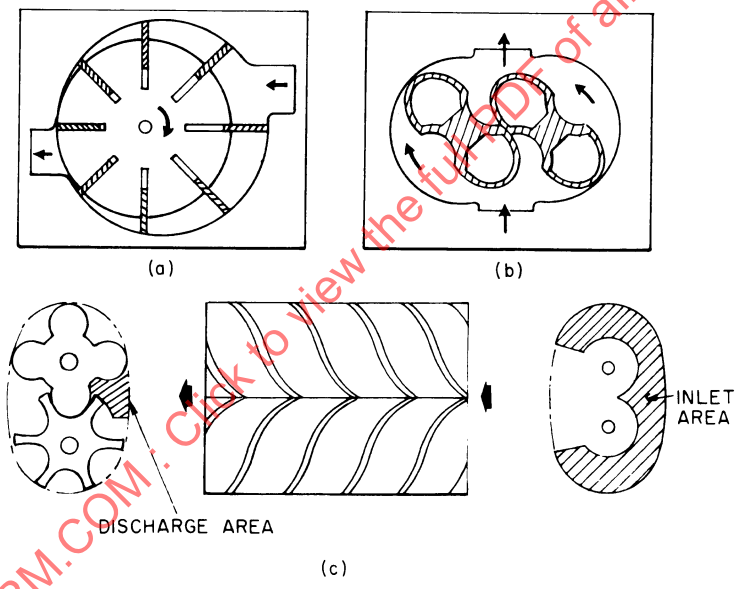

Figure 3H-31 - Rotary Compressors: (a) sliding vane; (b) lobe (Roots); (c) axial flow helical lobe

4.3.2 Dynamic Compressors

These compressors, shown in Fig. 3H-32, act continuously on the gas by inducing a change of angular momentum to the fluid as it flows through the compressor blading. Dynamic compressors are generally classified by the flow path through the compressor. The types are centrifugal, mixed, and axial.

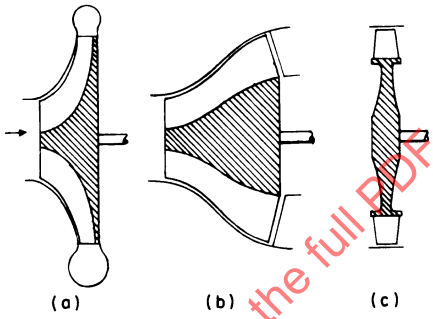

Figure 3H-32 - Dynamic Compressors: (a) centrifugal; (b) mixed; (c) axial

4.4 Fundamental Considerations

4.4.1 Positive Displacement Machines

The following discussion of these machines refers to the nomenclature of Fig. 3H-33.

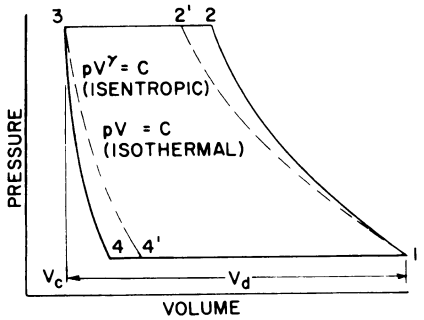

Figure 3H-33 - Ideal Pressure-volume Diagram for a Reciprocating Compressor

4.4.1.1 Pressure-Volume Diagram for a Piston Compressor

The compression process of a positive displacement piston machine having a clearance volume V_3 is best examined on the pressure-volume diagram, Fig. 3H-33, where:

1–2 = Compression
2–3 = Expulsion
3–4 = Expansion
4–1 = Suction
V_c = Clearance volume
V_d = Displacement volume

The area 1-2-3-4 represents the net work on the gas delivered by the compressor for an isentropic process. Area 1-2′-3-4′ represents the work for an isothermal process.

Work for isentropic compression:

$$\text{Work} = \frac{\gamma p_1 (V_1 - V_4)}{\gamma - 1}\left[\left(\frac{p_2}{p_1}\right)^{(\gamma-1)/\gamma} - 1\right] \text{ ft-lb/cycle} \quad \text{(3H-38)}$$

where $p_2 = p_3$ and $p_1 = p_4$

Work for isothermal compression:

$$\text{Work} = p_1 (V_1 - V_{4'}) \ln \frac{p_1}{p_{2'}} \text{ ft-lb/cycle} \quad \text{(3H-39)}$$

where $p_{2'} = p_3$ and $p_1 = p_{4'}$

In an actual reciprocating compressor, the valves are spring loaded and operate by a difference in pressure. Because of the valve spring forces, valve inertia, and valve friction losses, p_4 is at a lower pressure than p_1, and p_2 is greater than p_3.

The theoretical flow per two stroke cycle of a piston compressor is

$$W = \rho g_{intake} (V_1 - V_4) \text{ lb/cycle} \quad \text{(3H-40)}$$

4.4.1.2 Volumetric Efficiency

Volumetric efficiency is defined as the ratio of the actual flow to the ideal flow of the displacement volume (V_D)

$$\eta_v = \frac{W_{actual}}{\rho g_{intake} V_D} \quad \text{(3H-41)}$$

where $V_D = V_1 - V_3$, ft^3

ρg = Specific weight determined by intake conditions, lb/ ft^3

It should be noted that the volumetric efficiency will decrease as the compressor is operated at higher pressures. The point at which the intake valve opens (V_4) is a function of the expansion of the gas in the clearance volume. By examining Fig. 3H-33, it can be seen that as p_3 becomes higher, V_4 must move closer to top dead center, reducing the ratio of admission volume, $(V_1 - V_4)$, to swept volume, V_D.

4.4.1.3 Compression Efficiency

The adiabatic compression efficiency can be expressed as the ratio of the isentropic work to the indicated work:

$$\eta_{ad} = \frac{\text{Isentropic work}}{\text{Indicated work}} \tag{3H-42}$$

while constant temperature compression efficiency can be expressed as

$$\eta_{iso} = \frac{\text{Isothermal work}}{\text{Indicated work}} \tag{3H-43}$$

where indicated work is the actual work imparted to the gas delivered by the compressor, as determined by the indicator card.

4.4.1.4 Overall Efficiency

The overall efficiency can be expressed as the product of the mechanical efficiency (mechanical friction losses) and the compression efficiency:

$$\eta_{ov} = \eta_m \cdot \eta_{ad}$$

$$\text{or} \quad \eta'_{ov} = \eta_m \cdot \eta_{iso} \tag{3H-44}$$

4.4.2 Dynamic Compressors

The fluid moving through a dynamic compressor is acted upon by the impeller, which imparts angular momentum to the fluid, as in a dynamic pump or fan. Guide vanes ahead of the impeller or diffuser section, or both, downstream of the impeller are used to minimize the kinetic energy losses in the compressor.

Euler's equations (Eqs. 3H-1 and 3H-18) apply to dynamic compressors, except for compressibility effects. The velocity triangles and the stator and rotor design require refinements to account for the continual change in density of the fluid as it passes through the compressor.

The form of Euler's equation given in Eq. 3H-18 is general and is derived from Newton's laws of motion, which state that the time rate of change of angular momentum about an axis is equal to the moment of the applied force. Thus, the angular momentum of an increment, dW, of fluid entering a rotor per increment of time dt is $(r_1 c_{u1})/g$, and leaving is $(r_2 c_{u2})/g$, where c_{u1} *and* c_{u2} are the tangential components of the entering and leaving absolute velocities.

The change in angular momentum in time dt is the difference in these two quantities. Thus, equating the rate of change of momentum to the moment:

$$M = \frac{dW}{dt}\left(\frac{r_2 c_{u2} - r_1 c_{u1}}{g}\right) \quad \text{(3H-45)}$$

Multiplying this moment by the angular velocity n yields the power

$$Mn = \frac{n}{g}\frac{dW}{dt}(r_2 c_{u2} - r_1 c_{u1}) \quad \text{(3H-46)}$$

Substituting u_1 and u_2 for nr_1 and nr_2, the energy per pound of fluid flowing (ft-lb/lb), which is equivalent to the ideal head (ft) against which the compressor could deliver the flow, can be expressed as

$$H_e = \left(\frac{1}{g}\right)(u_2 c_{u2} - u_1 c_{u1})$$

For adiabatic compression, the ideal head can also be expressed as

$$H_e = Jc_p T_{t1}\left[\left(\frac{P_{t2}}{P_{t1}}\right)^{(\gamma-1)/\gamma} - 1\right] \quad \text{(3H-47)}$$

$$= Jc_p T_{t1} Y$$

For the case of the radial (centrifugal) compressor, certain special alternate forms of the equation are convenient. If there is no tangential component of fluid velocity at the rotor inlet ($c_{u1} = 0$),

$$H_e = \frac{u_2 c_{u2}}{g} \quad \text{(3H-48)}$$

If, as is nearly the case with a 90 deg (radial) exit blade angle and moderately low values of W_2, the tangential component c_{u2} is approximately equal to the peripheral velocity u_2, then

$$H_e = \frac{u_2^2}{g} \quad \text{(3H-49)}$$

In actual machines, Eq. 3H-49 is commonly used as a basis for defining the pressure coefficient K', so that

$$H_e = K' \frac{u_2^2}{g}$$

$$\text{and} \quad K' = \frac{gJc_pT_{t1}Y}{u_2^2} \tag{3H-50}$$

This coefficient accounts for head losses in the rotor and also in the diffuser and/or scroll. For a radial bladed compressor, K' tends to have a value between 0.5 and 0.75.

Another useful coefficient, λ, relates the actual temperature rise of the compressed fluid to the tip speed u_2:

$$\Delta T_t = T_{t2} - T_{t1} = \lambda \frac{u_2^2}{Jgc_p} \tag{3H-51}$$

$$\text{or, for air,} \quad \Delta T_t = \lambda \frac{u_2^2}{6080} \tag{3H-51a}$$

For a 90 deg radial, high speed, compact machine (small external heat transfer), λ tends to have a value between 0.9 and 1.0.

For any appreciable impeller backward curvature, both coefficients are reduced to lower values than indicated above, but in any case,

$$\eta_{ad} = \frac{K'}{\lambda} = \frac{T_{t1}Y}{T_{t2} - T_{t1}} \tag{3H-52}$$

The higher pressure ratios associated with a compressor imply higher velocities (kinetic energy), and require careful consideration of local flow Mach number.

4.4.2.1 The Compression Process

The temperature-entropy diagram is a convenient method of describing the compression process of a dynamic machine. Fig. 3H-34 shows the compression process for a dynamic machine with a discharge diffuser.

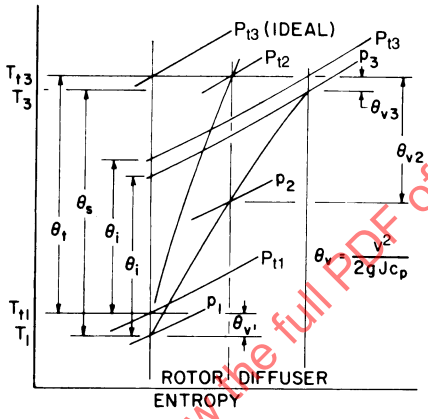

Figure 3H-34 - Temperature-entropy Diagram for Adiabatic Compression

4.4.2.2 Total Efficiency

The total efficiency can be defined (Fig. 3H-34) for adiabatic compression as

$$\eta_{ad} = \frac{\text{Total isentropic temperature increase}}{\text{Actual total temperature increase}} = \frac{\theta_i}{\theta_t}$$

$$= \frac{T_{t1}[(P_{t2}/P_{t1})^{(\gamma-1)/\gamma} - 1]}{T_{t2} - T_{t1}} = \frac{T_{t1}Y}{T_{t2} - T_{t1}} \qquad \text{(3H-53)}$$

4.4.2.3 Static Efficiency

The static efficiency can be defined (Fig. 3H-34) for adiabatic compression as

$$\eta_{ad} = \frac{\text{Static isentropic temperature increase}}{\text{Actual total temperature increase}} = \frac{\theta_i}{\theta_s} \qquad \text{(3H-54)}$$

4.4.2.4 Isentropic Enthalpy Change

The enthalpy increase for an isentropic compression process can be defined by

$$\Delta h_{ad} = c_p \theta_i = c_p T_{t1} Y \tag{3H-55}$$

4.4.2.5 Compressor Power

The actual compressor power can be defined for adiabatic compression by

$$P_{hp} = \frac{w \Delta h_{ad}}{42.4 \eta_m \eta_{ad}} \tag{3H-56}$$

4.5 Compressor Performance

In general, compressors used for in-flight installations represent a class of equipment that has been specially designed for the intended application, to provide maximum performance with minimum size and weight. The compressor is usually required to meet several operating and installation conditions that dictate extreme care in the selection of the type of compressor as well as design refinements in the internal aerodynamics of the machine.

4.5.1 Specific Speed

Because of the many considerations involved in the design of a compressor, it is difficult to generalize compressor performance. While specific speed is usually considered a tool for pumps and fans (incompressible flow), it can also serve to evaluate the best type and the efficiency range for a particular compressor application. Specific speed, when related to speed, flow, and head, can be rearranged into common compressor parameters such that

$$N_s = \frac{n(Q/60)^{1/2}}{H^{3/4}}$$

$$\approx \frac{(n/\sqrt{T})(w\sqrt{T}/p)^{1/2}}{(H/T)^{3/4}} \tag{3H-57}$$

Fig. 3H-35 presents variations in specific speed with efficiency for three types of compressors.

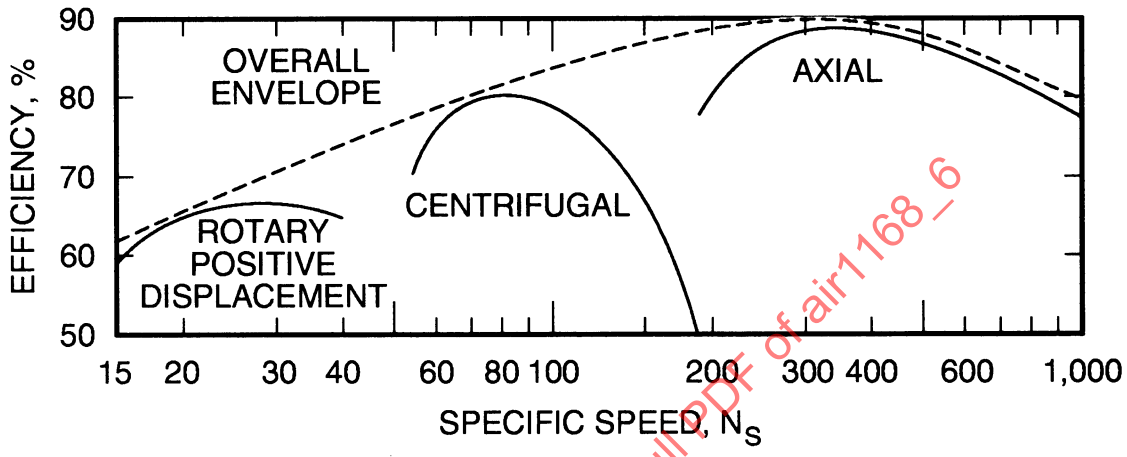

Figure 3H-35 - Variations of Efficiency with Specific Speed

4.5.2 Dimensionless Dynamic Compressor Performance

Generally, the performance of a dynamic compressor can be presented by relating the dimensionless parameters: impeller tip Mach number, inlet flow Mach number, pressure ratio, and efficiency. Other factors that affect compressor performance are compressor geometry, which is fixed for most compressors (except for variable guide or diffuser vanes), and Reynolds number. Reynolds number effects usually are not noted on a compressor map.

Fig. 3H-36 shows a typical presentation of dimensionless compressor performance. As a convenience for relating both flow and speed to actual values, the inlet pressure and temperature can be referenced to standard conditions.

At standard sea level conditions, the compressor weight flow and speed can be read directly. The flow function when expressed as

$$\frac{w\sqrt{T_{t1}}}{A_1 P_{t1}}$$

is a function of inlet Mach number and reaches a theoretical maximum value of 0.53 at Mach 1.0 for air, but because of the local interference effect of the blading, choking will occur at lower values of the flow function.

4.5.3 Compressor Performance Characteristics

The effects of compressor losses and Reynolds number are discussed below.

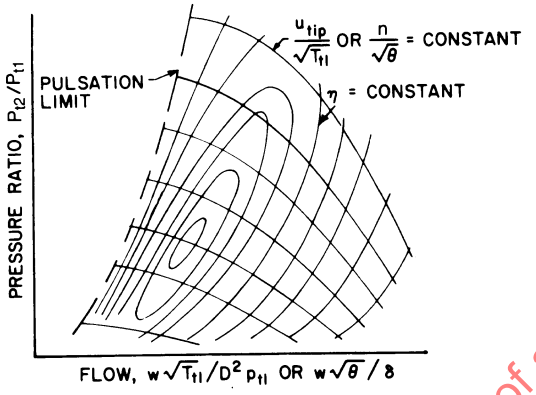

Figure 3H-36 - Dimensionless Compressor Performance

4.5.3.1 Dynamic Compressor Losses

Fig. 3H-37 shows the general characteristics of the losses in a dynamic compressor.

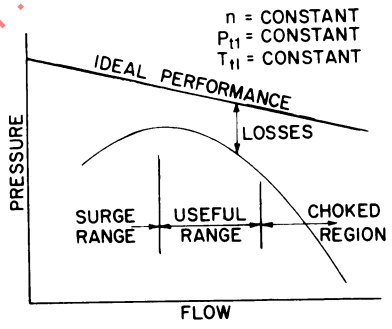

Figure 3H-37 - General Characteristics of a Dynamic Compressor

Choking occurs at the higher flow rates as the flow Mach number and dynamic pressure increase. With increased flow, a greater portion of the compressor power is lost in fluid friction from the compressor blading, and as the flow approaches the local critical Mach number at the compressor inlet, the compressor will become fully choked with near vertical pressure-flow performance characterisics in the choked region.

Surge is a violent instability of the pressure and flow, which occurs when a portion of the compressor blading is stalled. This is represented by the portion of the compressor pressure-flow performance curve which has a positive slope. A typical apportionment of losses in a dynamic compressor is shown by Fig. 3H-38.

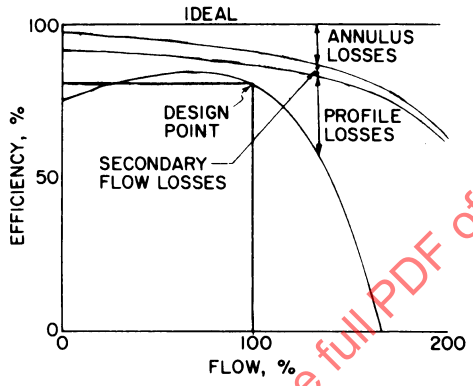

Figure 3H-38 - Losses in a Dynamic Compressor

The annulus losses are the wall friction losses associated with the kinetic energy of the fluid passing through the compressor. As the blade or passage height is decreased, the annulus losses become a more significant part of the compressor losses. The secondary flow losses occur near the tip and root of the compressor blades and represent a loss that is converted to internal energy as the trailing vortices set up velocity components normal to the through-flow direction. The profile losses represent the portion of the kinetic energy that is lost because of skin friction and separation as the flow passes through the blade channels.

4.5.3.2 Effect of Reynolds Number

Determining quantitative values of Reynolds number that are satisfactory for different compressor designs is difficult because of the number of design variables involved. However, the Reynolds number (based on blade chord for axial, and inlet diameter for centrifugal compressors) should be large (greater than 200,000) so that the flow is above the critical transition value, and laminar boundary layer separation is prevented by an early transition to a turbulent boundary layer. Subcritical flow conditions lead to high drag coefficients and reduced efficiency, whereas Reynolds numbers much greater than the critical value provide only small improvements in efficiency.

4.6 Dynamic Compressor Control Methods

The design of a compressor is influenced by the configuration requirements of the installation, the design operation point, and the off-design overall operating requirements. The last is concerned with selecting the most effective control method to adapt the compressor performance characteristics to the off-design considerations.

The pressure requirements for most installations are determined by the pressure required at the point of use, plus the connecting duct friction losses. This is shown on Fig. 3H-39, where pressure B is the pressure required at the use point and B-C is the friction loss in the ducting as determined by characteristic line B-A. If all the developed pressure is used to overcome friction, such as with a fan, the characteristic line D-A establishes the operating point.

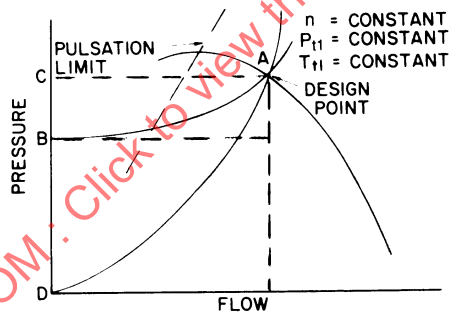

Figure 3H-39 - Compressor System Operation

The off-design requirements may involve a variation in the pressure delivered with a constant weight flow or a change in weight flow with constant pressure, or a combination of both. Fig. 3H-40 shows a typical off-design requirement for which a reduction in flow and pressure is necessary. The pressure difference B′-C′ is the duct friction loss as determined by the fixed system restriction characteristic B′-A′.

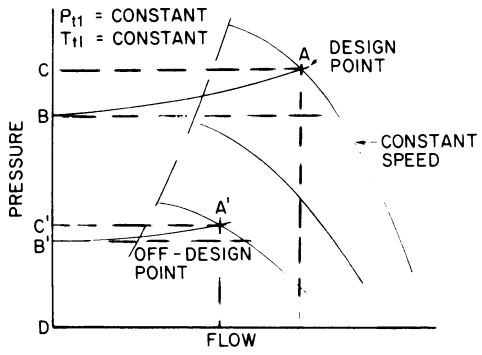

Figure 3H-40 - Off-design System Operation

Fig. 3H-41 shows the design and off-design requirements on the dimensionless compressor performance map.

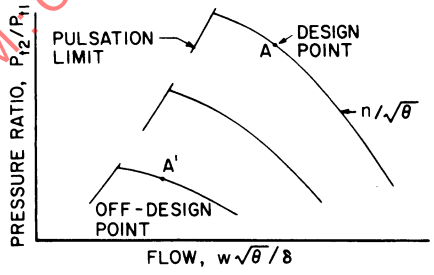

Figure 3H-41 - Off-design Dimensionless Operation

In essence, the design of a control system for off-design operation includes the following major components: sensor, controller, and controlled elements effecting compressor performance. Because of the specialized nature of the design of the overall control system, only controlled elements are discussed in this presentation.

Compressor performance variation can be effected by one or a combination of these basic techniques:

(1) Variable compressor geometry.

(2) Devices external to the basic compressor used to divert or throttle the compressor flow.

(3) Variation in compressor flow.

4.6.1 Variable Compressor Geometry

Geometries of inlet guide, impeller, and diffuser vanes are described.

4.6.1.1 Variable Inlet Guide Vanes

Adjustable vanes or blades at the compressor inlet (usually the inlet of each stage if more than one stage) can be adjusted to reduce the capacity and extend the stable operating range. The primary function of the vanes is to provide prerotation into the impeller. In addition, because of losses across the vanes, they act as a throttle, reducing the density at the impeller inlet, which also contributes to reduced flow.

It is common, particularly for centrifugal compressors, to design relatively simple guide vane geometry and accept the resulting throttling effects for control, which can result in a lower (5-10%) overall efficiency when compared to refined inlet guide vanes.

Fig. 3H-42a shows the performance effects of inlet vanes. It should be noted that the slope of the pulsation limit is quite flat and that a wide range of performance (as low as 30% of design flow) is obtainable without a change in the rotational speed.

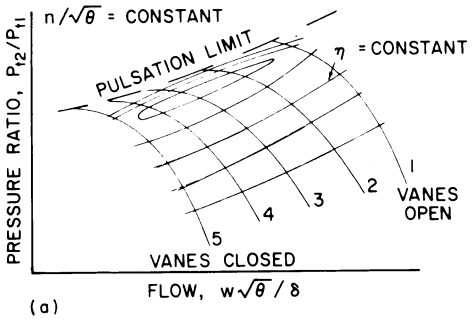

Figure 3H-42a - Compressor Performance with Inlet Guide Vanes

4.6.1.2 Variable Impeller Vanes

Adjustable impeller vanes represent an extremely complex method of affecting compressor performance. As such, they are not often used and are restricted to axial compressors.

4.6.1.3 Variable Diffuser Vanes

Diffuser vanes of variable angle have been used to extend the performance range of centrifugal compressors. The compressor performance effects are similar to those of inlet guide vanes shown in Fig. 3H-42a. Designs have been produced that operated to 20% of the design flow.

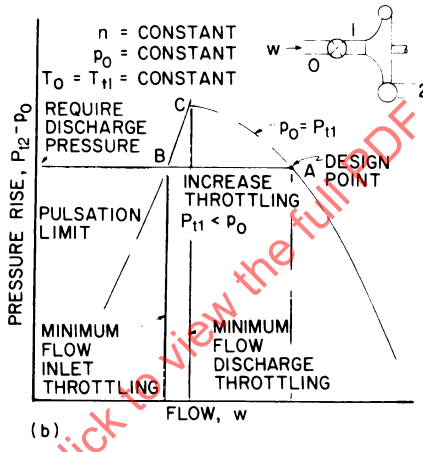

Figure 3H-42b - Compressor Operation with Inlet Throttling

4.6.2 External Control Methods

Several methods are used to control flow.

4.6.2.1 Inlet Throttling

Inlet throttling relies on the reduction of impeller inlet density due to the reduced pressure to effect a reduction in the delivered flow. The power to drive the compressor is reduced proportionately to the amount of throttling. This method of control is the cheapest and simplest, but does not have the operating economy and flow range of a well-designed variable inlet guide vane system.

Fig. 3H-42b shows compressor operation with inlet throttling for a constant discharge pressure. The extent of the reduction in flow is a function of the compressor characteristics.

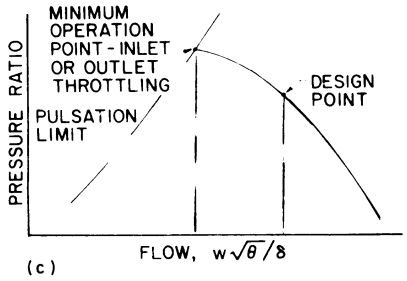

Figure 3H-42c - Throttling Effects on Dimensionless Compressor Performance

4.6.2.2 Discharge Throttling

Outlet throttling can be used to extend the flow range for constant pressure operation, similar to inlet throttling. Discharge throttling is not generally used with compressors because inlet throttling accomplishes the same control effects with a slightly greater flow range. This is evident from Fig. 3H-42c, where the dimensionless performance for inlet or discharge is the same with constant temperature and speed, and the delivered weight flow is proportional to impeller inlet pressure.

Also, generally less power is required for a given pressure ratio and weight flow, since the character of the efficiency lines is such that a system working on inlet throttling will usually operate at a slightly higher efficiency for the same flow.

4.6.2.3 Surge Blow-off Control

Where greater range is required than is available from the normal control scheme, a blow-off valve is provided to discharge flow that is not required at the use point, diverting it to the atmosphere or back to the compressor inlet. This control serves mainly as an additional control for protection against the possibility of operating the compressor in the surge or pulsation region.

4.6.3 Speed Control

When the prime mover for the compressor is a variable speed device, such as a turbine, speed can be controlled within the limits of the compressor performance for off-design operation. If large pressure ratios are required at low flows, it may be necessary to employ another control scheme in conjunction with the control of speed.

Special gear boxes have been used to provide either step or continuous gear ratio changes that can be controlled to permit varying operating characteristics.

4.7 Application of Accessory Compressors in Flight Vehicles

4.7.1 Positive Displacement Compressors

In flight-vehicle applications, positive displacement compressors are restricted to specialized applications that fall into three categories:

(1) High pressure (2000 – 3000 psi) gas systems where the flow is in the order of 1 – 3 ft^3/min. These small, air cooled, reciprocating compressors use several stages to obtain the high pressures.

(2) Low pressure (15 psi) lobe type machines that are used mainly in cabin pressure and air conditioning systems. Because of the simplicity of the controls and the lower operating speeds, these machines provide good service life.

(3) For low tonnage (less than 5 – 7 tons) systems the positive displacement compressor is the only practical machine because of the higher vapor density of most vapor cycle refrigerants. Ideally, it is possible to design centrifugal compressors for the smaller capacities, but to maintain realistic impeller passage widths (distance between wheel and shroud), impractical speeds (80,000 – 120,000 rpm) are necessary to develop the head requirements for a two- or three-stage machine.

4.7.2 Dynamic Compressors

The dynamic compressor is capable of operating at significantly higher rotational speeds than positive displacement machines. Since the dynamic compressor is inherently a balanced machine, rotative speeds in excess of 100,000 rpm are possible with small single stage units.

The other limiting factor is the wheel stress which, with a carefully designed and manufactured radial machine, can permit wheel tip speeds to approach 2,000 ft/sec. Although equipment can be designed and built with these high tip and rotational speeds, it is desirable from a cost and reliability standpoint to limit rotational speeds to the lowest practical speed for the installation and to limit tip speed to 1200-1500 fps.

The main advantages of a dynamic compressor over the positive displacement machine are the corresponding reductions in size and weight that result from the higher rotative speeds and the generally greater simplicity of mechanical design.

The centrifugal compressor received greater design and development emphasis in earlier compressors (prior to 1940). Since the advent of the jet engine, axial compressor technology has expanded at such a rate that its state of the art exceeds that of the centrifugal compressor.

Inherently, a centrifugal compressor can be designed to provide a reasonable level of performance with a minimum of design and development, since a large portion of the pressure is developed by centrifugal forces, and pressure ratios of the order of 1.5-3.0 are easily obtainable with a single stage. An axial compressor for comparable performance would require two to five stages, with greater design and mechanical complexity. The maximum efficiencies obtainable with an axial compressor exceed those of a comparable centrifugal machine.

Table 3H-1 lists some of the advantages of the axial and centrifugal compressors. The mixed flow compressor attempts to incorporate some of the advantages of the axial and centrifugal machines and, as such, is a complex machine that has specialized design applications where frontal area is important and pressure ratios in the order of 3 or 4:1 are required in a single stage.

Table 3H-1 - Comparative Advantages of Centrifugal and Axial Compressors

Centrifugal	Axial
Greater flow range for a constant speed and a specified efficiency variation	Smaller frontal area
Larger pressure ratio per stage (approaching 6:1 for special design	Higher peak efficienceies (exceeding 90%)
Less design risk	Adaptable to multistage construction
Best application: small auxiliary gas turbine, cabin compressor, superchargers, and larger vapor cycle compressors	Best application: high performance gas turbine engines, and low pressure ratio, high performance blowers
Less complex when used as single-stage machine	

Source: Data compiled from Valve Engineering Data Handbook, Crane Co.

4.8 References

Elaboration of the material on compressors presented above can be found in Refs. 13-22.

5. TURBINES

5.1 Nomenclature

c = Absolute velocity, ft/sec
C_b = Blade loss coefficient, dimensionless
C_n = Nozzle loss coefficient, dimensionless
D = Rotor tip diameter, ft
H = Pressure head, ft
H_e = Euler rotor head, ft
p = Pressure, lb/in.^{2}
P_{hp} = Horsepower
Q = Volume flow rate, ft^3/min
q_{th} = Head coefficient, dimensionless
R = Characteristic gas constant, ft-lb/lb-^{o}R

R' = Degree of reaction, dimensionless
r = Turbine pressure ratio, dimensionless
u = Rotor peripheral velocity, ft/sec
w = Relative velocity of fluid, ft/sec
Y = $[(P_{t1}/P_{t3})^{(\gamma-1)/\gamma}] - 1$, dimensionless
Z' = Restriction factor, dimensionless
β = Blade angle, deg
λ = Specific gravity, dimensionless
μ = Absolute viscosity, lb/ sec-ft, lb / hr-ft
η = Efficiency, dimensionless

Subscripts

ad = Adiabatic
B = Blade
m = Meridional
n = Nozzle
op = Optimum
ov = Overall
pa = Partial admission
s = Static
t = Turbine
th = Theoretical
u = In tangential direction
1 = Nozzle inlet
2 = Wheel inlet
3 = Wheel exit

5.2 General Considerations

A turbine is a compact mechanical device used for the conversion of potential pressure energy to shaft work. The device consists generally of the following:

(1) Stationary nozzles through which the working fluid is made to pass, converting the inlet static pressure energy largely to velocity energy.

(2) A rotor or rotors containing blades or passages through which the high-velocity working fluid passes. The manner in which the working fluid passes through the rotor is such that a large percentage of the fluid kinetic energy is imparted to the rotor by the impulse force of the fluid striking the rotor blades, or by the reaction force of the working fluid leaving the blades, or by a combination of these effects.

The turbine is used frequently in aircraft and missile fluid systems because of it's relative simplicity, compactness, light weight, and performance rangeability for a given power level as compared with other power generation devices. Typical aircraft applications vary from the driving means for electrical and hydraulic power generation systems to air cycle refrigeration systems.

5.3 Turbine Types

The turbine types that have evolved over the period of usage of the device are the following basic, single stage configurations.

5.3.1 Radial Flow Machines

All turbine types have many variations in application. Many of these variations, rather than possessing any aerodynamic superiority, are configurations that achieve only a lower level of aerodynamic acceptability but which result in an overwhelming mechanical or producibility advantage in a specific application (Figs. 3H-43 and 3H-44).

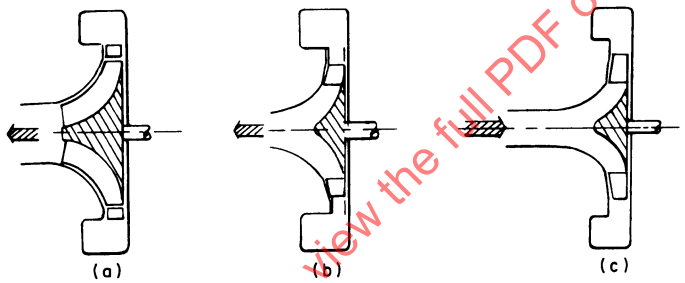

Figure 3H-43 - Radial Flow Types: (a) inward radial flow, Francis type; (b) inward radial flow, cantilever type; (c) outward radial flow

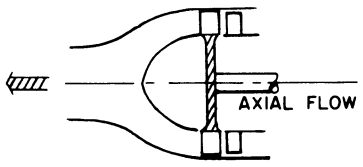

Figure 3H-44 - Axial Flow Type

The following sections treat the single stage inward radial and axial turbine types in some detail, with emphasis on machines in which the working fluid is compressible. The outward radial turbine has had a very limited history of application in aircraft and missile accessories, and no specific treatment of performance effects of this type are included in this section.

No attempt is made to treat the complex subject of detail turbine design. Rather, this section attempts to present treatment of the important factors affecting turbine performance of a known design.

5.4 Turbine Fundamentals

Various characteristics are discussed.

5.4.1 Torque-Momentum Relationship (Fig. 3H-45)

For a radial flow turbine, the derivation of the Euler equation relating torque to the change in fluid angular momentum is virtually identical to that of the radial flow compressor given in paragraph 4.4.2, and after appropriate changes in sign, the "ideal or Euler rotor head" becomes

$$H_e = \frac{u_2 c_{u2} - u_3 c_{u3}}{g} \tag{3H-58}$$

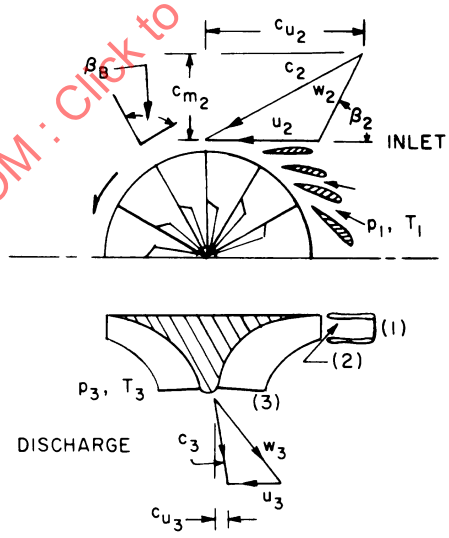

Figure 3H-45 - Torque-momentum Relationship

In an axial flow machine, the inlet and outlet radii are equal so that $u_2 = u_3$ and Eq. 3H-58 becomes

$$H_e = \frac{u(c_{u2} - c_{u3})}{g} \tag{3H-59}$$

These, as well as additional fundamental equations, are derived in Refs. 23 and 24. In a turbine, the actual applied head must be larger than the "ideal head" by the magnitude of the head losses in the machine.

Eqs. 3H-58 and 3H-59 apply regardless of fluid characteristics, that is, regardless of either compressible or incompressible flow, or of rotor form (axial, radial, or other type).

5.4.2 Flow and Efficiency

The characteristics of most turbine types may be expressed generally in terms of two functions: effective nozzle area, A, and turbine efficiency as a function of u/c_{th}, where:

u = Rotor tip blade speed, ft/sec

c_{th} = Theoretical nozzle spouting velocity for the gas at the given overall turbine pressure ratio and inlet temperature, ft/sec

$$= \sqrt{2gH_e}$$

$$= \left(2gJc_pT_{t1}\left[1 - \left(\frac{p_{s3}}{p_{t1}} \right)^{(\gamma-1)/\gamma} \right] \right)^{1/2}$$

$$= \left[2gJc_pT_{t1}\left(\frac{Y}{Y+1} \right) \right]^{1/2} \tag{3H-60}$$

for which

$$Y = \left[\left(\frac{p_{t1}}{p_{s3}} \right)^{(\gamma-1)/\gamma} - 1 \right] \tag{3H-61}$$

Eq. 3H-61 is the same definition as that given in paragraph 4.4.2.

The effective nozzle area A_n is a measure of the amount of fluid that passes through the turbine, since

$$w = \frac{A_n p_{t1}}{\sqrt{RT_{t1}}} Z' \tag{3H-62}$$

where

$$Z' = \sqrt{\frac{2g\gamma}{\gamma - 1}} \cdot \sqrt{\left(\frac{p_{s2}}{p_{t1}}\right)^{2/\gamma} - \left(\frac{p_{s2}}{p_{t1}}\right)^{(\gamma+1)/\gamma}}$$

Fig. 3H-46 characterizes the variation in Z′ with pressure ratio p_{t1}/p_{s2} and γ.

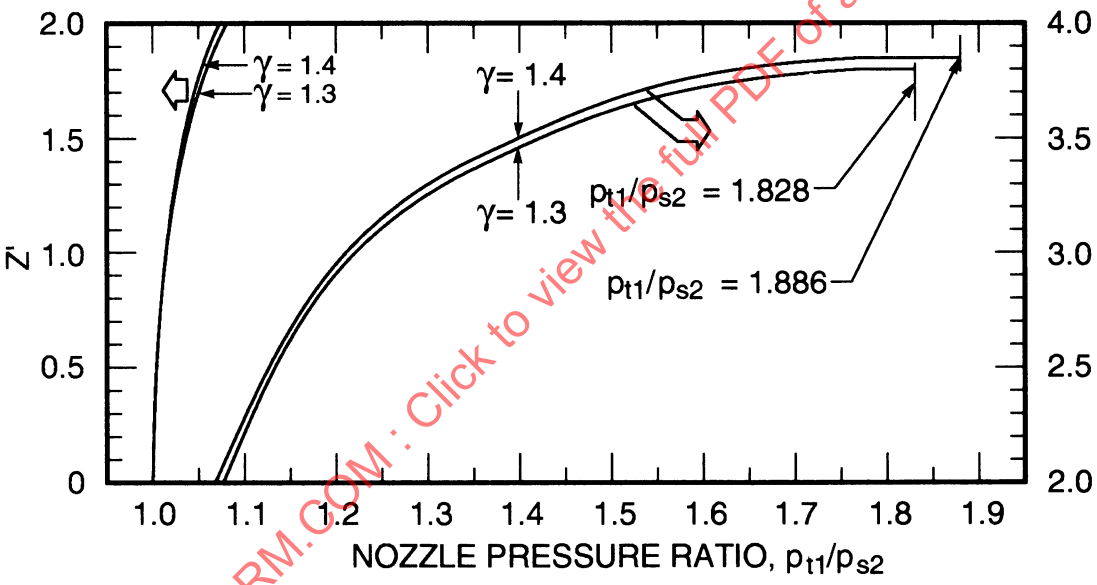

Figure 3H-46 - Z′ in Terms of Pressure Ratio for γ=1.3 and γ=1.4

Turbine horsepower may be expressed by

$$P_{hp} = \frac{wc_{th}^2 \eta_t}{550(2g)} = \frac{wJc_p \eta_t T_{t1}}{550}\left(\frac{Y}{Y+1}\right) \tag{3H-63}$$

5.4.3 Head Coefficient

The turbine head coefficient in terms of H_e is defined nondimensionally as

$$q_{th} = \frac{H_e}{u_2^2/g} \tag{3H-64}$$

Note that q_{th} for turbines corresponds directly to K′ for compressors, shown in paragraph 4.4.2. Large values of q_{th} permit low values of rotor speed for a given available head.

For single stage turbines, the optimum exit condition corresponds to a zero tangential component of velocity or zero "swirl," thus minimizing the residual energy remaining in the exhaust flow.

For minimum shock and separation losses at the rotor entrance, the relative fluid entry angle β_2 and the rotor blade entry angle β_B should be equal at design conditions. When this is the case, it can be shown (Ref. 24) by means of the inlet velocity triangles (see Fig. 3H-45) that

$$q_{th-op} = 1 + \frac{c_{m2}}{u_2} \cot \beta_B \tag{3H-65}$$

This relationship is plotted in Fig. 3H-47 for a range of values of β_B and c_{m2}/u_2. Note that at β_B = 90 deg, q_{th} = 1.0 for any value of c_{m2}/u_2.

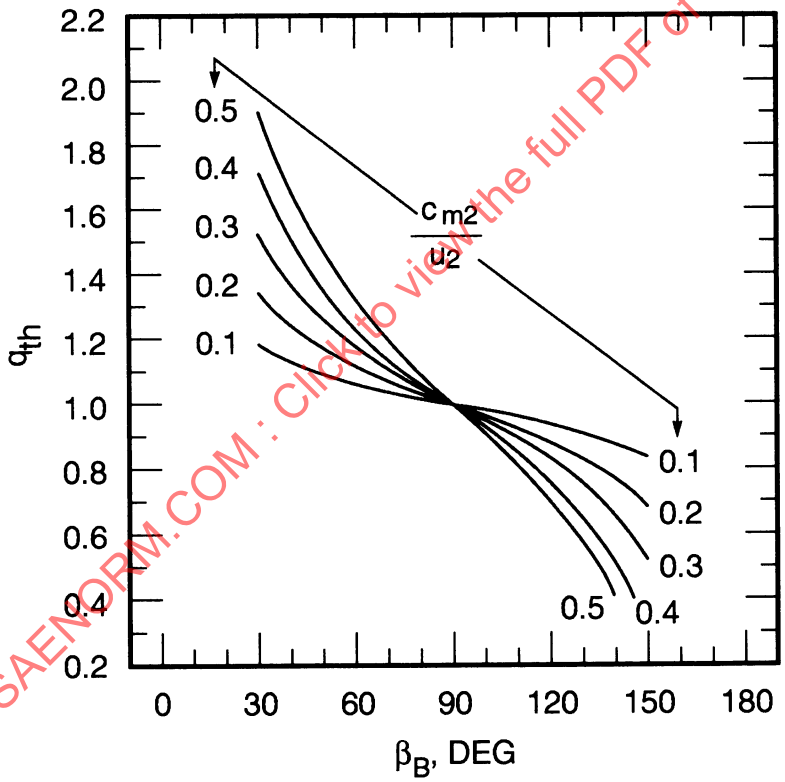

Figure 3H-47 - Turbine Head Coefficient in Terms of Blade Angle and Velocity Ratio

In most rotor designs, c_{m2}/u_2 varies between 0.2 and 0.5. The high end of the through-flow factor c_{m2}/u_2 range signifies the use of turbine designs incorporating discharge diffusers.

5.4.4 Relation Between Theoretical Head Coefficient Efficiency and Velocity Ratio

From the definitions of c_{th} (Par. 5.4.2) and q_{th} (Par. 5.4.3), the relationship between u_2/c_{th} and q_{th} can be found to be

$$\frac{u_2}{c_{th}} = \frac{1}{\sqrt{2q_{th}}} \tag{3H-66}$$

In high speed radial turbines, reasonable stress levels dictate the use of 90 deg blade angles, β_B, corresponding to an optimum value of $q_{th} = 1.0$. For this case, u_2/c_{th} becomes approximately 0.7. In axial turbines, the blade angle β_B has little effect on blade stresses and is, therefore, not dependent on this consideration. For the single stage impulse turbine, Ref. 24 derives the following expression for stage efficiency:

$$\eta_t = 2(1 + C_b)\left(\frac{u_2}{c_{th}}\right)\left(C_n \cos\beta_2 - \frac{u_2}{c_{th}}\right) \tag{3H-67}$$

where C_b = 0.97 for average conditions
C_n = 0.85 for average conditions
β_2 = Nozzle angle with respect to plane of rotation of buckets

The corresponding expression for q_{th} for the axial flow impulse turbine is

$$q_{th} = (1 + C_b)\left(\frac{C_n \cos\beta_2}{u_2/c_{th}} - 1\right) \tag{3H-68}$$

For maximum output and maximum efficiency, β_2 should be as small as practical.

Fig. 3H-48 is a plot of η_t for a range of values of u_2/c_{th} *for* β_2 = 12 deg, C_b = 0.85, and C_n = 0.97 for an axial flow impulse turbine. Also shown is a typical efficiency curve for a radial flow turbine with a 90 deg blade angle. Note that peak efficiency for the axial flow machine occurs at about u_2/c_{th} = 0.47 and for the radial flow turbine at about u_2/c_{th} = 0.7. The corresponding values of q_{th} are 1.87 for the axial flow and 1.0 for the radial flow machine.

With proper choice of blade angle, when stress considerations permit, it is possible to obtain peak efficiencies at values of u_2/c_{th} ranging from 0.5 to 1.0.

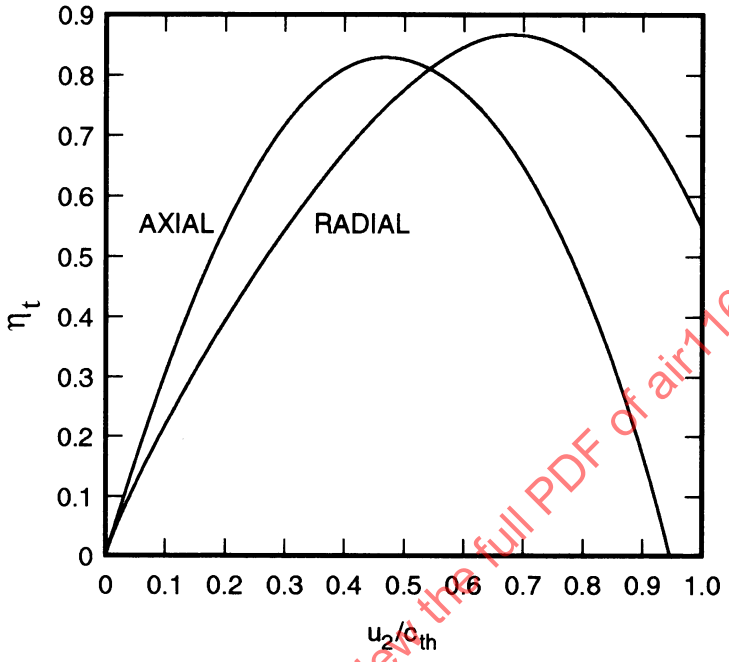

Figure 3H-48 - Efficiency of Axial and Radial Flow Impulse Turbines

5.4.5 Degree of Reaction

In a pure impulse turbine, all pressure energy is converted to kinetic energy in the nozzle. In a pure reaction turbine, this occurs entirely in the rotor. In most practical machines this conversion is divided to a varying degree between nozzles and rotor.

The degree of reaction of a turbine is determined by the ratio of the head (H_{ad}) expended in the rotor to the overall head across the turbine. The degree of reaction R′ varies with the head coefficient q_{th}, as shown in Fig. 3H-49.

5.4.6 Turbine Nozzle Restriction Factor

As mentioned in paragraph 5.4.2, the turbine nozzle restriction factor Z′ is dependent on nozzle pressure ratio, and therefore on the degree of reaction R′ shown in Fig. 3H-49.

Given the turbine operating conditions and selecting the wheel geometry that yields q_{th-op}, the required turbine nozzle area to pass a given flow may be approximated using the relationship in paragraph 5.4.2 and Fig. 3H-49.

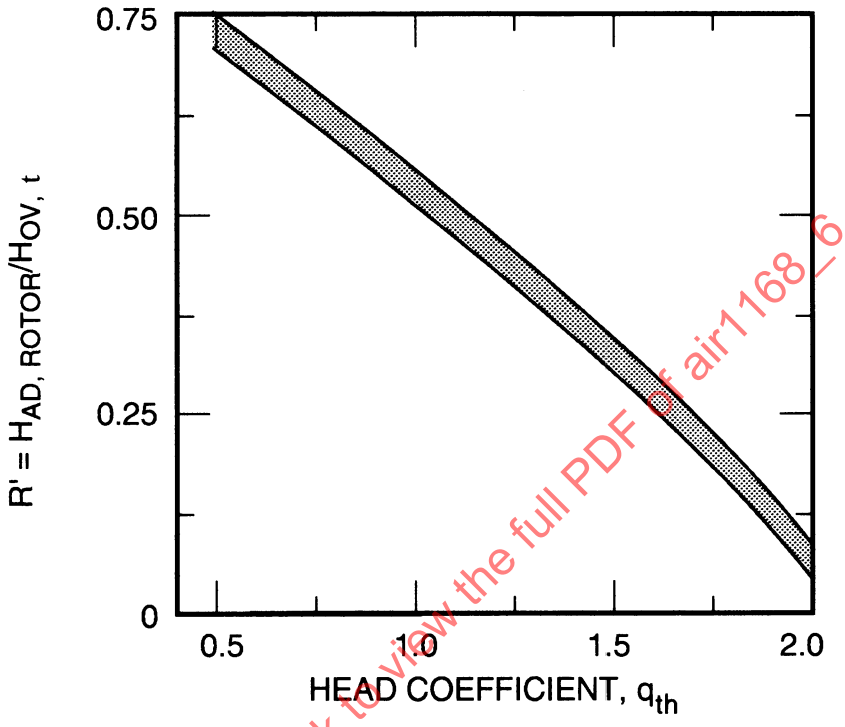

Figure 3H-49 - Degree of Reaction as a Function of Head Coefficient

5.5 Performance Effects

5.5.1 Specific Speed

Specific speed is a turbine evaluation and design parameter showing the influence of rotor geometry. Although an outgrowth of hydraulic turbomachinery (pumps), it is extremely useful as applied to compressible fluid turbines. Specific speed may be defined in two forms:

$$N_s = \frac{n\sqrt{Q_3/60}}{H_{ad}^{3/4}} \qquad (3H\text{-}69)$$

or $$N_s' = \frac{n\sqrt{P_{hp}/\lambda}}{H_{ad}^{5/4}} \quad \text{(3H-70)}$$

where $$H_{ad} = Jc_pT_1\left(\frac{Y}{Y+1}\right)$$

The radial turbine cross sections shown in Fig. 3H-50 depict the specific speed categories.

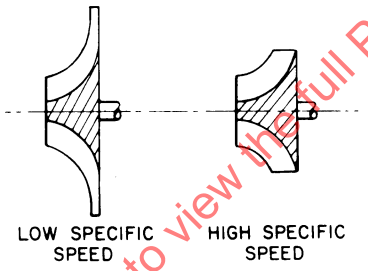

Figure 3H-50 - Radial Turbine Cross Sections

Fig. 3H-51 correlates N_s with η_t , turbine efficiency, based on a series of modern turbines of different designs. Referring to the figure, the points indicate the following:

(1) 3.5 in. Francis turbine, $r = 9{:}1$

(2) 5.0 in. axial turbine, $r = 6{:}1$

(3) 120 in. Francis water turbine

(4) 9.0 in. Francis gas turbine, $r = 3.4{:}1$

(5) 14.0 in. axial air turbine, NACA

(6) Axial gas turbine (small jet engine)

(7) Typical Kaplan water turbine

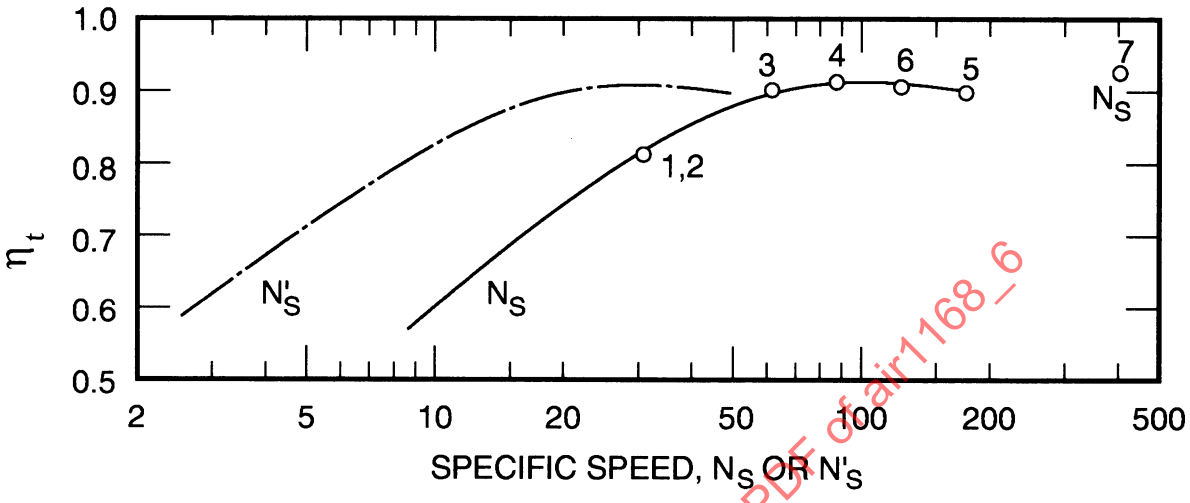

Figure 3H-51 - Turbine Efficiency Versus Specific Speed

The predominant effects of low specific speed, indicative of low through-flow, which degrades peak turbine performance, are high disc friction and leakage losses compared to useful output. At extremely high specific speed (high through-flow) exit kinetic energy loss is high compared to useful output. A typical variation in peak efficiency with specific speed demonstrating this trend is shown in Fig. 3H-52 for a 90 deg radial turbine.

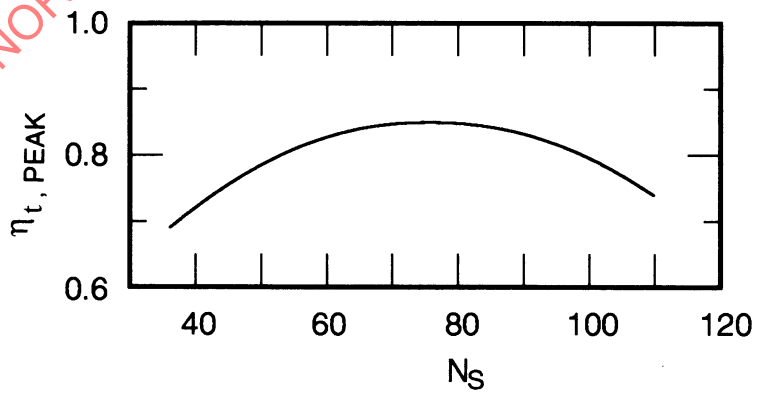

Figure 3H-52 - Peak Turbine Efficiency Versus Specific Speed

5.5.2 Reynolds Number and Absolute Size Effects

It has been shown that the absolute size of the rotor affects the peak efficiency of the turbine as depicted generally in Fig. 3H-53. This effect occurs partly because of the pure Reynolds number effect (that is, the momentum and viscosity influences), and partly because of quality control and manufacturing limitations. Factors such as clearances, surface roughness, and contour accuracy are all increasingly difficult to control in smaller machines at reasonable manufacturing cost, and as such become sources of the degradation in efficiency with decreasing absolute size.

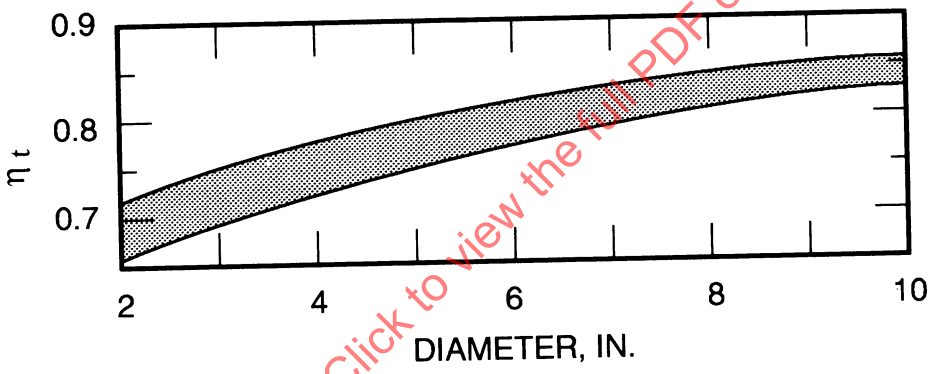

Figure 3H-53 - Effect of Reynolds Number (dia) on Turbine Efficiency

The Reynolds number[1] influence is established empirically for a specific design and can be utilized as a single function in evaluating machines that are geometrically similar. It has also been established that each class or design has a critical value of N_{Re} above which little, if any, influence on performance exists. At values of N_{Re} less than critical, the degradation in performance due to this effect is significant. Critical values of N_{Re} in modern turbines are in the range of 2×10^6 to 4×10^6.

[1]Defined for use in turbomachinery as $N_{Re} = g\rho Du_2/\mu$

5.5.3 Compressibility Effects

Most modern turbines designed for high efficiency have blade passages that accelerate the flow relative to the rotor, minimizing the noticeable compressibility effects. A limitation is the point at which the exhaust absolute velocity approaches sonic velocity. See Fig. 3H-53.

5.6 General Comparison of Axial and Radial Turbine Types

There appears to be no overwhelming justification for a consistent preference of one type over the other for the range of aircraft turbine applications, since, for comparable design conditions:

(1) Both types require approximately the same rotational speed for a given horsepower output.

(2) The axial turbine will be slightly smaller in diameter, implying lower disc stress levels than in the radial rotor, but the radial turbine rotor is commonly a better structural shape.

(3) The radial turbine is somewhat superior in potential peak performance at low specific speeds and, conversely, the axial rotor appears better at high values of specific speed.

(4) The radial rotor is generally cheaper to manufacture, being less sensitive to contour and surface finish than the axial counterpart.

5.7 Partial Admission

Often, in the case of aircraft and missile turbines, the application of a turbine at high pressure ratios or a desired low rotational speed or both, results in a large diameter rotor with low through-flow. In this situation, it is often impossible to design a producible configuration having a nozzle ring that introduces flow to the entire periphery of the wheel.

In this case, it is possible to utilize a "partial admission" nozzle where flow is admitted through a nozzle that occupies a portion of the periphery. This "partial admission" effect has a depreciating effect on attainable peak performance. This is shown approximtely by Fig. 3H-54 for both radial and axial rotor configurations.

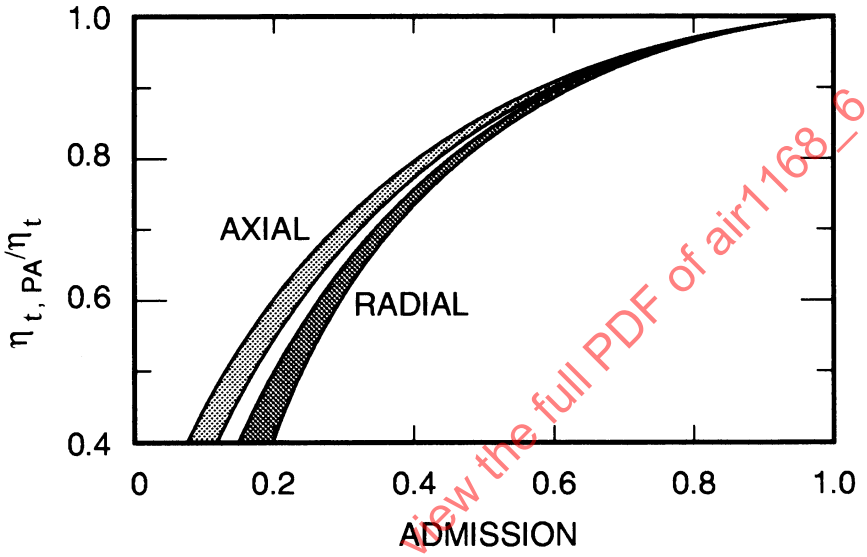

Figure 3H-54 - Effect of Partial Admission on Turbine Efficiency

5.8 Variable Nozzle

A convenient means of varying the through-flow capacity and power output of a given turbine in many accessory applications is to mechanically vary the nozzle throat area. This technique, while theoretically adaptable with either the axial or radial type rotors, is used commonly with the radial wheel because of greater mechanical feasibility.

Fig. 3H-55 illustrates the most common mechanical arrangement employed for varying the radial turbine nozzle area. The nozzle vanes are pivoted and moved in unison by an external control device and actuator, typically a turbine speed control or flow control.

The variable nozzle mode of control is by far a more efficient means of accommodating variable load as compared with the alternative means, such as an upstream throttle and fixed nozzle area turbine, where the energy saving warrants the complexity. Fig. 3H-56 shows the off-design characteristics of a typical 90 deg radial turbine with a variable nozzle at constant tip speed as compared to a throttle control.

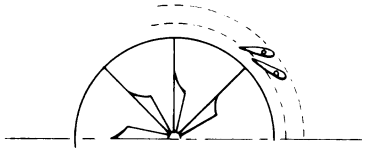

Figure 3H-55 - Radial Turbine Nozzle Area

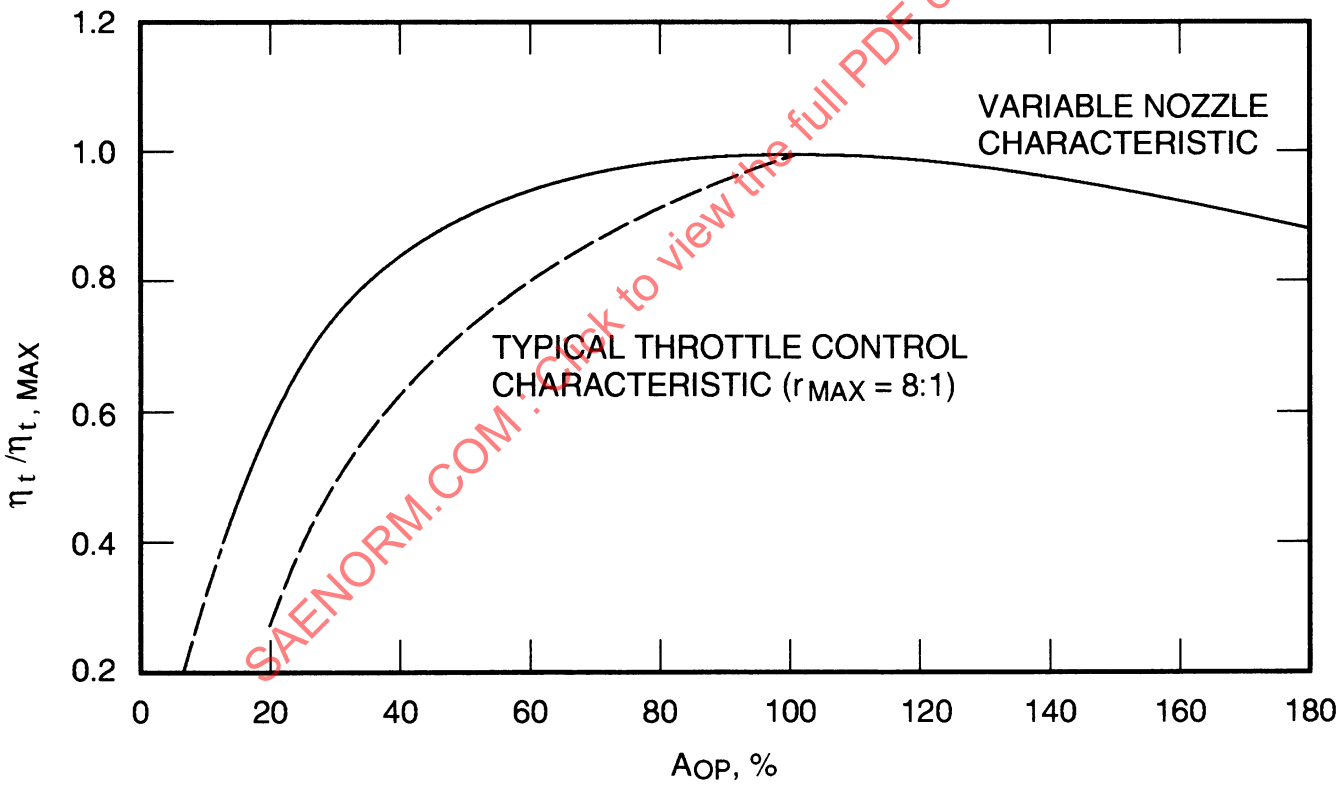

Figure 3H-56 - Effect of Variable Nozzle Control, r = turbine pressure ratio

5.9 Multistaging

Referring to the specific speed criteria described in Par. 5.5.1, another means of designing efficiently for an application that would be a low specific speed application for a single stage machine is the technique of multistaging. As can be seen by inspecting the specific speed parameter (Eq. 3H-69), the H_{ad} per stage is reduced, and speed and volume flow can be adjusted to allow each of the stages to operate at higher specific speed, thus resulting in an improvement in potential design peak efficiency.

Reference to rotor sketches in previous paragraphs will show that the axial configuration is mechanically easier to produce in multistage design than the radial configuration.

5.9.1 Multiple Reentry Type

A unique form of multistage turbine developed by NASA (Ref. 25), in which the multiple stages are arranged on a single rotor, is shown on Fig. 3H-57a. This type is particularly adaptable to very low specific speed applications such as missile auxiliary power units, which use very high pressure hot gas as a driving fluid.

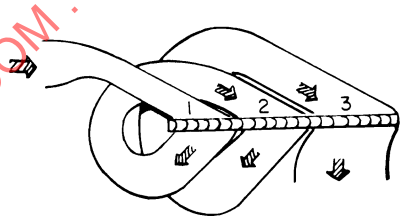

Figure 3H-57a - Developed View of Rotor Periphery

5.10 Generalized Turbine Performance Maps

The turbine performance presentation as desired from the user's point of view should have parameters that are most familiar and useful to him. These are power output, P_{hp}, weight flow rate, w, turbine rotational speed, n, nozzle inlet temperature, T_{t1}, nozzle inlet total pressure, p_{t1}, exhaust static pressure, p_{s3}, and turbine efficiency, η_t.

Using Eqs. 3H-60 and 3H-63, the power output may be expressed as follows:

$$P_{hp} = \frac{wJc_pT_{t1}\eta_t}{550}\left[1-\left(\frac{p_{s3}}{p_{t1}}\right)^{(\gamma-1)/\gamma}\right] \tag{3H-71}$$

Dividing by p_{s3} and $\sqrt{T_{t1}}$,

$$\frac{P_{hp}}{p_{s3}\sqrt{T_{t1}}} = \frac{wn}{p_{s3}}\frac{\sqrt{T_{t1}}}{n}\frac{Jc_p\eta_t}{550}\left[1-\left(\frac{p_{s3}}{p_{t1}}\right)^{(\gamma-1)/\gamma}\right] \tag{3H-72}$$

The desirable parameters from the users' standpoint are:

Horsepower function = $P_{hp}/(p_{s3}\sqrt{T_{t1}})$, dimensionless

Flow rate function = wn/p_{s3}, dimensionless

Speed parameter = $n/\sqrt{T_{t1}}$, dimensionless

Pressure ratio = p_{t1}/p_{s3}, dimensionless

Turbine efficiency = η_t, dimensionless

All five parameters can be plotted on one performance map, as shown in Fig. 3H-57b.

5.10.1 Variable Nozzle Area

A different performance map is needed to represent each nozzle area under consideration, as shown in Figs. 3H-57c and 3H-57d.

5.11 References

Elaboration of the material on turbines presented above can be found in Refs. 23-28.

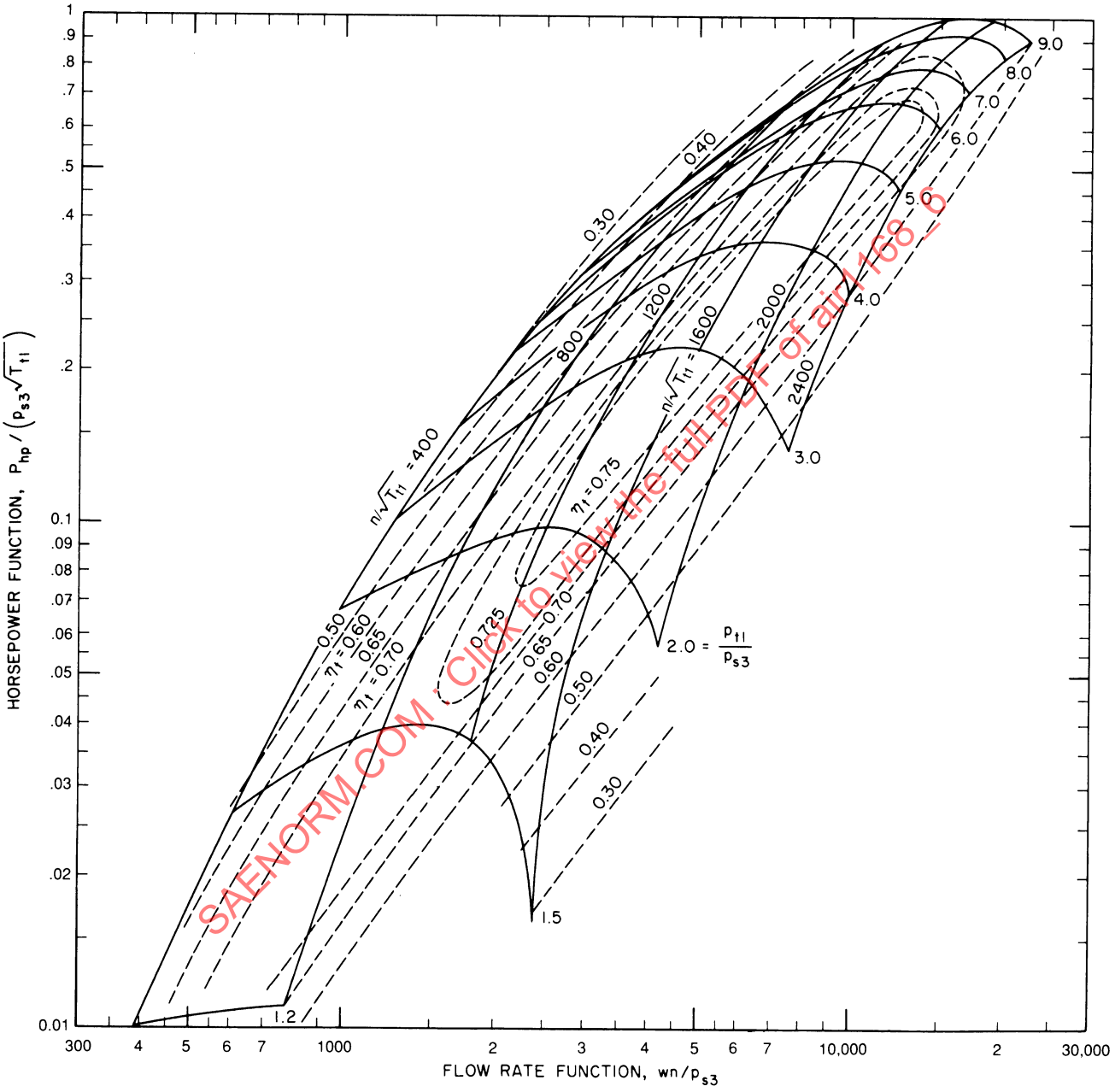

Figure 3H-57b - Fixed Nozzle Turbine Performance Chart

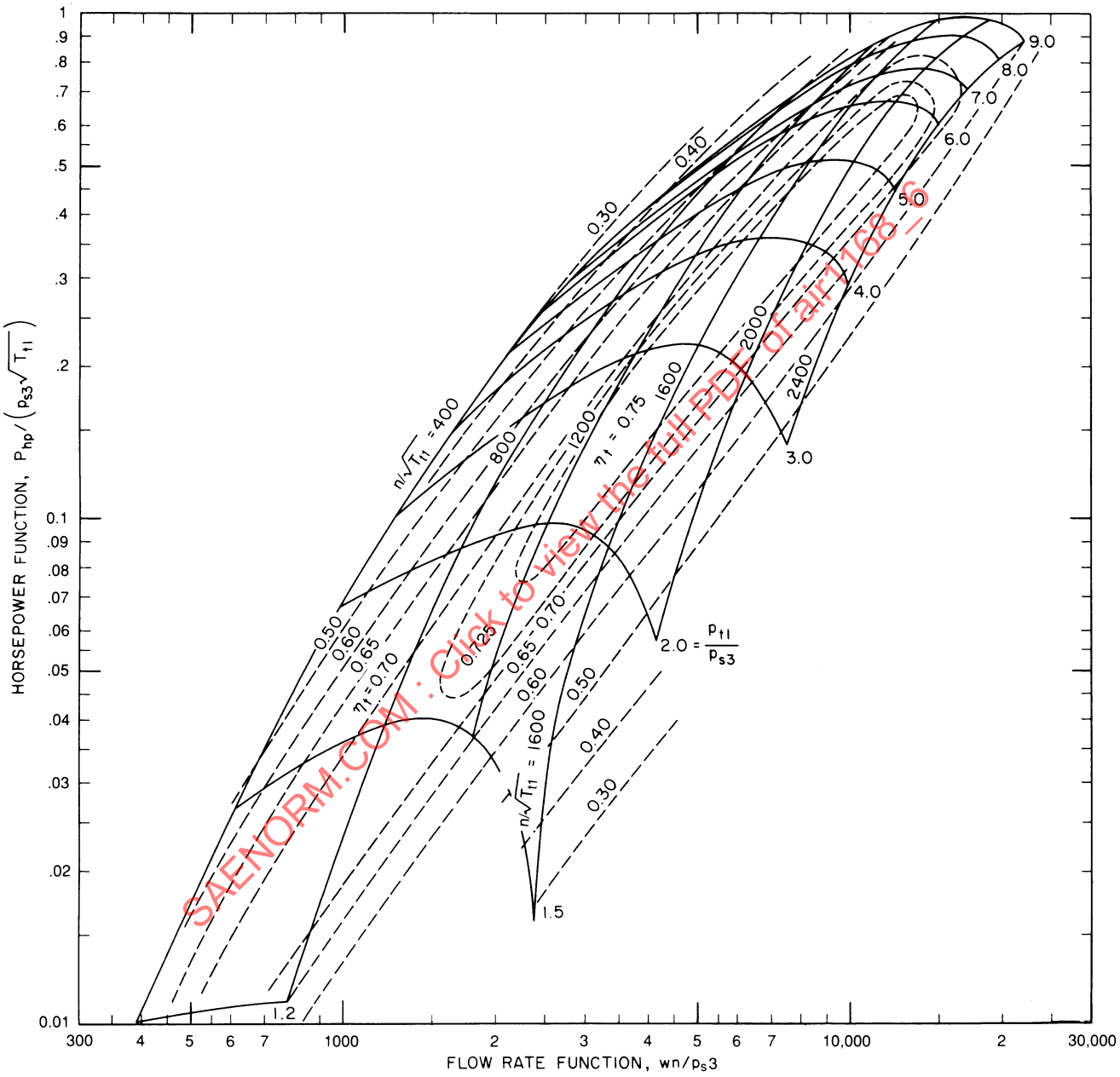

Figure 3H-57c - Variable Area Nozzle Turbine Performance Chart; A_n = 100% Maximum Nozzle Area

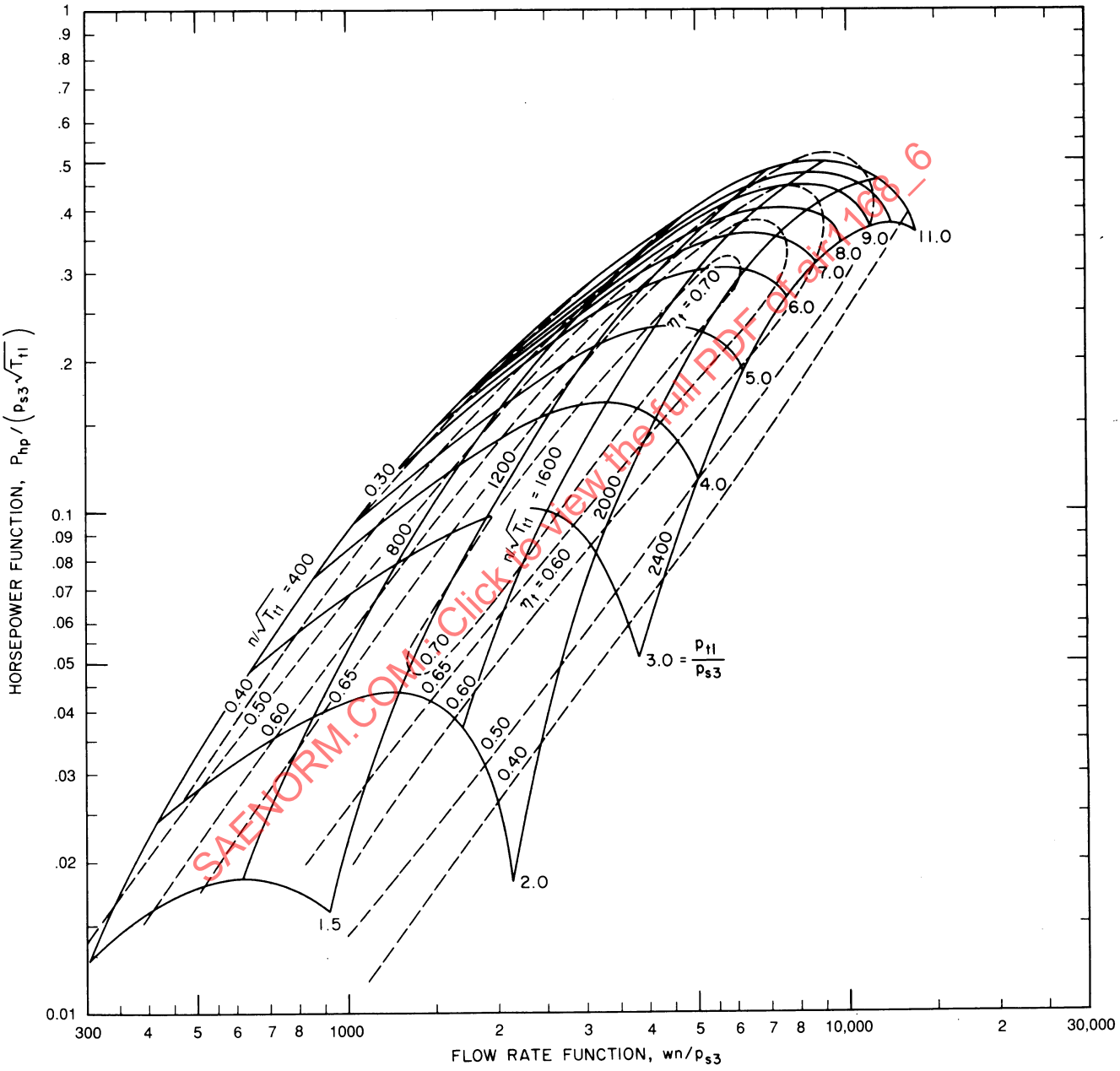

Figure 3H-57d - Variable Area Nozzle Turbine Performance Chart;
A_n = 50% Maximum Nozzle Area

6. JET PUMPS

6.1 Nomenclature

A = Area, ft^2, $in.^2$
C = Function of geometry, dimensionless
D = Diameter, ft
f = Friction factor (0.003 average value for most jet pump designs with air), dimensionless
F_{fr} = Wall friction shear force, lb
h = Enthalpy, Btu/lb
K_m = Momentum correction factor, dimensionless
K_p = Static pressure correction factor, dimensionless
L = Mixing length, ft
L/D = Length - to - diameter ratio, dimensionless
P = Pressure, lb/ft^2, $lb/in.^2$
ΔP = Pressure loss, lb/ft^2
S = Wall surface area, ft^2
v = Fluid velocity, ft/sec
w = Weight flow rate, lb/sec, lb/min, lb/hr
α = Area ratio, dimensionless
ϕ = Function of [ ]
η_d = Diffuser efficiency, dimensionless
η_e = Jet pump efficiency, dimensionless

Subscripts

d = Diffuser exit
E,e = Energy
m = Mixed stream
0,1,2,3 = Stations at various positions in the jet pump, Fig. 3H-60

Superscripts

$*$ = Nondimensional parameter
$'$ = Primary stream
$''$ = Secondary stream

6.2 General Considerations

The jet pump (ejector), because of its low weight and mechanical simplicity, finds many uses in fluid systems. Where the efficiency of energy utilization in a pumping application may be justifiably compromised in favor of low weight and simplicity, the jet pump should be given serious consideration. In general, these applications apply where high fluid flow must be induced at relatively low head output and where a supply of high pressure fluid, usable as a driving means, exists.

This section limits the scope of treatment to jet pumps in which both the driving and driven streams are of the same fluid state.

6.3 Jet Pump Theory

The jet pump is a device that allows the exchange of the momentum and energy of a high energy fluid stream to a low energy fluid stream. The exchange is created by expanding the high energy stream through a nozzle so that the resultant jet is exposed to the low energy stream and a shear plane is set up between the two.

Through the mechanics of viscous shear and fluid diffusion, the momentum and kinetic energy of the high velocity jet is partially transferred to the low energy (driven) stream. If mixing of the two streams is completed, there will be a single stream with homogeneous energy and velocity distribution at the end of the mixing. In the ideal case, no heat transfer exists across the mixing section walls and no energy is lost through pressure loss at the mixing section wall. The mixing process must behave in the following manner:

(1) Mass is conserved:

$$w' + w'' = w_m \tag{3H-73}$$

(2) Total momentum is conserved:

$$\left(P'A' + \frac{w'}{g}v'\right) + \left(P''A'' + \frac{w''}{g}v''\right) = \left(P_m A_m + \frac{w_m}{g}v_m\right) \tag{3H-74}$$

(3) Energy is conserved:

$$w' c_p' T_t' + w'' c_p'' T_t'' = w_m c_{pm} T_{tm} \tag{3H-75}$$

Jet pump performance prediction then becomes the specific solution of the mixing process, applying the physical laws stated above together with the specific character of the mixing process and the properties of the fluids involved.

The ideal performance result must be adjusted to account for the deviations from the ideal process which are encountered in a real pump:

(1) Fluid wall friction.

(2) Heat transfer.

(3) Turbulence.

(4) Imperfect mixing.

(5) Nonuniform velocity at the exit.

Most jet pump applications in existence have been designed uniquely by specifying the fourth boundary condition, that is, the detailed mixing process involved, which allows a unique analytical solution to the design.

6.4 Jet Pump Types

The two types of specific mixing processes generally considered in jet pump design are described below.

6.4.1 Constant Area Mixing

Where the mixing process is completed in a constant area duct or pipe, a portion of the pressure rise obtained in the secondary stream will occur in the mixing section and a part in the diffuser, if a diffuser is used. See Fig. 3H-58.

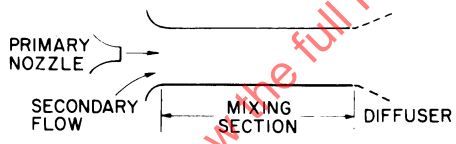

Figure 3H-58 - Constant Area Mixing

6.4.2 Constant Pressure Mixing

This is the case in which the mixing process is completed at constant static pressure by proper contour of the mixing section wall. In this case, all the pressure rise obtained in the driven stream occurs in the diffuser downstream of mixing. See Fig. 3H-59.

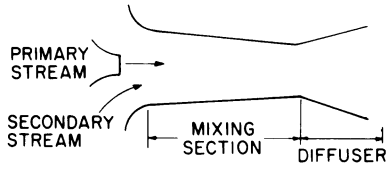

Figure 3H-59 - Constant Pressure Mixing

6.5 Jet Pump Performance

This section presents the performance criteria and the general method of data presentation together with representative test results for jet pumps, utilizing both compressible and incompressible fluids. This presentation and the sizing information presented in Refs. 29-32 will be restricted to the constant area mixing type, since this type has the greatest engineering utility.

Most investigators have determined that convergent or divergent mixing section configurations, including the constant pressure case, do not lead to higher theoretical or experimental performance than the constant area case except when the high Mach number case of the secondary or driven stream is greater than Mach 0.25.

The performance criteria given here are applicable to jet pumps of relatively low pressure rise, using subsonic primary pressure ratios. Dynamic pressures are assumed to be small relative to the absolute static pressures. All pressures and temperatures in the equations are taken to be static or stream values.

6.5.1 Analytical Criteria

The physical laws completely describing the mixing process and the resultant characteristic of the mixed fluid are the following (the nomenclature refers to Fig. 3H-60):

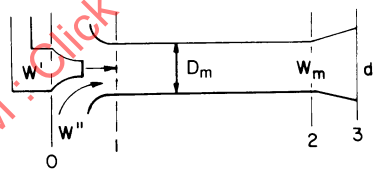

Figure 3H-60 - Constant Area Mixing

Conservation of mass:

$$w' + w'' = w_m \tag{3H-76}$$

Conservation of momentum:

$$\frac{w'}{g} v' + \frac{w''}{g} v'' + P_1 A_1 = K_m \frac{w_m v_m}{g} + K_p P_2 A_2 + F_{fr} \tag{3H-77}$$

Conservation of energy:

$$w'h' + w''h'' = w_m h_m \tag{3H-78}$$

6.5.2 Static Pressure, Momentum Correction Factors, and Fluid Friction (Ref. 29)

The terms K_p, K_m, and F_{fr} in Eq. 3H-77 are correction factors accounting for the following phenomena in the mixing process:

(1) Nonuniform flow accelerations and decelerations result in a nonuniform static pressure distribution across the mixing streams at sections 1 and 2. This static pressure gradient is accounted for by the nondimensional pressure correction factor K_p, relating actual mean stream static pressure to wall static pressure at section 2. K_p as a function of jet pump geometry is given in Fig. 3H-61.

(2) Incomplete mixing of the primary and secondary streams at section 2 together with wall friction results in nonuniform velocity distribution; this is accounted for by the momentum correction factor K_m, which relates the actual momentum rate at section 2 to the bulk average momentum rate based on average velocity and density at section 2.

(3) Wall friction between sections 1 and 2 is evaluated by utilizing the conventional friction factor based on average velocity v_m and the wetted wall area of the mixing tube, S_m ($=\pi D_m L_m$).

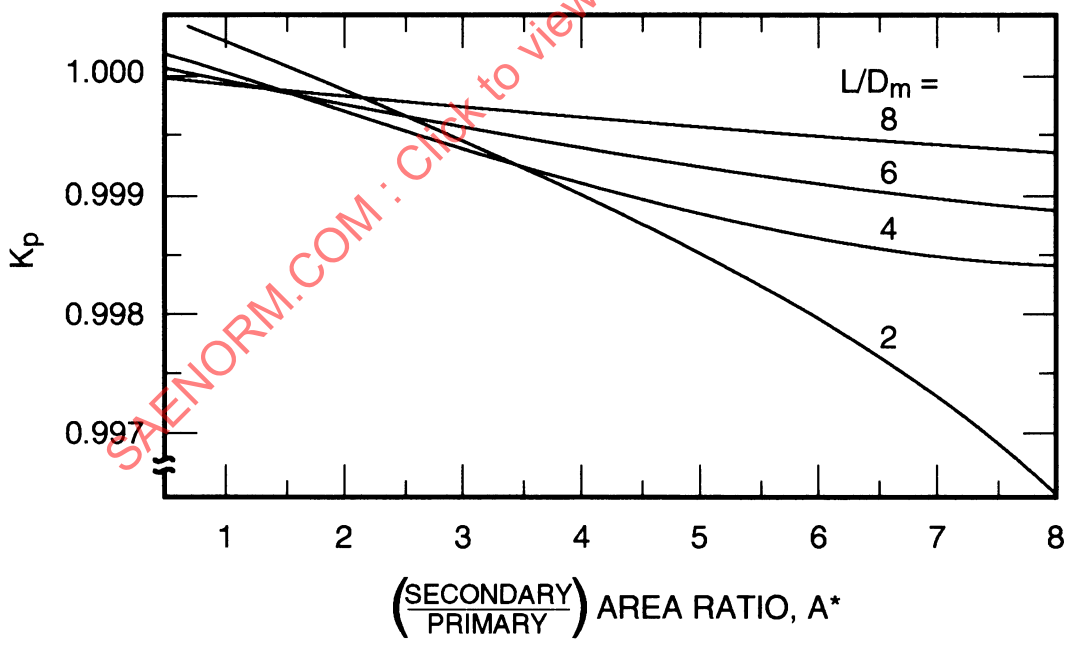

Figure 3H-61 - Variation of K_p with L/D_m and A^*

6.5.3 Analytical Solution for Jet Pump Performance

The combination of the physical laws described in paragraph 6.5.1 yields the following expressions for jet pump performance:

(1) Constant area mixing without diffuser:

$$(P_2 - P_0'') = \frac{1}{gA_m}\left[\frac{(w')^2}{A'\rho'g} + \frac{(w'')^2}{A''\rho''g}\left(1 - \frac{1}{2}\frac{A_m}{A''}\right) - \frac{w_m^2}{A_m\rho_m g}\left(K_m + \frac{f}{2}\frac{S_m}{A_m}\right)\right] + P_2(1 - K_p) \quad \text{(3H-79)}$$

(2) Constant area mixing with diffuser:

$$(P_3 - P_0'') = \frac{1}{gA_m}\left[\frac{(w')^2}{A'\rho'g} + \frac{(w'')^2}{A''\rho''g}\left(1 - \frac{1}{2}\frac{A_m}{A''}\right) - \frac{w_m^2}{A_m\rho_m g}\left(K_m + \frac{f}{2}\frac{S_m}{A_m} - \frac{\eta_d}{2}\left(1 - \frac{A_m^2}{A_d^2}\right)\right)\right] + P_2(1 - K_p) \quad \text{(3H-80)}$$

6.5.4 Nondimensional Parameters

The application of nondimensional parameters to the jet pump design equation greatly increases its utility in design calculations. The following parameters may be utilized as described in Ref. 29:

$$\Delta P^* = \frac{(P_2 - P_0'')/\rho''g}{(v')^2/2g} \quad \text{(3H-81)}$$

$$w^* = \frac{w''}{w'} = \text{Flow rate ratio} \quad \text{(3H-82)}$$

$$T^* = \frac{T''}{T'} \quad \frac{\text{Ratio of secondary to}}{\text{primary abs. temp}} \quad \text{(3H-83)}$$

$$A^* = \frac{A''}{A'} \quad \frac{\text{Ratio of secondary to}}{\text{primary area}} \quad \text{(3H-84)}$$

$$K_p^* = \frac{P_2(1 - K_p)}{(v')^2/2g} \quad \text{(3H-85)}$$

Utilizing the preceding parameters with fixed jet pump geometry, the performance equation of paragraph 6.5.3, Eq. 3H-80, reduces to

$$\frac{\Delta P^*}{T^*} = C_1 - C_2(W^*)^2 T^* - C_3 w^*(T^* + 1) + \frac{K_p^*}{T^*} \tag{3H-86}$$

where C_1, C_2, and C_3 involve geometry and K_m, f, and η_d.

6.5.4.1 Nondimensional Design Equations

Equation 3H-86 is further simplified by introducing the combination term $w^*(T^*)_{0.40}$, approximately valid for values of $T^* \geq 0.3$ (Ref. 29). Then

$$\frac{\Delta P^*}{T^*} = C_1 - C_2[w^*(T^*)^{0.4}]^2 - 2C_3[w^*(T^*)^{0.4}] + \frac{K_p^*}{T^*} \tag{3H-87}$$

where $C_1 = \left(2\frac{A'}{A_m}\right)\left(1 - \frac{A'}{A_m}\beta\right)$

$$C_2 = \left(\frac{A'}{A_m}\right)\left[\frac{A'}{A_m}\beta - \frac{1}{A^*}\left(1 - \frac{A_m}{A'2A^*}\right)\right]$$

$$2C_3 = 4\left(\frac{A'}{A_m}\right)^2\beta$$

for which $\beta = \left[K_m + \frac{f}{2}\left(\frac{S_m}{A_m}\right) - \frac{\eta_d}{2}\left(1 - \frac{A_m^2}{A_d^2}\right)\right]$

6.5.4.2 Momentum Correction Factor Correlation

Experimental results have shown that the momentum correction factor K_m may be correlated as follows:

$$K_m = \phi[w^*(T^*)^{0.5}, (L/D_m), A^*] \tag{3H-88}$$

Further, it is shown that K_m varies significantly with $w^*(T^*)^{0.5}$ only for $(L/D_m) < 4.0$, and depends on geometry alone for $(L/D_m) \geq 4.0 K_m$.

Figs. 3H-62 through 3H-65 depict the variation of K_m with the factors given above.

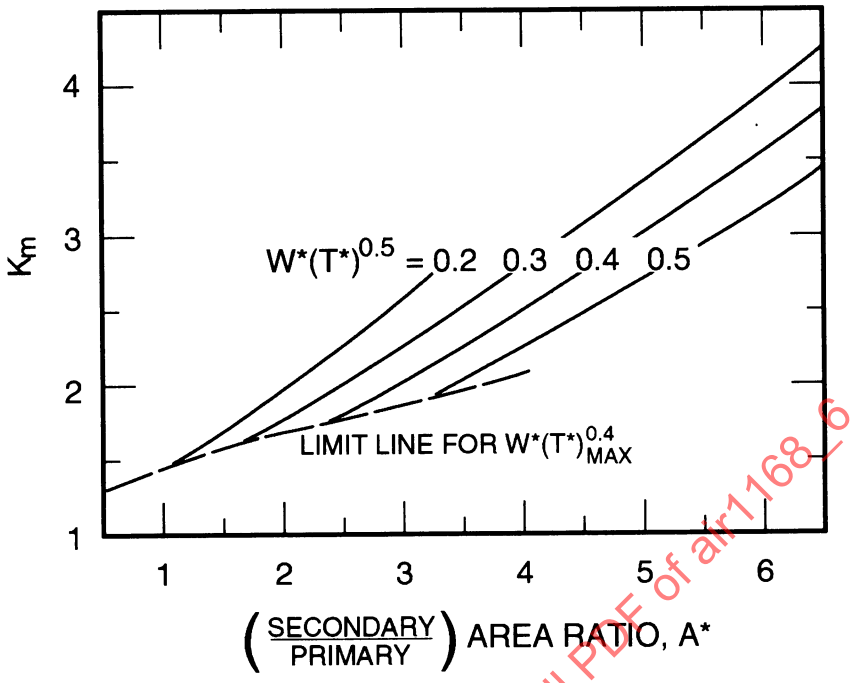

Figure 3H-62 - Variation of K_m with A^* and $(w^*)(T^*)^{0.5}$, $L/D_m = 1.0$

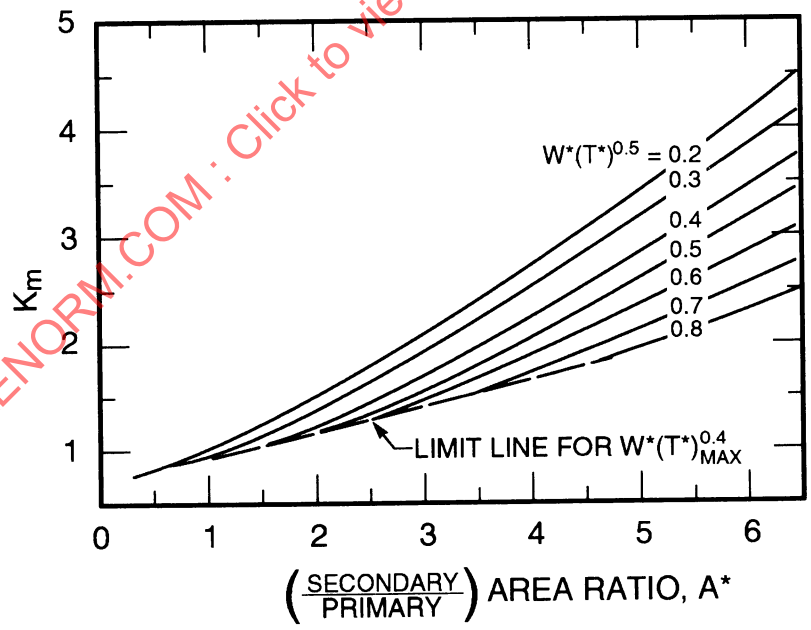

Figure 3H-63 - Variation of K_m with A^* and $(w^*)(T^*)^{0.5}$, $L/D_m = 2.0$

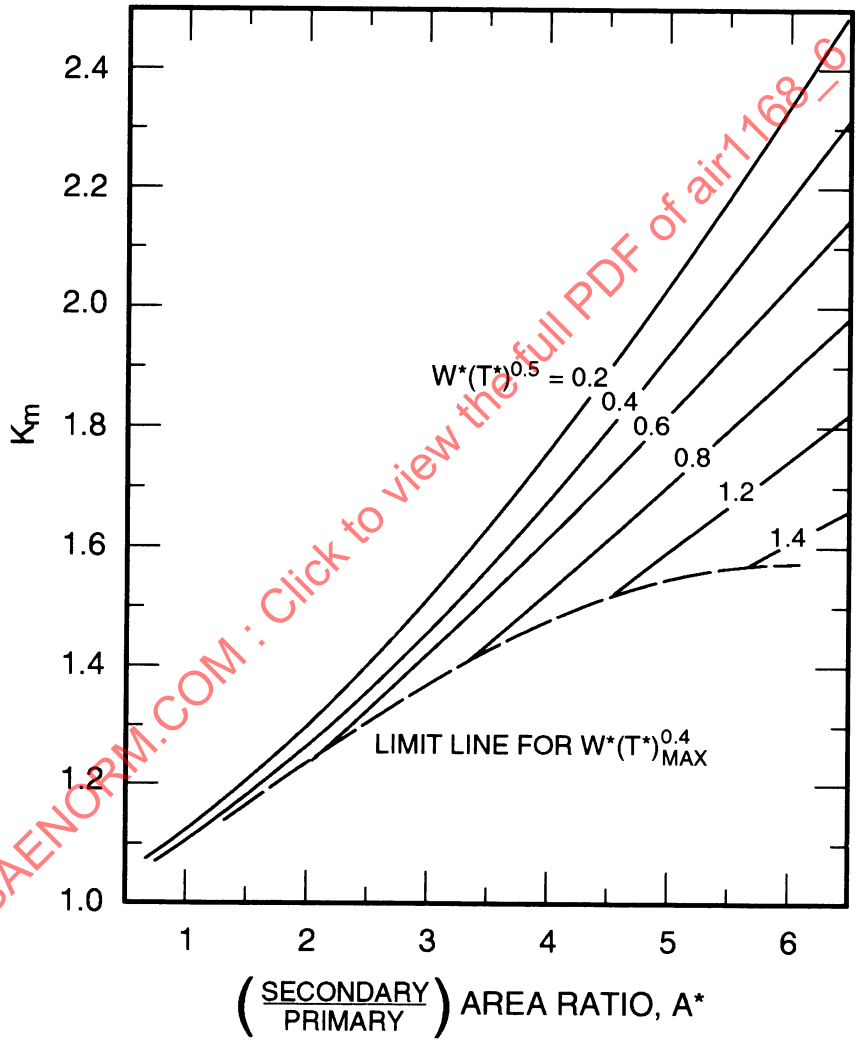

Figure 3H-64 - Variation of K_m with A^* and $(w^*)(T^*)_{0.5}, L/D_m = 3.0$

6.5.5 Jet Pump Efficiency

The significant expression defining the efficiency of conversion of primary stream kinetic energy to secondary stream flow work is

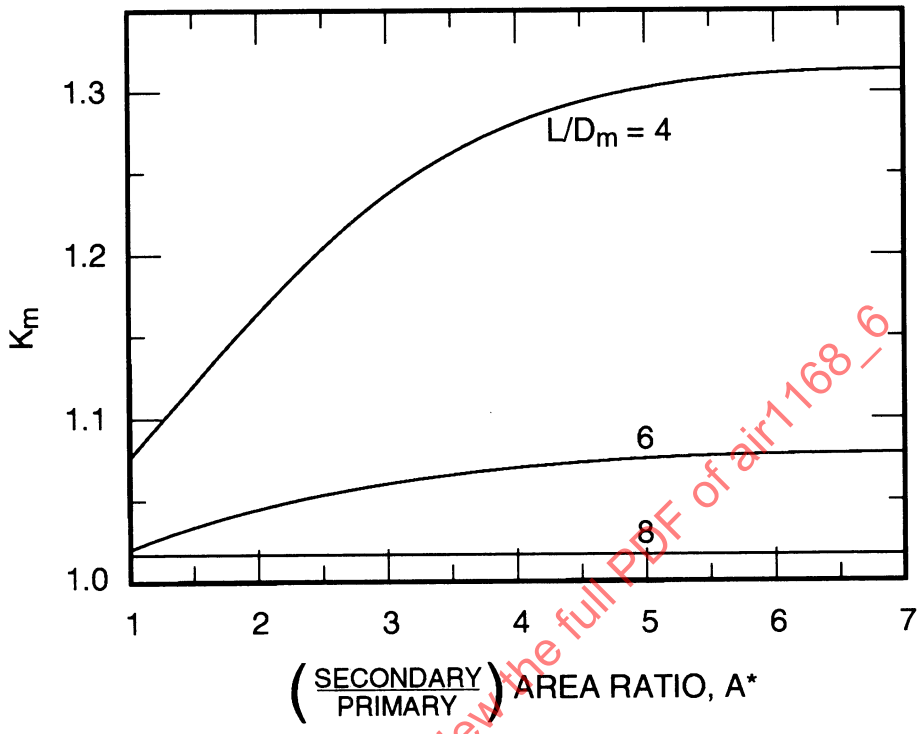

Figure 3H-65 - Variation of K_m with A^* and L/D_m (K_m to large values of L/D_m)

$$\eta_e = \frac{[w''(P_2 - P_o'')]/g\rho''}{[w'(v')^2]/2g}$$

$$= w^*(T^*)^{0.4}\left(\frac{\Delta P^*}{T^*}\right)(T^*)^{0.6} \qquad (3H\text{-}89)$$

From Ref. 30 an approximate expression for maximum jet pump efficiency in terms of the non-dimensional parameters previously discussed is

$$\eta_{e,\,max} = \frac{1}{4}[w^*(T^*)^{0.40}]_{max} \cdot \left[C_1 + \frac{K_p^*}{T^*}\right](T^*)^{0.6} \qquad (3H\text{-}90)$$

Fig. 3H-66 depicts the variation of $\eta_{e,max}/(T^*)^{0.6}$ versus the jet pump geometry, A^* and L/D_m. Fig. 3H-67 presents the parameter $[(w^*)(T^*)^{0.40}]_{max}$ as a function of A^* and L/D_m for use with Eq. 3H-90.

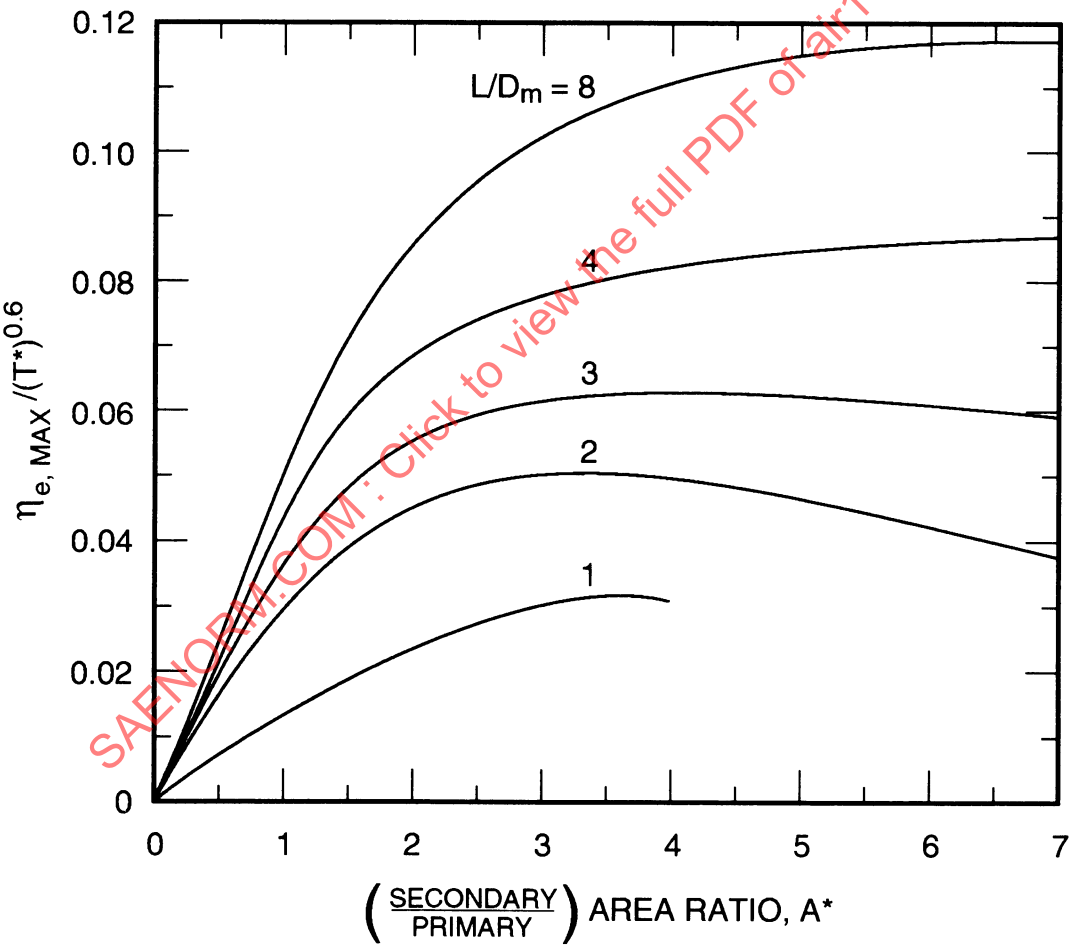

Figure 3H-66 - Variation of Efficiency in Terms of L/D_m and A^*

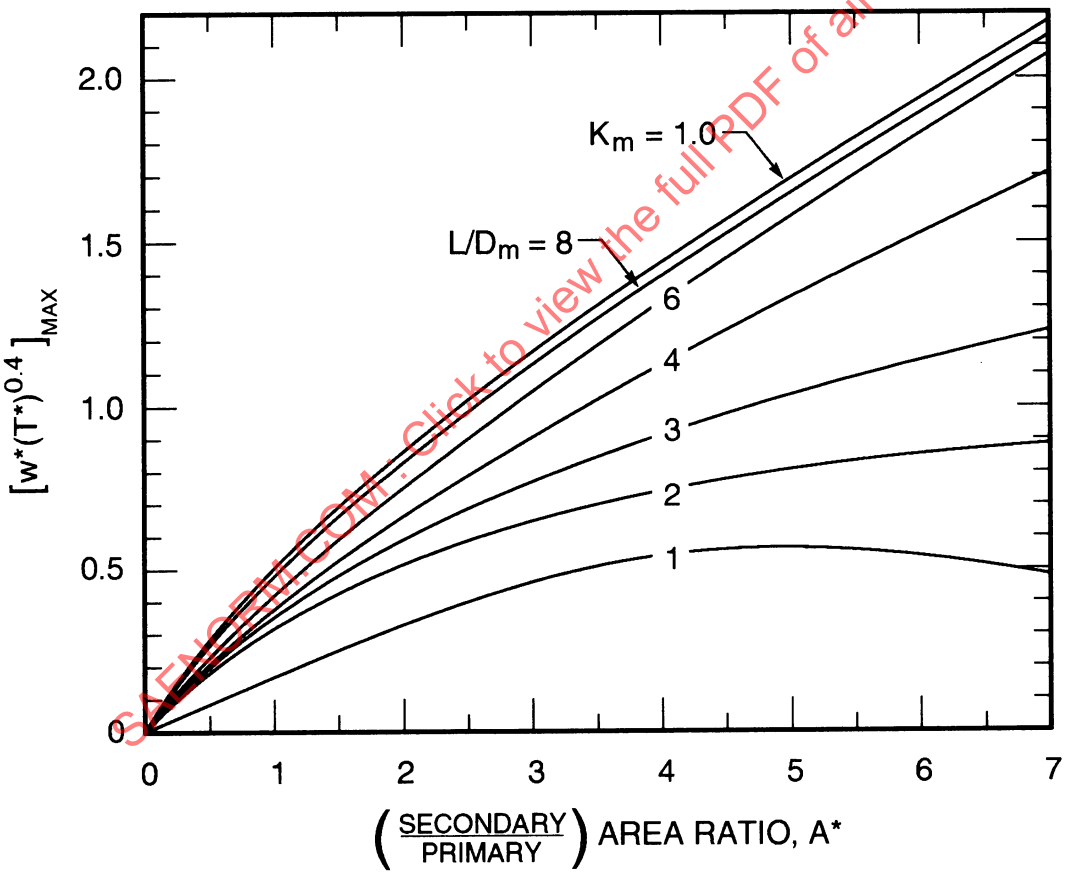

Figure 3H-67 - Variation of $[(w^*)(T^*)^{0.4}]_{max}$ with A^* and L/D_m

6.5.6 Design Calculation Procedure

The following procedures utilize the jet pump performance criteria described above in the design of a specific jet pump.

Design specifications that compose the jet pump problem statement are:

(1) Problem statement

(a) Primary flow:

Weight flow rate	$= w'$, lb/sec
Flow area	$= A'$, ft^2
Density	$= \rho' g$, lb/ft^3
Nozzle exit static pressure	$= P_1'$, lb/ft^2
Temperature	$= T_0'$, ^oR

(b) Secondary flow:

Desired weight flow rate	$= w''$, lb/sec
Temperature	$= T_0''$, ^oR
Desired pressure rise	$= (P_3 - P_0'')$, lb/ft^2

Utilizing problem statement (1), calculate the following:

(2) $w^*(T^*)^{0.4}$ at the design point and $\Delta P^*/T^*$ at the design point.

(3) $[w^*(T^*)^{0.4}]_{max}$ is obtained by doubling the value obtained in (2).

(4) Enter Fig. 3H-67 with this value of $[w^*(T^*)^{0.4}]_{max}$, and a series of compatible L/D_m and A^* are tabulated.

(5) Values of $\Delta P^*/T^*$ corresponding to L/D_m and A^* are computed using the following expression:

$$\left(\frac{\Delta P^*}{T^*}\right)_{max} = C_1 + \frac{K_p^*}{T^*} \qquad \text{(3H-91)}$$

with C_1 defined by the equation given in paragraph 6.5.4.1, K_m taken from Figs. 3H-62 through 3H-65, and K_p taken from Fig. 3H-61.

(6) The values of $(\Delta P^*/T^*)_{max}$ and $[w^*(T^*)^{0.4}_{max}]$ are plotted as shown on Fig. 3H-68, and the design characteristics are approximated by straight lines.

(7) Enter the design value of $w^*(T^*)^{0.4}$ and $\Delta P^*/T^*$ on this plot and select the geometry design characteristic (value of L/D_m and A^*) that passes through the design point.

(8) With the approximate geometry established, verify the results, using Eq. 3H-87 to determine the accurate operating characteristic line, that is, $w^*(T^*)^{0.4}$ versus $\Delta P^*/T^*$.

(9) Compute the value of η_e at the design point.

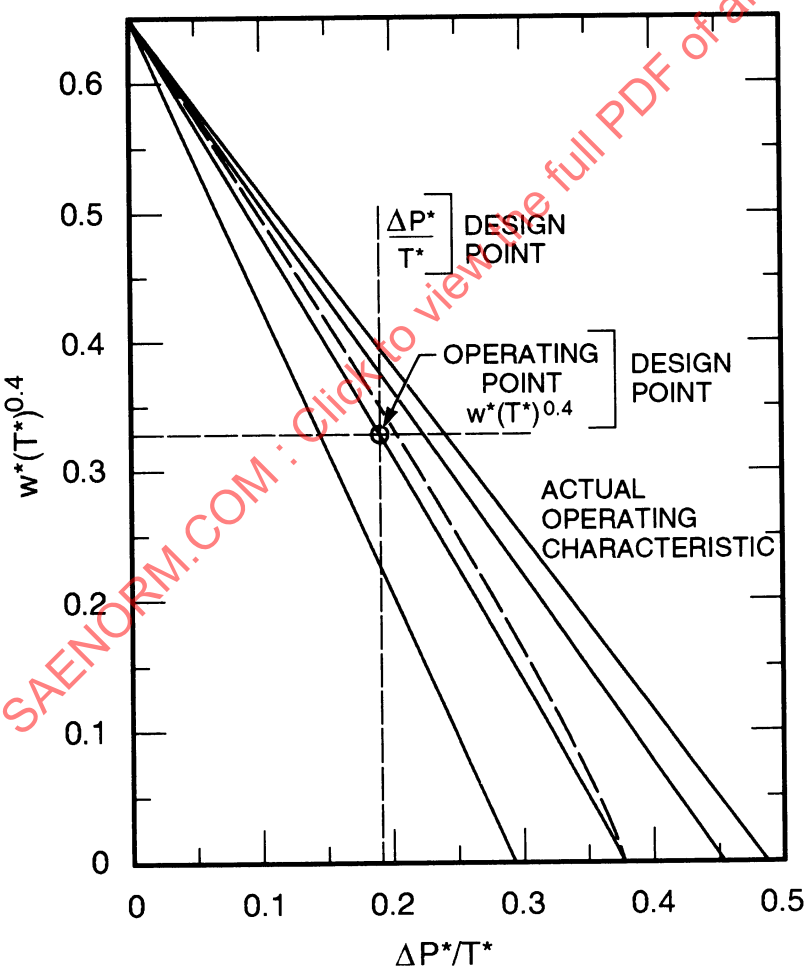

Figure 3H-68 - Method of approximately establishing design operating conditions

6.5.7 Primary Nozzle Position

The optimum location for the primary nozzle exit face is approximately 1 dia outside the mixing section throat.

6.5.8 Effect of Varying Design Parameters

Jet pump applications vary widely from low mass ratio and high secondary pressure rise to high mass flow ratio and low pressure rise. It is apparent from Fig. 3H-69, taken from Ref. 30, that there is a unique mixing section area which yields the greatest pump pressure rise for various weight flow ratios and exit diffuser area ratios.

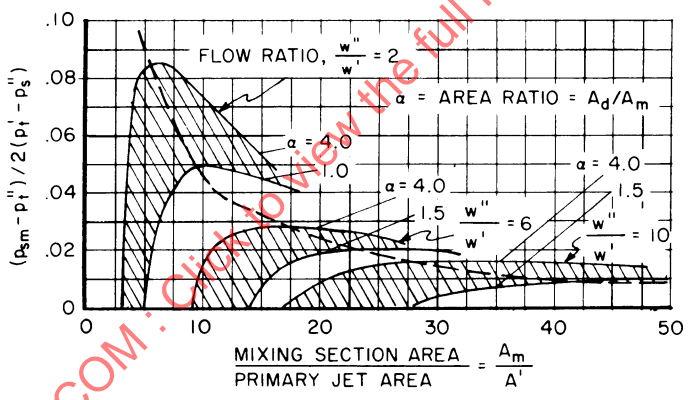

Figure 3H-69 - Pump Pressure Rise Versus Flow Ratio and Area Ratio

6.5.9 Multiple Primary Nozzle Jet Pump Configurations

The use of multiple primary jet nozzles offers the designer a means of reducing the mixing section length required to achieve complete mixing. Fig. 3H-70 gives a correlation between nozzle arrangement and mixing section length for complete mixing. This is based on data from Ref. 30. Radial mixing spread is the radius of the primary flow cone compared with the mixing section diameter.

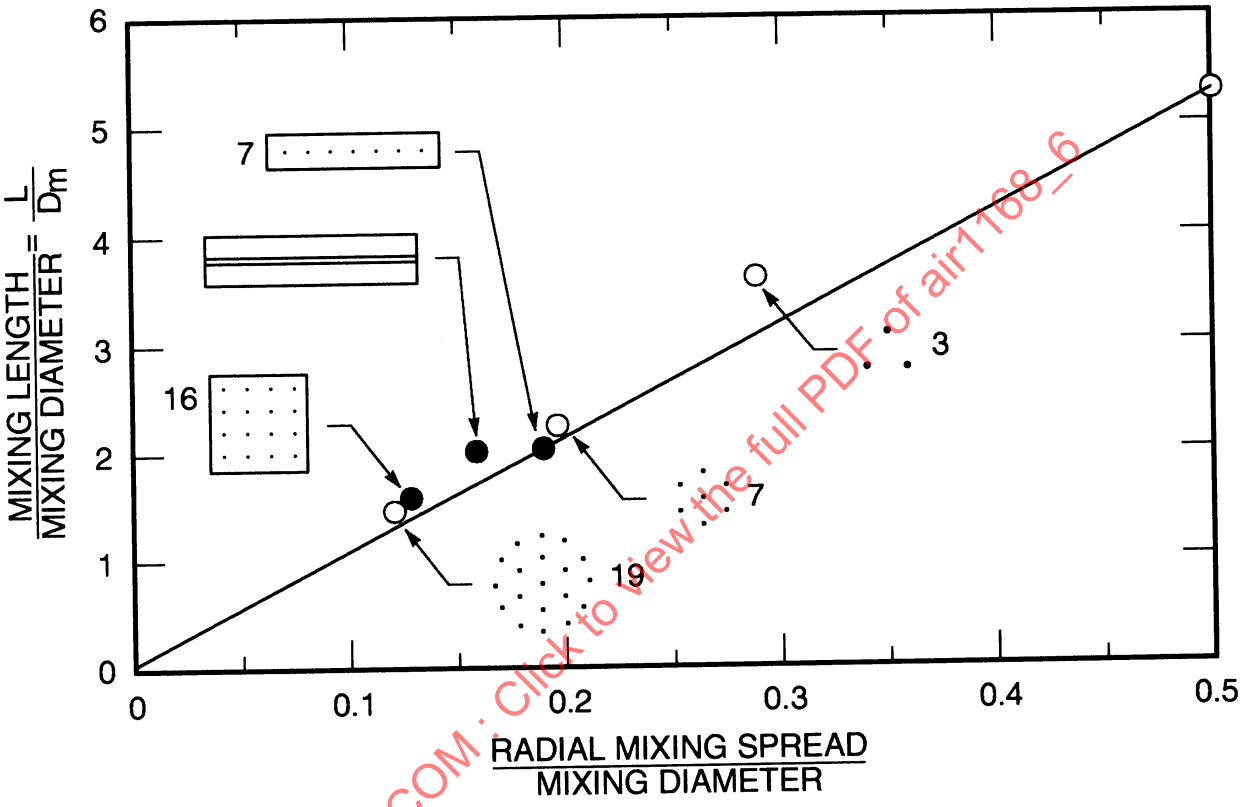

Figure 3H-70 - Correlation of Mixing Length and Nozzle Arrangement

6.5.10 Supersonic Primary Stream Velocities

The design of a jet pump using supersonic velocities in the primary stream may be treated by the method outlined in Par. 6.5.6. The designer is cautioned, however, that some inaccuracy is introduced in so doing, in that the method used treats both fluids as incompressible. The design results should be verified, using data presented in Ref. 31 which accounts for compressibility effects.

6.6 References

Elaboration of the material on jet pumps presented above can be found in Refs. 29-32.

7. VALVES

7.1 Nomenclature

A = Geometrical area of restriction, in^2
C = Orifice coefficient, dimensionless
C_e = Effective flow coefficient of combination, (gal/min)/(lb/in^2.)
C_1 = System flow coefficient exclusive of valve, (gal/min)/(lb/in^2.)
C_t = Torque coefficient, dimensionless
C_v = Valve flow coefficient, (gal/min)/(lb/in^2.)
D = Duct inside diameter, ft
h = Height, ft
K_t = Loss coefficient $\Delta p_t / q$, dimensionless
K_v = Gain, rad/sec-volt
Δp = Pressure loss, lb/ft^2, lb/$in.^2$
p = Pressure, lb/$in.^2$
p_n = Normal seal pressure, lb/in. of seal length
Q = Volume flow rate, gal/min
r = Pressure drop ratio $(p_1 - p_2)/(p_1 - p_3)$, dimensionless
s = Laplace operator
S = Fluid specific gravity, dimensionless
t = Thickness, ft
T = Torque, in.-lb
V = Velocity, ft/sec
W = Weight flow rate, lb/sec
W_{ch} = Choked flow rate, lb/sec
X = Stroke, in.
α = Closing angle, deg
μ = Coefficient of friction, dimensionless
τ_e = Electrical time constant, sec
τ_m = Mechanical time constant, sec

Subscripts

0 = Midpoint of valve
1 = Upstream of valve
2 = Downstream of valve
3 = Downstream of system
a = Actuator
cr = Critical
e = Exit
s = Supply
t = Total

7.2 General Considerations

Control valves are used in fluid control systems as variable restrictions to accomplish the changes in fluid flow or pressure required by the automatic control system. The complete control valve, not including the sensing, computation, and amplification functions of an automatic control, consists of the valve and the valve actuator. In the performance of its control function, the valve is usually required to:

(1) Contain the fluid without leaking, and without undue corrosion or erosion.

(2) Pass the maximum required fluid flow with a minimum of pressure loss.

(3) Provide a continuously variable flow restriction between shutoff and maximum flow.

As a portion of an automatic control system, the valve may further be required to:

(1) Have a particular known relationship between percent flow and percent of maximum opening when installed in the fluid duct system.

(2) Operate only in response to the actuator input control signal, without being influenced by spurious signals.

7.3 Valve Types

Valves are available in numerous general and special purpose types. The type of valve best suited to a given application will depend upon consideration of the following factors:

(1) Properties of working fluid:

(a) Temperature and pressure.

(b) Differential pressure at shutoff.

(c) Corrosion and erosion.

(d) High viscosity fluids or presence of solids.

(2) Control requirements:

(a) Modulating versus on-off. Flow characteristics.

(b) Pressure drop at open position.

(c) Leakage at closed position.

(3) Actuation requirements:

(a) Pressure or flow unbalance force.

(b) Inherent friction.

The most important valve types are listed below, along with their salient features.

(1) Butterfly valves (Fig. 3H-71):

(a) Relatively high flow, low pressure drop.

(b) Limited shutoff pressure differential.

(c) Relatively high leakage at shutoff.

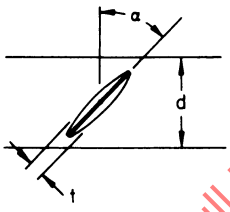

Figure 3H-71 - Butterfly Valve; *t*/*d* = Thickness,%

(2) Poppet valves (Fig. 3H-72):

(a) Relatively low flow, high pressure drop.

(b) Suitable for high pressure.

(c) Low shutoff leakage, especially with resilient seat.

(d) Large pressure unbalance, but can be balanced with piston or second poppet.

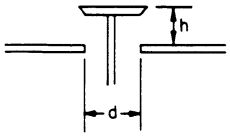

Figure 3H-72 - Poppet Valve

(3) Plug valves (Fig. 3H-73):

(a) Similar to poppet, but usually employing contoured flow passages for lower pressure drop.

(b) Suitable for relatively high pressure.

(c) Low shutoff leakage, especially with resilient seat.

(d) Frequently fluid-actuated, by its own working fluid or by a separate source, by means of a piston integral with the plug valve.

(e) Can be contoured to produce desired flow characteristics.

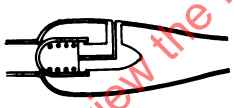

Figure 3H-73 - Plug Valve

(4) Gate valve (Fig. 3H-74):

(a) Relatively high flow, low pressure drop.

(b) Generally larger and heavier than butterfly valve, but capable of higher shutoff pressure and lower leakage.

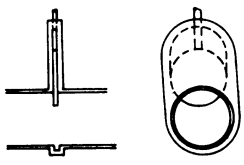

Figure 3H-74 - Gate Valve

(5) Spool valves (Fig. 3H-75):

(a) Low flow, small size only.

(b) May be very closely balanced for low operating force.

(c) May be notched or grooved for desired flow characteristics.

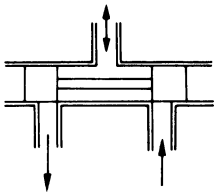

Figure 3H-75 - Spool Valve, Three Way

(6) Shutter valves or louver valves (Fig. 3H-76):

(a) High flow, low pressure drop applications only.

(b) Very limited shutoff pressure differential.

(c) Relatively high leakage at shutoff.

(d) Light weight and short length in comparison to other high flow valves.

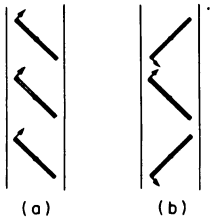

Figure 3H-76 - Louver Valve: (a) unirotational; (b) counterrotational

7.4 Valve Performance and Sizing

The correct sizing of a valve for a given application generally involves a compromise between valve full open pressure drop and valve size and weight. In modulating control applications, valve "rangeability" (defined below) must also be considered.

7.4.1 Valve Sizing for Capacity

For the purpose of estimating the characteristics of valves for which data are not available, the valve opening may be considered to be an orifice, and the standard equations for orifice flow (Ref. AIR1168/1) may be applied. However, since the flow patterns and recovery factors through various types of valves may be complex and difficult to estimate, it is preferable to use experimental data.

The most common method of empirical data presentation for commercial valves uses the valve flow coefficient C_v, defined as the valve flow in gpm of water at a pressure differential of 1.0 psi. It is typically measured with an accuracy of 5 to 10%. Typical values of C_v for various types of valves are given in Table 3H-2.

Table 3H-2 - Typical Values [1] of K_t and C_v for Various Valve Types

Type	K_t	C_v/D^2
Butterfly valves, 7% thick	0.13	12,000
35% thick	0.60	5,570
Swing Check[2]	2.50	2,725
Recessed swing check[2]	0.95	4,420
Angle poppet, unobstructed, with stem 45 deg from line of pipe	2.75	2,600
With stem 60 deg from line of pipe	3.40	2,340
In 90 deg pipe bend	6.50	1,690

1. All values shown are for wide open position.

2. Check valves may require a minimum ΔP to obtain wide open position.

The valve flow coefficient C_v is related to the loss coefficient K_t as follows:

$$C_v = 4310 \frac{D^2}{\sqrt{K_t}} \qquad \text{(3H-92)}$$

The valve flow coefficient C_v is related to effective area by means of the incompressible orifice flow equation:

$$C_v = 300 \frac{CA}{\sqrt{\rho g}} \quad \text{(3H-93)}$$

For gases and vapors,

$$W = 0.0176 C_v \sqrt{\rho g \Delta p} \quad \text{(3H-94)}$$

If the valve pressure drop exceeds the critical value, the Δp is taken at critical pressure ratio. For air, this pressure drop is $\Delta p_{cr} = 0.472\, p_{1t}$, where p_{1t} is the valve upstream total pressure.

For liquids,

$$Q = C_v \sqrt{\frac{\Delta p}{S}} \quad \text{(3H-95)}$$

For viscous fluids, the valve flow coefficient C_v must be multiplied by the correction factor obtained from Fig. 3H-77. The "factor R" given in this curve is an approximation of Reynold's number in terms of the valve parameters:

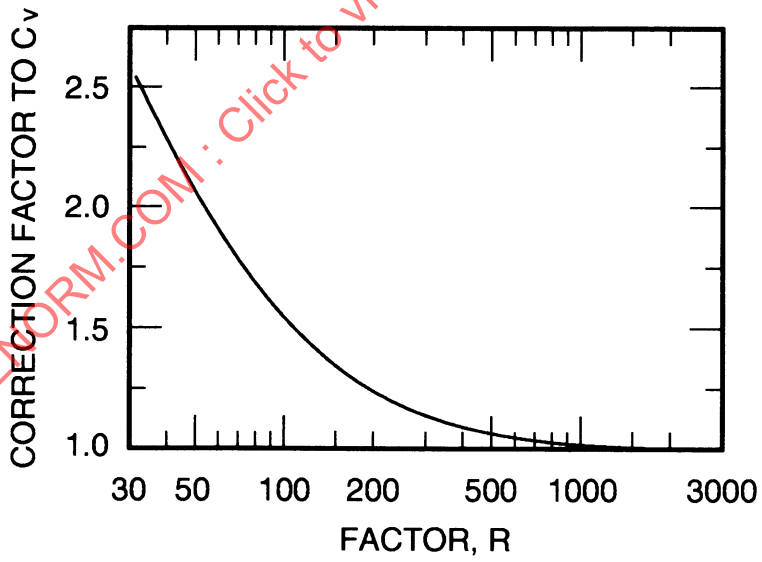

Figure 3H-77 - Viscosity Correction Curve

$$R = \frac{10{,}000 \text{ (flow in gpm)}}{\sqrt{C_v} \text{ (Centistokes at flow temp)}} \quad \text{(3H-96a)}$$

$$R = \frac{46{,}500 \text{ (Flow in gpm)}}{\sqrt{C_v} \text{ (SUS at flow temp)}} \quad \text{(3H-96b)}$$

(Note: Centistokes = Centipoises/S)

Note: Eq. 3H-96b is accurate at viscosities of 200 SUS or higher. With viscosities below 200 SUS, convert to centistokes and use Eq. 3H-96a. ("SUS" is defined as "Saybolt Universal Seconds" per SAE J916.)

7.4.2 Valve Flow Characteristics

The flow characteristic of a valve defines the relationship between valve opening and valve flow at constant valve pressure drop.

The effective flow characteristics of a valve in a complete system are affected by the duct losses as discussed in paragraph 7.4.3. The flow characteristics of typical butterfly valves and gate valves are shown in Figs. 3H-78 and 3H-79. Fig. 3H-80 shows the flow characteristics of a louver such as that used at heat exchanger inlets.

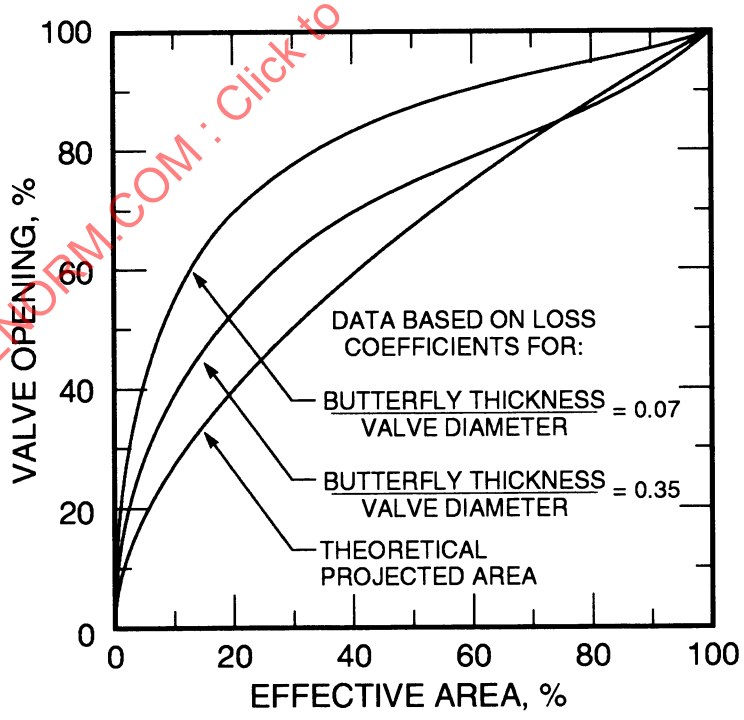

Figure 3H-78 - Typical Butterfly Valve Flow Characteristics

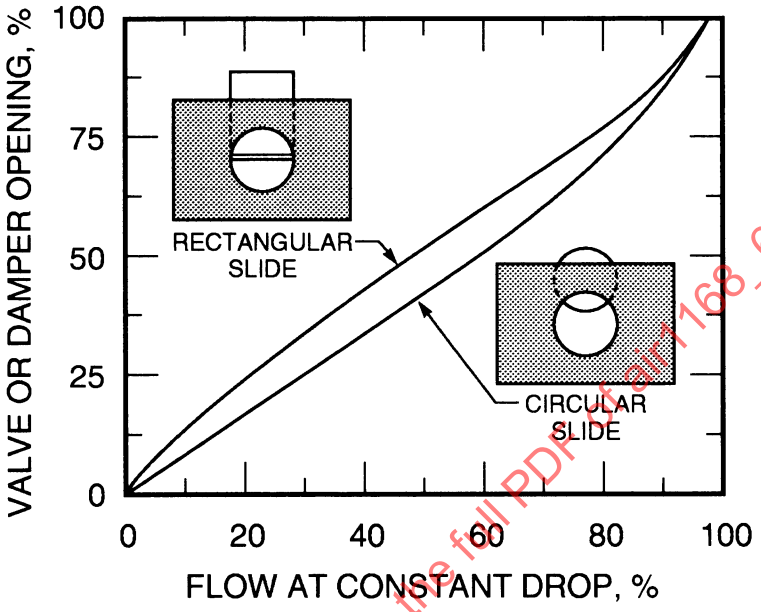

Figure 3H-79 - Typical Gate Valve Characteristics

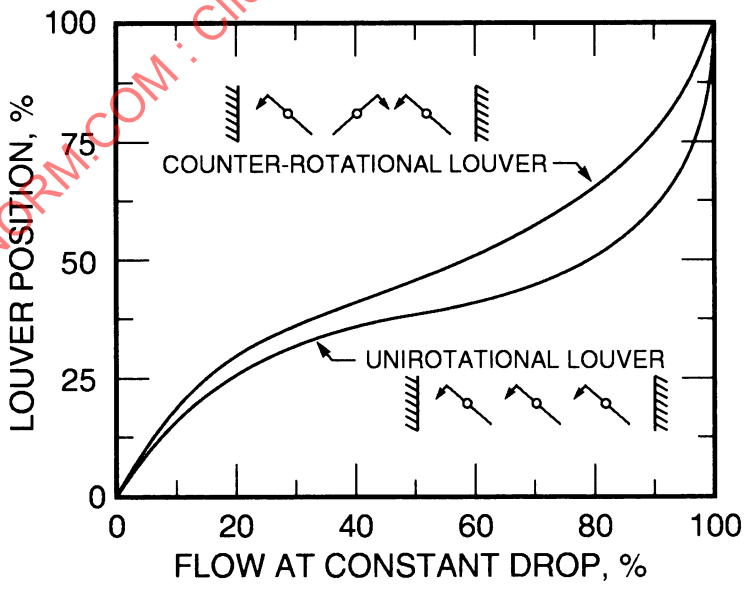

Figure 3H-80 - Typical Louver Valve Characteristics

Poppet, plug, and spool valves may be contoured to give a wide variety of flow characteristics. The most commonly used characteristics are: linear, and exponential (equal percentage).

The linear characteristic results in flow proportional to valve stroke (at constant valve pressure drop). The exponential (equal percentage) results in equal percent change in flow per unit valve stroke, the percent being of the variable flow rather than of the maximum flow. This characteristic is a straight line on a semilogarithmic plot, its slope being determined by the ratio of flows between the valve operating extremes. Obviously, the equal percentage characteristic has an infinite number of values and cannot be maintained at shutoff. The linear characteristics are shown in Figs. 3H-81 and 3H-82 (same curves, note the straight lines for A,B, and C on the plot of Fig. 3H-82 which has a log scale on the abscissa) where values for the curves are:

Curve	Theoretical Rangeability	Unit Sensitivity
A	100:1	4.7
B	50:1	4.0
C	20:1	3.0

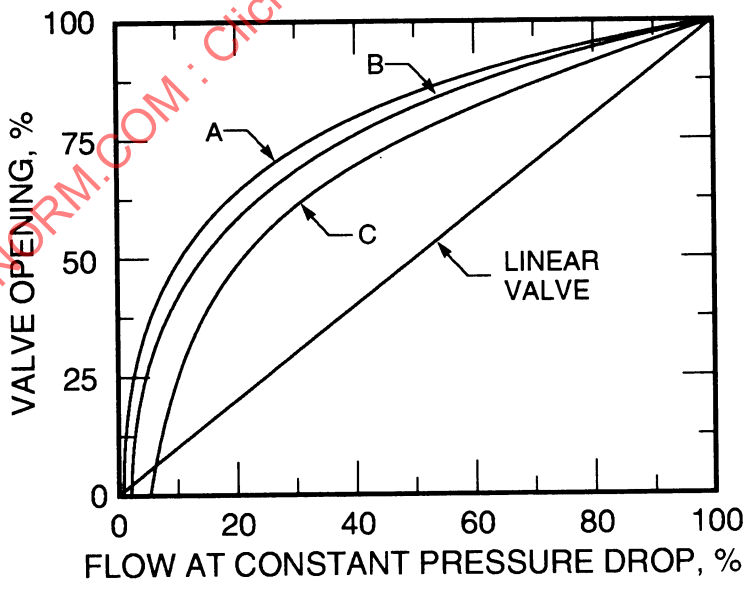

Figure 3H-81 - Characterized Valve Functions, Exponential (Equal Percentage) Valves

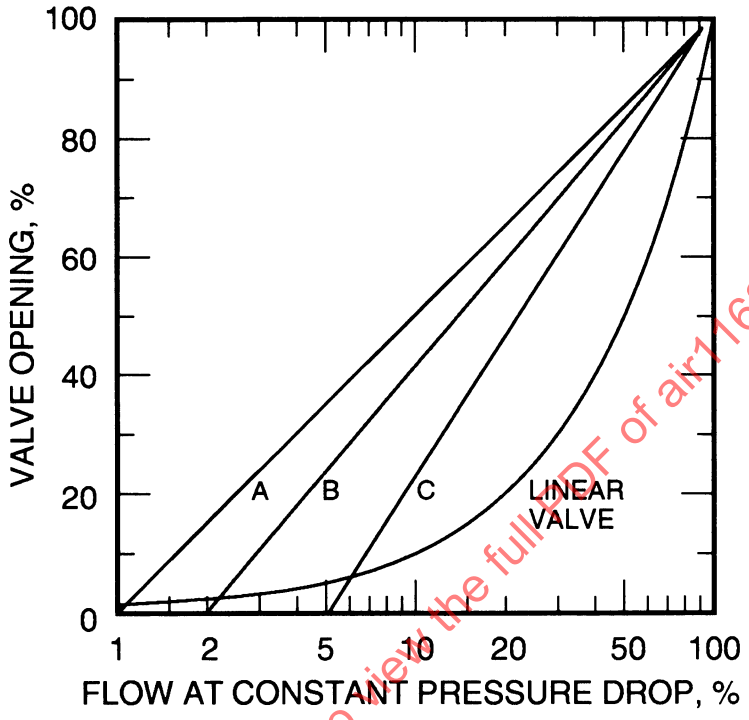

Figure 3H-82 - Characterized Valve Functions, Exponential (Equal Percentage) Valves

7.4.3 Effective Flow Characteristics

The duct system in which a valve is installed will combine with the valve characteristic to provide a modified effective characteristic of the complete system. For the system shown in Fig. 3H-83a, let

C_v = Valve flow coefficient, gpm at $(p_1 - p_2) = 1.0$ psi
C_1 = System flow coefficient exclusive of valve, gpm at $(p_2 - p_3) = 1.0$ psi
C_e = Effective flow coefficient of combination, gpm at $(p_1 - p_3) = 1.0$ psi

Then $$\frac{1}{C_e^2} = \frac{1}{C_v^2} + \frac{1}{C_1^2} \qquad \text{(3H-97a)}$$

or $$C_e = C_v \left(\frac{C_1^2}{C_1^2 + C_v^2} \right)^{1/2} \qquad \text{(3H-97b)}$$

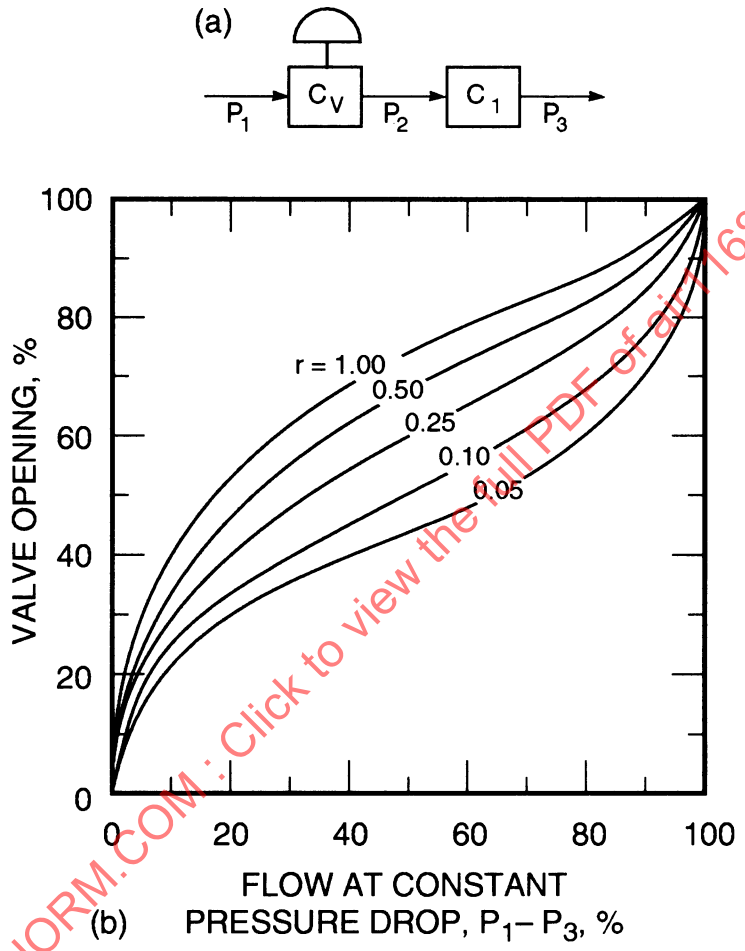

Figure 3H-83 - Effective Flow Characteristics: (a) valve installed in restrictive line; (b) effective characteristics of butterfly valve; $r = (p_1 - p_2)/(p_1 - p_3)$, wide open

The manner in which the inherent valve characteristic is modified by the connecting system loss is illustrated in Figs. 3H-83b, 3H-84, and 3H-85.

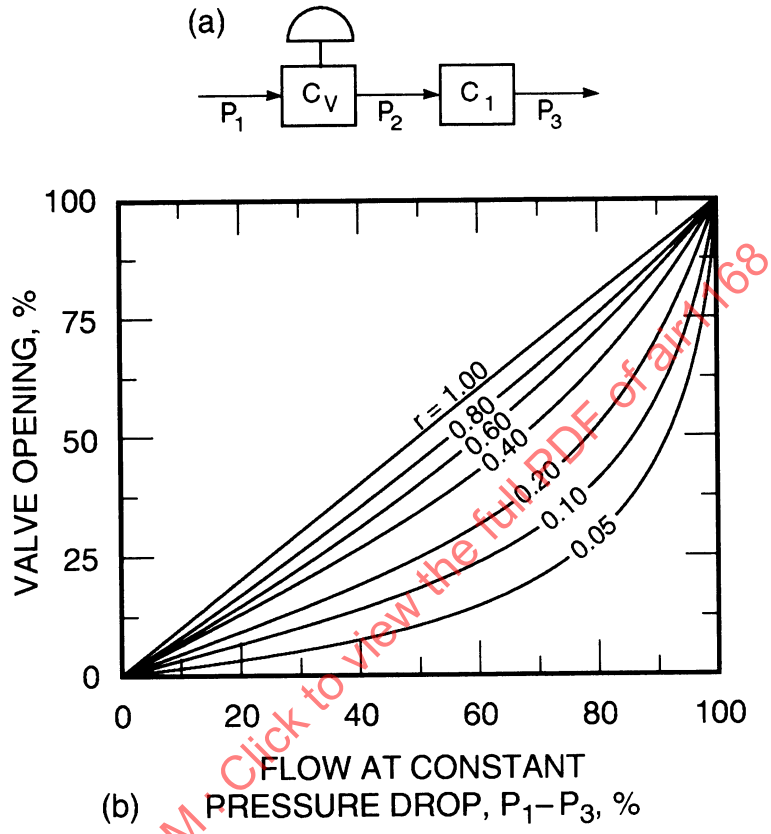

Figure 3H-84 - Effective Characteristics of a Linear Valve: (a) valve in restrictive line; (b) effective characteristics of linear valve; $r = (p_1 - p_2)/(p_1 - p_3)$, in wide open position

7.4.4 Rangeability and Unit Sensitivity

The rangeability of a valve is defined as the flow range (taken as a ratio of maximum to minimum flow) through which the inherent valve characteristic is maintained within prescribed limits. The definition is somewhat vague in that the minimum controllable flow is not clearly defined.

Valve unit sensitivity is defined as the percent change in flow for each percent change in valve opening, based on the flow rate just before the change. Unit sensitivity should not be confused with valve sensitivity coefficient or valve gain as used in feedback control analysis.

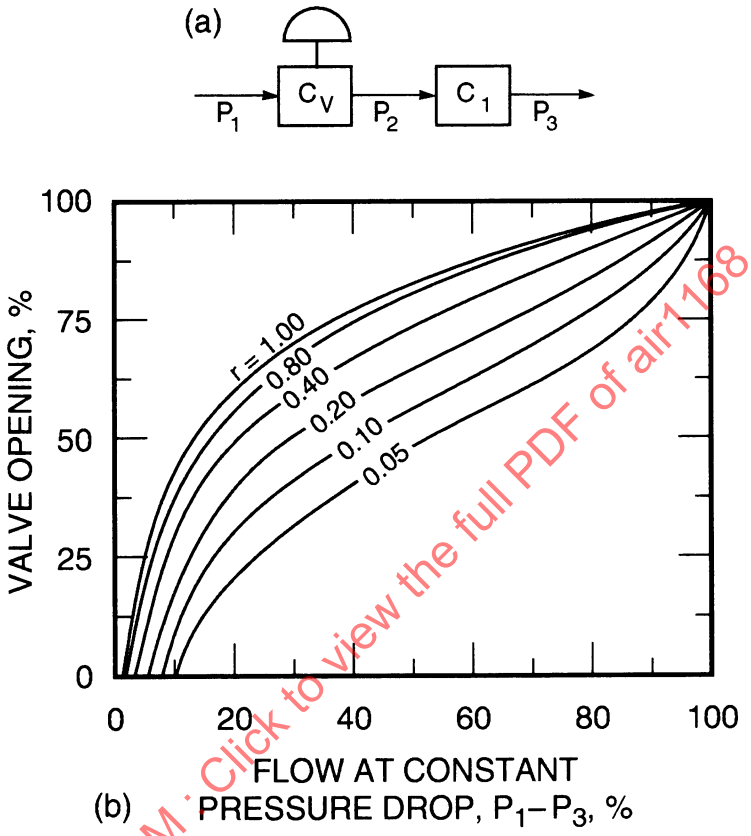

Figure 3H-85 - Effective Characteristics: (a) valve in restricting line; (b) effective characteristics of 50:1 equal percentage valve; $r = (p_1-p_2)/(p_1-p_3)$, wide open

The valve gain is defined as the ratio of the change in flow rate to an incremental change in valve stroke with constant pressure drop across the valve. Valve gain is constant for a linear valve, whereas unit sensitivity is constant for an equal percentage valve.

The unit sensitivities of the equal percentage valves shown in Figs. 3H-81 and 3H-82 are noted on the curves. The unit sensitivity of the linear valve as related to size in a given duct system is shown in Fig. 3H-86. Fig. 3H-87 illustrates the unit sensitivity of butterfly valves of various sizes in a given duct system.

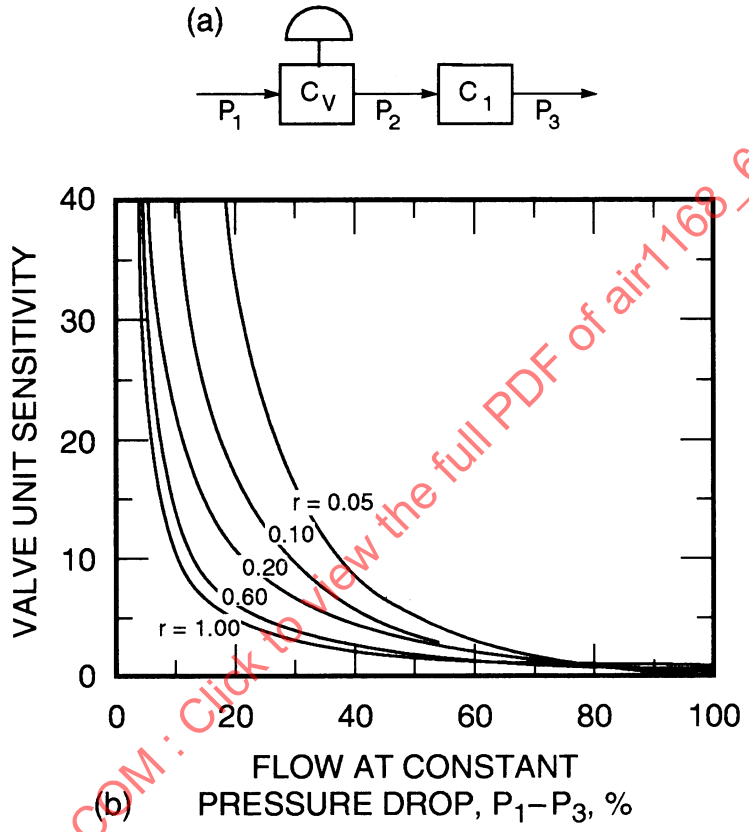

Figure 3H-86 - Sensitivity versus flow at constant drop: (a) valve in restrictive line; (b) linear valve unit sensitivity, where unit sensitivity $= \frac{\text{\% Flow change}}{\text{valve opening change}} / \frac{\text{Valve flow}}{\text{wide open flow}}$ and $r = (p_1 - p_2)/(p_1 - p_3)$, wide open

These curves indicate the concept of a valve's being too sensitive near the closed position, particularly when the value is relatively large (that is, low pressure drop) for the system in which it is operating. This problem is less severe for the butterfly valve because of its slow opening characteristic.

7.4.5 Selection of Valve Characteristics

The proper selection of valve characteristics for a given application is not an exact science. The proper selection of a valve type may depend entirely upon factors such as size, weight, reliability, and fail-safe characteristics, or may be determined by performance characteristics in the modulating range.

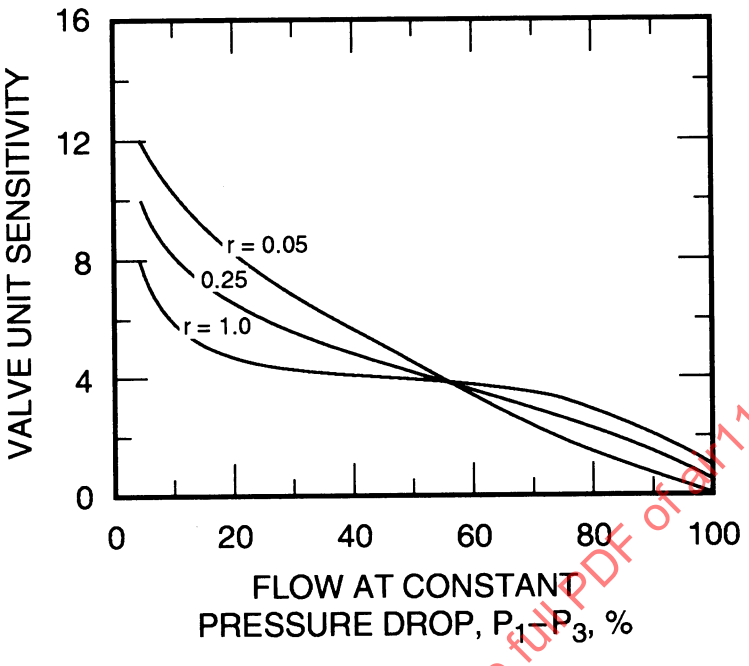

Figure 3H-87 - Butterfly Valve Unit Sensitivity

If a modulating control is used, it is desirable to obtain a valve characteristic that, in combination with the remainder of the system processes, tends to maintain constant gain in the control loop regardless of extreme variations of other operating parameters.

It was seen in paragraph 7.4.4 that the effect of a line drop is to cause an equal percentage valve to become more linear, and a linear valve to become more quick-opening. These characteristics are arbitrarily defined at constant pressure drop of the duct section involved. Concurrent and directly related changes in the remainder of the system may define a different effective operating characteristic.

In addition to consideration of the effective control characteristic in the system is the compensation for other system nonlinearities, which may be directly counteracted by the use of an appropriate valve characteristic. Typical of these nonlinearities are the square root pressure-flow function and the vapor pressure curves for filled thermal systems.

Over a load range of up to 3:1, the performances of a linear and an equal percentage valve may be made nearly identical. Proper sizing is more important in the application of the linear valve than of the equal percentage valve, primarily because of the quick-opening characteristics of an oversized linear valve. Such oversizing of butterfly valves is common in air conditioning applications in order to obtain low pressure drop in the wide open position. The resulting characteristic does not have an important effect in most applications because of the relatively slow opening characteristics of the butterfly valves.

7.4.6 Valve Leakage

The minimum leakage of shutoff valves is generally limited by the basic valve design and force or torque available for seating the valve. Poppet, plug, and gate valves are commonly made with resilient seat materials, giving bubbletight shutoff.

Butterfly valves often do not seal properly, particularly at operating temperatures that preclude the use of organic resilient seat materials. In such applications, leakage may be estimated as 0.1 lb/min. of air per inch of valve diameter at a pressure differential of 200 psi and a temperature of 750 ^{o}F. Lower leakage may be obtained with ingenious seating designs or high actuating torques. Higher leakage (for example, double) may be expected from valves that are required to modulate flow as well as shut off.

7.5 Valve Actuation

Types and requirements are discussed below.

7.5.1 Actuation Requirements

The following requirements determine the type and size of valve actuator to be used:

(1) Actuation Force or Torque - The force or torque required to actuate the valve results from fluid pressure unbalance, friction, and acceleration forces. In most applications, either the friction or the unbalance forces are dominant, and acceleration may be neglected. Typical butterfly valve torques are shown by the fluid dynamic pressure unbalance curve (Fig. 3H-88), for which

$$T = C_t D^3 \Delta p \quad \text{in.-lb}$$

where D = Valve ID, in.

Δp = Valve static pressure drop, psi

The data in Fig. 3H-88 represent a range of typical torque coefficient curves for several valve types operating on air.

Fig. 3H-89 shows the "jam-in" and "crackout" torque curves, for which

$$T = p_n D^2 \left(\mu \cos \alpha \pm \frac{\pi}{4} \sin \alpha \right) \text{ in.-lb}$$

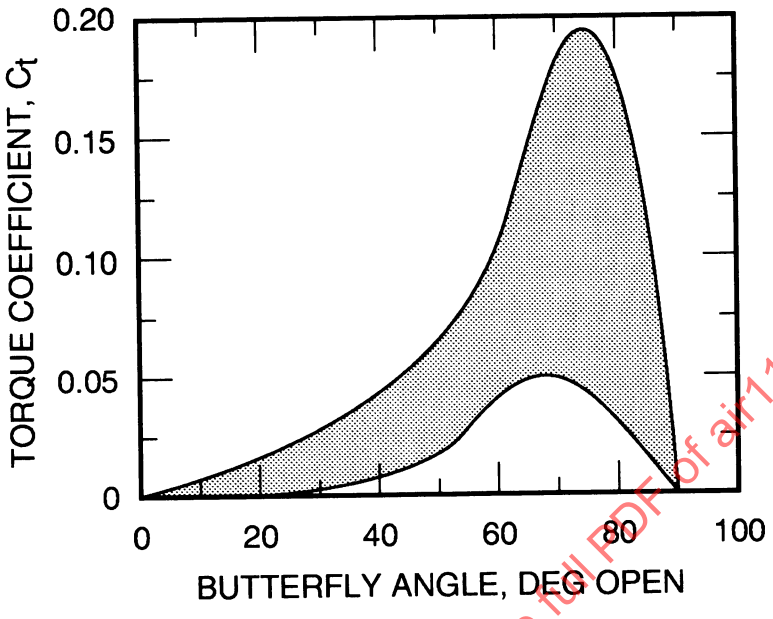

Figure 3H-88 - Butterfly Valve Aerodynamic Torque

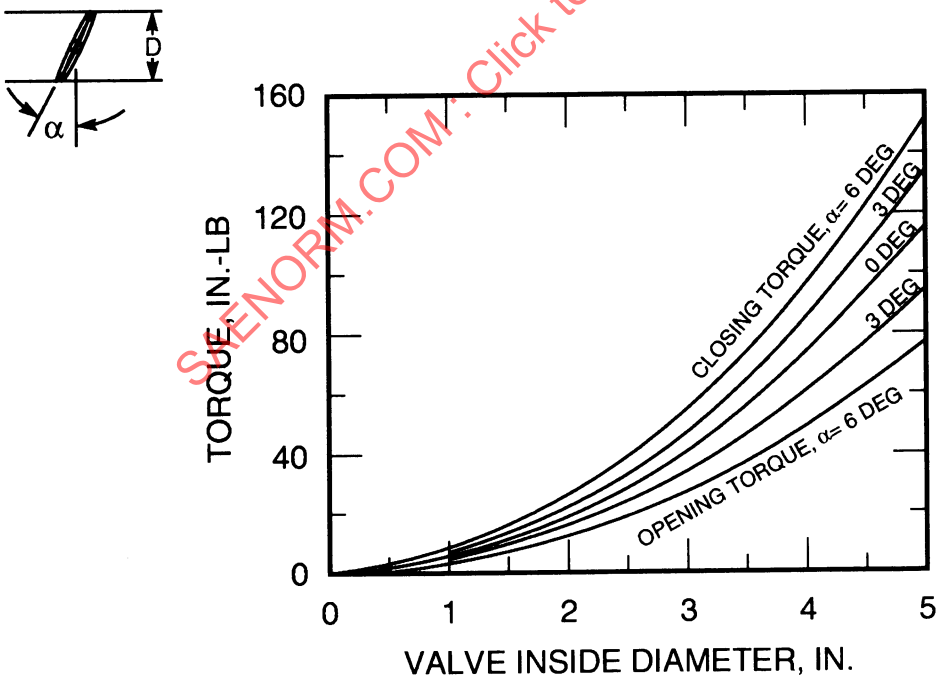

Figure 3H-89 - Butterfly Valve Sealing Torque

(2) Actuation Speed - The maximum required actuation speed may determine the actuator type, since snap action is easily obtained with pneumatic, hydraulic, or solenoid operated valves, but may impose an undue size and weight penalty with an electric motor drive.

(3) Energy Source - The relative penalties associated with the use of AC or DC electric supplies or with pneumatic or hydraulic power must be evaluated along with the suitability of the available energy sources in terms of actuator type, power supply regulation, reliability, fail-safety, and similar specifications and characteristics.

(4) Controllability - The type of actuator selected has a profound influence on the complexity of equipment required for control, and on the performance of the control (frequency response, ratio of maximum to minimum controllable speed, resolution in the presence of dry friction, and other operating efficiencies).

(5) Fail-safety, Reliability - The requirement of a valve to fail in a given position requires a clutch in most electric motor drives, but is inherent in most fluid - actuated valves. The reliability of the energy source directly affects valve reliability unless interrelated requirements preclude valve operation in the absence of the energy source (for example, self-powered regulators).

(6) Size and Weight - The smallest and lightest actuator for a given application will depend upon the operating characteristics and the characteristics of the available energy sources. No one type is lightest under all circumstances.

7.5.2 Types of Actuators

Valves may be actuated electrically, hydraulically, pneumatically, or manually. Combinations of these means are sometimes used for purposes of reliability, independent override, fail-safety, computation, or transfer of control signal type.

7.5.2.1 Electric Actuators

In shutoff applications, electrically driven valves are controlled by on-off switches and may be stopped at the extreme position by limit switches. Small actuator motors may be designed to run stalled against the stops indefinitely, giving an increase in reliability by elimination of the limit switches. The associated power and weight penalty is significant with larger actuators, however.

In modulating applications, the electric motor may be controlled by continuous speed modulation or by full power on-off pulses. Available transistorized controllers convert continuous modulated signals into time - modulated full power pulses. This method has the advantages of wider range average speed control and greater crackout torque to move against dry friction with low level signals.

Alternating current motors have the advantage of not requiring commutators, but starting torque is inferior to series DC machines. The highest starting torques are achieved in AC machines by the use of starting windings, or a wound rotor with slip rings, or both. The starting winding is generally not practical for valve applications, since starting acceleration may comprise the majority of the running time. The following AC motors are the more common types:

(1) Permanent Split Capacitor, Single Phase (Fig. 3H-90) - A good general purpose type for small or large size. Speed control is accomplished by time - modulated full power pulses or by control of applied voltage. A wound rotor gives better starting torque, but requires slip rings.

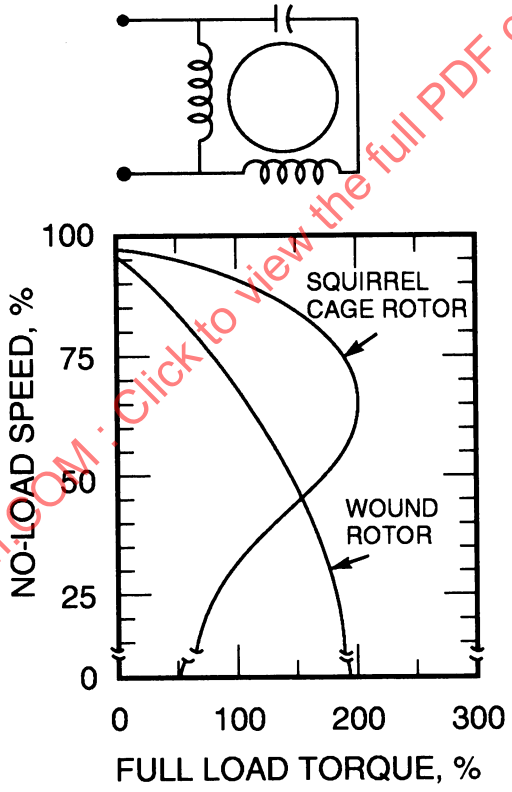

Figure 3H-90 - Permanent Split Capacitor Motor Characteristics

(2) Servomotors (Fig. 3H-91) - Specifically designed for linearity of the torque-speed characteristic for critical servo control applications. Relatively heavy in larger power applications. Various designs feature low rotor inertia, high inherent damping, either viscous or inertial, and low starting voltage (drag cup type). The linear torque-speed characteristic permits the servomotor devices to be represented by the linear transfer function:

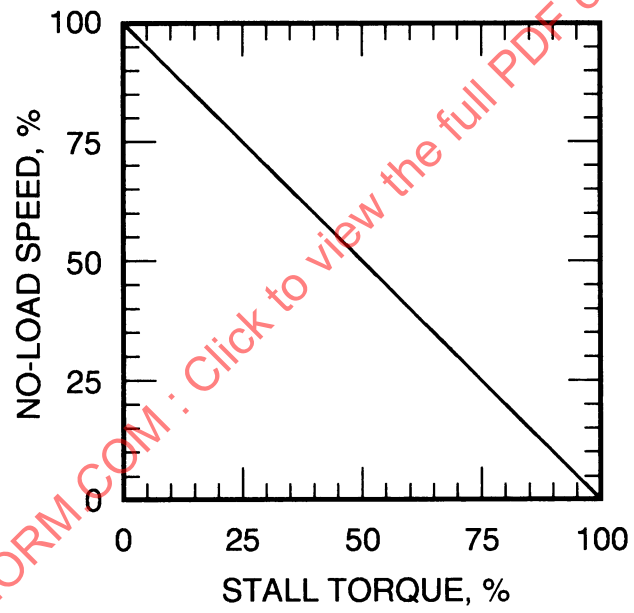

Figure 3H-91 - Servomotor Characteristics

$$\frac{\theta_o}{\theta_i} = \frac{K_v}{s(1+\tau_m s)(1+\tau_e s)} \qquad \text{(3H-98)}$$

where θ_o = Output position, rad
θ_i = Input signal, V
K_v = Gain, rad/sec-V
s = Laplace operator
τ_m = Mechanical time constant, sec

$$= \frac{\text{Rotor inertia}}{\text{Stall torque/no-load speed}}$$

≈ 0.020 sec (typical)

τ_e = Electrical time constant, sec

= Circuit inductance/resistance

≈ 0.001 sec (typical)

(3) Shaded Pole (Fig. 3H-92) - Relatively cheap, but large and inefficient. May be reversed by reversing the shading coils.

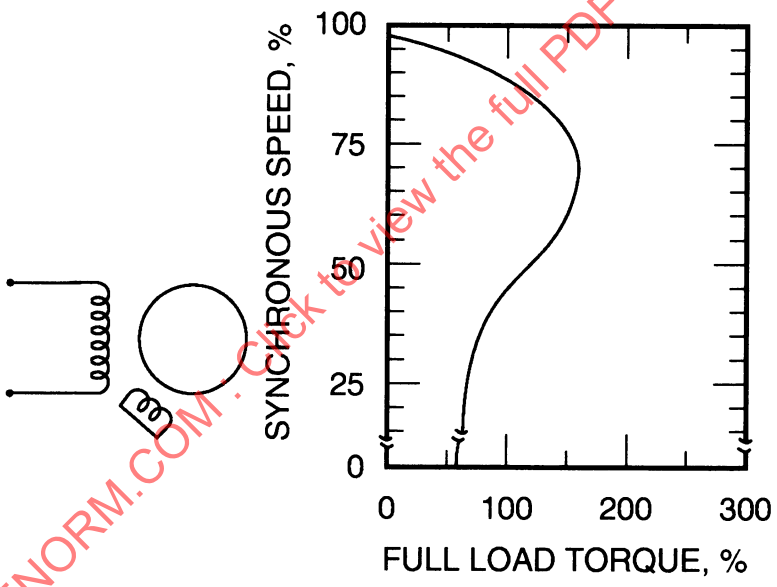

Figure 3H-92 - Shaded Pole Motor Characteristics

Direct current motors, while requiring commutators, are well suited to continuous speed modulation in conjunction with automatic control circuits. Series machines are most commonly used in actuators because of their high starting torque. Series, shunt, and compound types are compared in Fig. 3H-93.

Permanent magnet fields may be used in both AC and DC types. The magnet tends to be larger and heavier than an equivalent wound coil, but leads to greater electrical efficiency because there is no field loss. These machines are either DC or synchronous, and have a shunt characteristic.

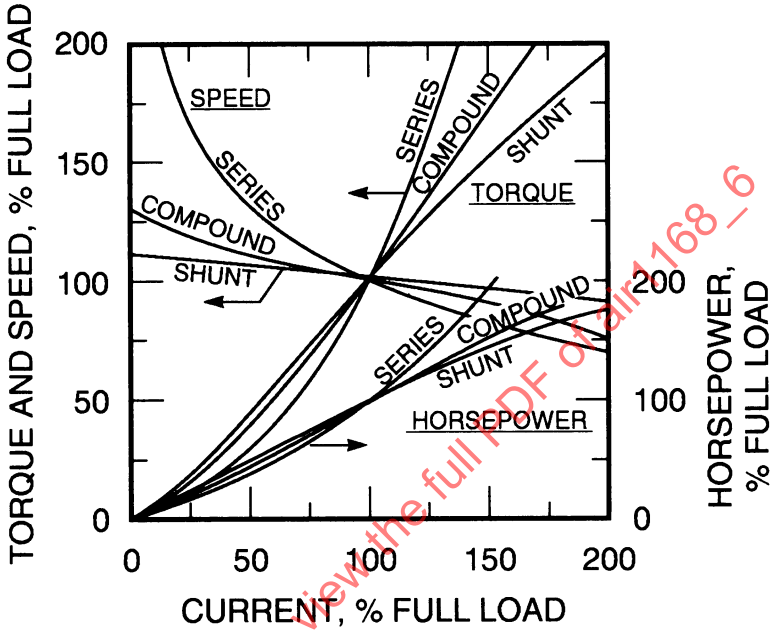

Figure 3H-93 - DC Motor Characteristics

7.5.2.2 Pneumatic Actuators

Pneumatic actuation is frequently used for valves in air duct systems because of the following advantages:

(1) Valves may be self-powered from the working fluid, requiring no external energy other than command signals.

(2) Fast actuation is possible without excessive actuator weight.

(3) Valves may be made to fail open or closed as desired without added fail-safe devices.

The pneumatic actuator is sized such that the force requirement may be met at the minimum differential pressure condition (for example, maximum altitude-minimum speed condition in an engine bleed system). The severity of the minimum pressure requirement typically determines the feasibility of pneumatic actuation.

Control of pneumatic actuators is accomplished by restrictions in the actuator supply and discharge ports. Either or both of these restrictions may be made variable for control. The appropriate configuration is determined by the fail-safe position, the starting requirements, and the condition during which control bleed flow is required to be a minimum.

The pressure-flow characteristics of the three common series orifice configurations are shown in Figs. 3H-94, 3H-95, and 3H-96. These curves are calculated for the arbitrary conditions of constant supply and exhaust pressure, steady flow, and 10:1 pressure ratio of supply to exhaust. Similar curves may be constructed for any steady flow conditions through the use of the orifice flow equations given in AIR1168/1 and the equation of continuity.

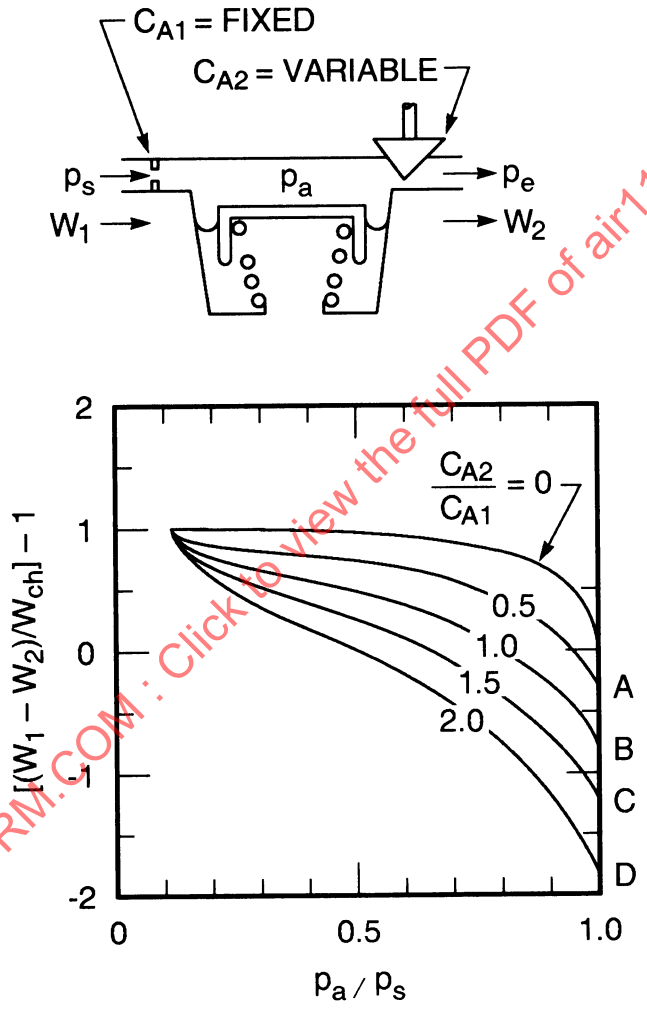

Figure 3H-94 - Air Flow Characteristics through Series Orifices, Downstream Orifice Variable; W_{ch} through C_{A1}; p_e/p_s= 0.1

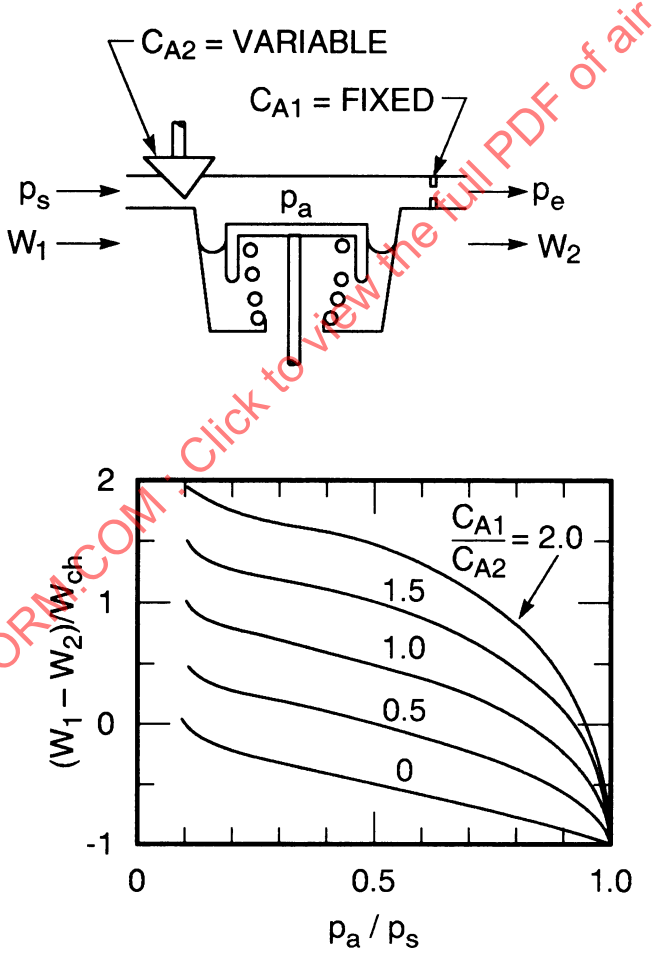

Figure 3H-95 - Air Flow Characteristics through Series Orifices, Upstream Orifice Variable; W_{ch} through C_{A1} when $C_{A1} = C_{A2}$; $p_e / p_s = 0.1$

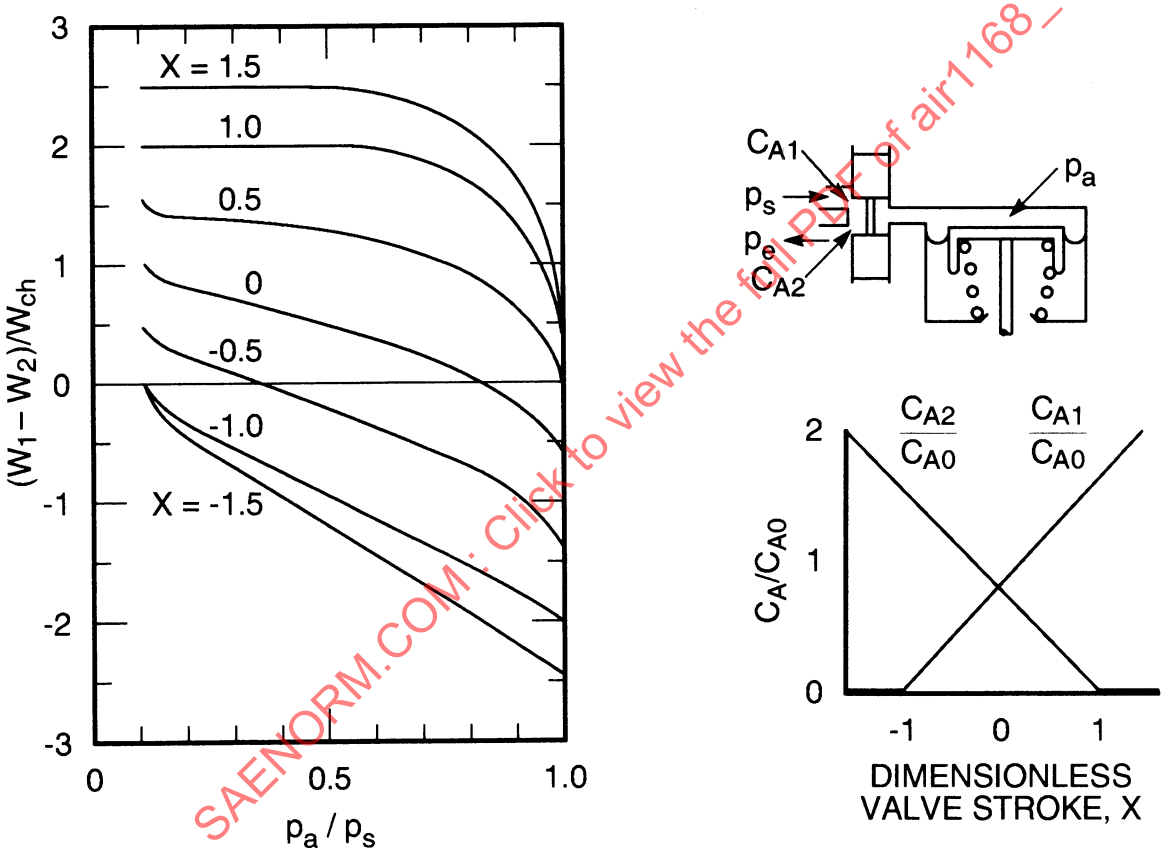

Figure 3H-96 - Air Flow Characteristics through Series Orifices, Both Orifices Variable; $p_e/p_s = 0.1$; W_{ch} through C_{A1} when $C_{A1} = C_{A2}$; $C_{A2} = 0$ for $X \geq 1$, and $C_{A1} = 0$ for $X \leq -1$. C_{A0} = Midpoint Orifice Coefficient.

The variable restrictions, or servo valves, may be on-off or modulating, and may be controlled pneumatically from a pressure signal operating on a bellows or diaphragm connected to the servo valve, or electrically by means of a solenoid or torque motor. Torque motor characteristics are discussed below under hydraulic actuators.

The most common valve types used for the control of the actuator working fluid are poppets and spool valves. Poppets tend to be more simple, rugged, and leaktight, but are difficult to balance against pressure and Bernoulli forces. Spool valves may have lower unbalance forces, but higher friction force. The force level is critical only in modulating applications.

At moderate temperatures and pressures, impregnated fabric diaphragms are commonly used for pneumatic actuators. Metallic diaphragms or bellows are used at higher temperature, but tend to have a relatively small displacement volume per unit of installed volume. (The displacement volume determines the output work per stroke at a given differential pressure.) Piston actuators are subject to dry friction and leakage, but utilize volume efficiently, have no inherent spring rate, and may be used at temperatures limited only by the seals.

7.5.2.3 Hydraulic Actuators

Electrohydraulic actuation is not frequently used in air conditioning applications because of the requirement for both electrical and hydraulic supply sources, neither of which is basic to most air duct systems. Electrohydraulic systems offer the advantages of high power per unit weight or volume and good frequency response, and they are easily compensated dynamically in the electronic portion of control.

(1) Electrohydraulic Servo Valves - The electrohydraulic servo valve converts an electrical input signal into a controlled hydraulic flow and pressure to the actuator. Most valves consist of an electromagnetic torque motor operating a first stage flapper valve, which in turn operates a second stage spool valve. Typical electrohydraulic servo valve characteristics are listed in Table 3H-3.

Table 3H-3 - Electrohydraulic Servo Valve Characteristics

Characteristic	Operating Range.
Fluid supply pressure	1500-3500 psi
Working fluid	Hydraulic fluid, MIL-0-5606, MLO-8200, MLO-8515, OS-45
Maximum fluid temperature	200-450°F
Maximum ambient temperature	200-700°F
Rated flow	0.15-10.0 gpm
Quiescent flow	0.03-0.40 gpm
Filtration required	2-100 μ, usually 5-10 μ
Input differential current	5-50 mA
Torque motor resistance	500-3500 ohms
Torque motor inductance	0.15-25 henrys
Size	5-15 $in.^3$
Weight	0.7-5.0 lb
Valve open-loop response	50-350 cps at 90 deg phase shift
Hysteresis	0.1-8.0% max signal
Threshold	0.05-1.5% max signal
Typical closed loop electrohydraulic actuation system response (airborne applications)	3-20 cps at 90 deg phase shift

(2) Hydraulic Actuators - Some servo valves are built in integral assemblies with their actuators, permitting integral position feedbacks or more compact construction. For rotary actuation, four basic types of actuators are used:

(a) Conventional, Linear, Double - acting Actuator with Bellcrank Linkage - This type is the simplest from the standpoint of stress, sealing, and producibility, but often requires an excessive space envelope for the linkages. Further, the output is nonlinear and subject to backlash. The cosine effect of the bellcrank at actuation extremes requires a degree of oversizing of the actuator piston to account for the reduction of the lever arm.

(b) Linear, Single - acting Actuators in Push-Push Configuration - Actuator stress, sealing, and producibility are similar to a conventional actuator. An involute yoke results in a constant lever arm and zero backlash. Since two cylinders are required, the installed size and weight may be greater than a conventional linear actuator, depending upon the linkage requirements.

(c) Rotary Vane Type Actuator - Sealing and producibility problems are greater with this type of actuator, but space is more efficiently utilized. Less efficiently stressed parts indicate that the weight must be higher unless offset by the more compact rotary output without linkages.

(d) Multistroke Rotary or Piston Expanders - The use of multiple stroke expansion is the only basic way of reducing the actuator compliance in a compressible fluid system, and therefore it has dynamic response advantages when a compliant working fluid is used. Normally, the complexity is considerably greater, and gearing is required.

7.6 Valve Weights

Typical weights for check valves, electric motor - driven butterfly shutoff valves, and pneumatically actuated butterfly shutoff valves from 0.5-8.0 in. ID are shown in Figs. 3H-97, 3H-98, and 3H-99. The ranges shown represent an envelope of manufacturers' data for typical aircraft air valves. The variation in weight for a given valve type and size is attributable to the following factors:

(1) Design concept, type of construction.

(2) Performance requirements: maximum temperature, pressure, valve actuation speed, leakage, life.

(3) Mechanical requirements: flanges, fittings, mounting.

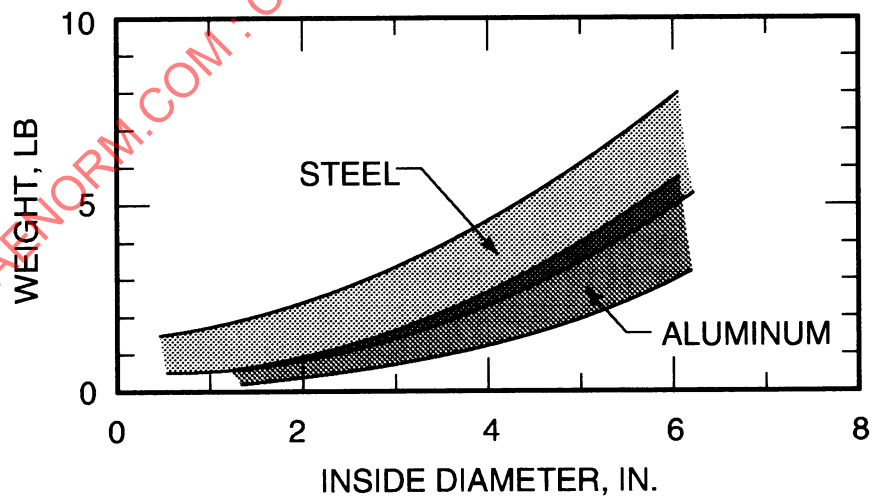

Figure 3H-97 - Weights of Typical Check Valves

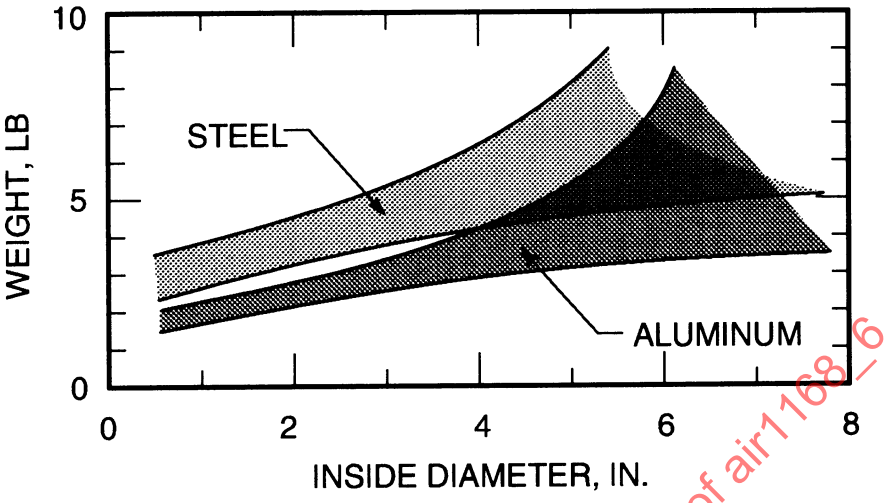

Figure 3H-98 - Weights of Typical Electric Motor Driven Butterfly Shutoff Valves

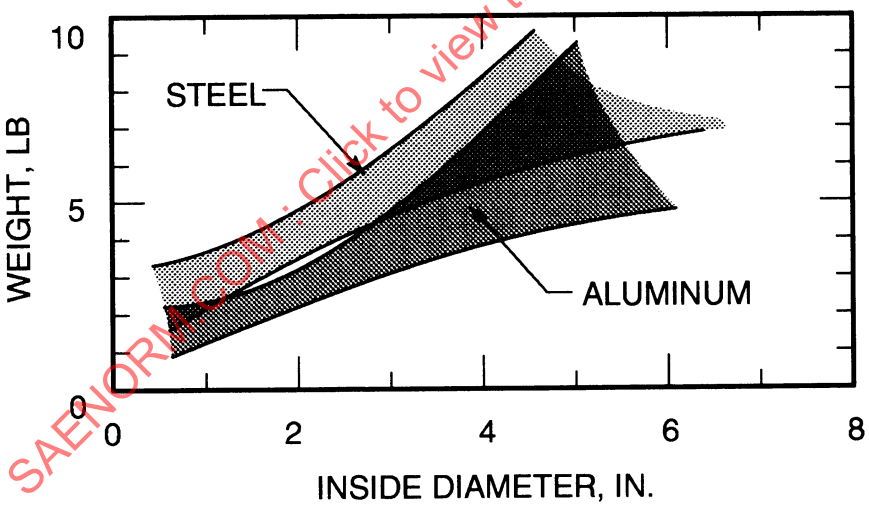

Figure 3H-99 - Weights of Typical Pneumatically Actuated Butterfly Shutoff Valves

7.7 References

Elaboration of the material on valves presented above can be found in Refs. 33-41.

8. HEAT EXCHANGERS

8.1 Nomenclature

A = Cross-sectional area, ft^2, $in.^2$
A_f = Fin area, ft^2
A_c = Minimum free flow area, ft^2
b = Plate spacing, in.
C = Heat capacity, Btu/sec-^oR
c = Wetted perimeter, ft
D_h = Hydraulic diameter of heat exchanger, ft
f = Fanning friction factor, dimensionless
F_g = Correction factor, dimensionless
G = Flow rate per unit area, W/A, lb/hr-ft^2
h = Heat transfer coefficient, Btu/hr-ft^2 - ^oR
j = Colburn parameter ($N_{St} N_{Pr}^{2/3}$), dimensionless
L = Total exchanger flow length, ft
L_f = Fin length, ft
$LMTD$ = Log mean temperature difference, ^oF
m = $\sqrt{hc/kA_f}$, dimensionless
n = Number of passes
NTU = Number of heat transfer units
N_{St} = Stanton No. , $h/g\ \rho\ Vc_p$ or h/Gc_p, dimensionless
N_{Pr} = Prandtl No. ,$\mu g c_p / k$, dimensionless
ΔP = Pressure loss, lb/ft^2
q = Rate of heat flow, Btu/sec
r_h = Heat exchanger hydraulic radius, ft
t = Temperature, ^oF
T = Temperature, ^oR
Δt = Temperature difference, ^oF
U = Overall thermal conductance, Btu/sec - ft^2 - ^oR
V = Velocity, ft/sec
W = Weight flow rate, lb/sec, lb/hr
x = $(t_{co} - t_{ci})/(t_{hi} - t_{ci})$, dimensionless
y = Distance, ft
z = $(t_{hi} - t_{ho})/(t_{co} - t_{ci}) = C_c/C_h$, dimensionless
α = Total heat transfer area/total volume, ft^2/ft^3
β = Total heat transfer area/volume between plates, ft^2/ft^3
ε = Effectiveness of heat exchanger, dimensionless
σ = free flow area/frontal area, dimensionless

Subscript

av	= Average
c	= Cold
f	= Fin
h	= Hot
i	= In
max	= Maximum
min	= Minimum
o	= Out
p	= Pass
ov	= Overall
tot	= Total

8.2 General Considerations

There are many places in aerospace vehicles where the transfer of heat is required. The use of compact airborne heat exchangers is extensive, and the utilization of compact units will continue to increase with the increasing complexity and advanced performance of aircraft and missiles. Many tasks are accomplished by heat exchangers; for example, aircraft air conditioning (heating and cooling), electronic equipment cooling, oil cooling, and a variety of other applications.

The utilization of various types of airborne heat exchangers may be grouped as follows (together with representative examples for each group):

(1) Air to Air - Examples: Primary and secondary air cycle refrigeration heat exchangers utilizing supercharger air and ambient (ram) air; ram air heat exchangers for cooling cabin supply air by means of ambient (ram) air.

(2) Air to Liquid - Examples: Ram air oil coolers, evaporator of vapor cycle refrigeration system utilizing cabin air and refrigerant, condenser of vapor cycle refrigeration system utilizing ambient (ram) air and refrigerant.

(3) Liquid to Liquid - Examples: Oil coolers, utilizing fuel as coolant; condenser of vapor cycle refrigeration system utilizing expendable water heat sink and refrigerant.

8.3 Basic Relationships for Heat Exchanger Design Definition

A heat exchanger is a device in which the two fluids exchanging thermal energy are separated by the heat transfer surface (see Figure 3H-99a).

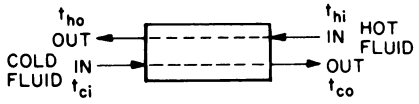

Figure 3H-99a - Typical Heat Exchanger Arrangement

8.3.1 Energy and Rate Equations

The following equations express the relationships.

Heat lost by hot fluid:

$$q_h = W_h c_{ph} (t_{hi} - t_{ho}) = C_h (t_{hi} - t_{ho}) \quad \text{(3H-99)}$$

Heat gained by cold fluid:

$$q_c = W_c c_{pc} (t_{co} - t_{ci}) = C_c (t_{co} - t_{ci}) \quad \text{(3H-100)}$$

Heat transfer rate equation:

$$\frac{dq}{dA} = U (t_h - t_c) \quad \text{(3H-101)}$$

Two methods exist for integrating the heat transfer rate equation:

(1) The heat exchanger effectiveness-*NTU* method (ε–*NTU*)

(2) The log mean temperature difference method *(LMTD)*

The *LMTD* method has been used extensively in the past. In the past few years, however, the effectiveness-*NTU* method has become the recommended and accepted method for heat exchanger calculations. Both methods are summarized, and the advantages of the effectiveness-*NTU* method are outlined below and compared to those of the *LMTD* method.

8.3.2 The Log Mean Temperature Difference Method

The rate of heat transferred through a differential element of area *dy* located a distance *y* from the entrance of the heat exchanger is (see figure 3H-99b)

$$dq = U\,dy\,(t_h - t_c) \tag{3H-102}$$

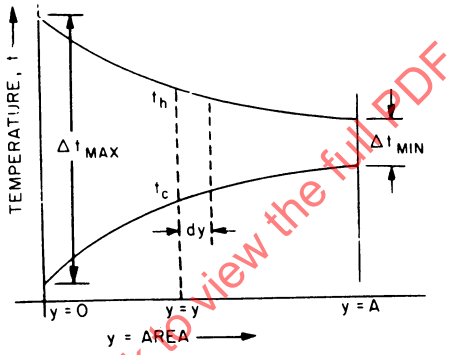

Figure 3H-99b - Example Of Hot and Cold Fluid Temperature Heat Exchange

It can be shown for counterflow and parallel flow heat exchangers (in addition to condensers and evaporators) that the total rate of heat, *q*, transferred through the total heat transfer area *A* is

$$q = UA\,(LMTD) \tag{3H-103}$$

where $$LMTD = \frac{\Delta t_{max} - \Delta t_{min}}{\ln \frac{\Delta t_{max}}{\Delta t_{min}}} \tag{3H-103a}$$

The *LMTD* must be altered for the more complex configurations of heat exchangers, that is, for shell and tube devices of multipass configuration, and for cross flow exchangers with different pass arrangements. Correction factors exist by which the *LMTD* for counterflow must be multiplied to give the true temperature difference. Designating the correction factor by F_g, the expression for the rate of heat transferred becomes

$$q = UAF_g\,(LMTD) \tag{3H-104}$$

8.3.3 The Heat Exchanger Effectiveness - *NTU* Method

The design of heat exchangers is simplified by collecting the various variables into a group of dimensionless parameters. This not only permits convenient computational procedures, but also visualization of the influence of the variables on heat exchanger performance. The following equations express these parameters.

Heat exchanger effectiveness ε:

$$\varepsilon = \frac{C_h (t_{hi} - t_{ho})}{C_{min} (t_{hi} - t_{ci})} = \frac{C_c (t_{co} - t_{ci})}{C_{min} (t_{hi} - t_{ci})} \quad \text{(3H-105)}$$

where C_{min} = Smaller of C_h and C_c magnitudes

C = Heat capacity = Wc_p

ε compares the actual heat transfer rate,

$$C_h (t_{hi} - t_{ho}) = C_c (t_{co} - t_{ci}) \quad \text{(3H-106)}$$

to the maximum possible heat transfer rate (realizable only in a counterflow heat exchanger of infinite heat transfer area).

NTU (number of exchanger heat transfer units):

$$NTU = \frac{AU_{av}}{C_{min}} = \frac{1}{C_{min}} \int_o^A U dA \quad \text{(3H-107)}$$

where A = Same transfer area used in the definition of U

The parameter *NTU* is a nondimensional expression of the "heat transfer" size of the exchanger. When the *NTU* value is small, the effectiveness is low, and when the *NTU* value is large, the effectiveness approaches asymptotically the limit imposed by the flow arrangement and thermodynamic considerations.

Consideration of the *AU* term in the *NTU* expression indicates the cost of attaining a high effectiveness: Increasing the area *A* means an increase in space, weight, and thus capitalization; increasing the *U* value means an increase in the power requirements to overcome the increased friction losses accompanying the higher film coefficients.

Capacity rate ratio:

$$\text{Capacity rate ratio} = \left(\frac{C_{min}}{C_{max}} \right) \quad \text{(3H-108)}$$

where C_{min} and C_{max} are, respectively, the smaller and the larger of the two magnitudes. Since the values represent energy storage rates in each stream per unit temperature change, they are used as parameters in plots of effectiveness versus *NTU* values. Therefore, it may be concluded:

$$\varepsilon = f\left(NTU, \left(\frac{C_{min}}{C_{max}}\right), \text{flow arrangement} \right) \tag{3H-109}$$

This function may be derived mathematically for each particular flow arrangement, the solutions for the various heat exchanger configurations being presented in a later section.

8.3.3.1 Advantages of Effectiveness-*NTU* Method

The effectiveness-*NTU* method for the solution of heat transfer problems possesses certain inherent advantages over the *LMTD* method:

(1) The effectiveness is a thermodynamically significant parameter (much like an efficiency factor).

(2) The effectiveness-*NTU* method clearly shows the application of both the heat transfer rate equation and the energy balance principles to heat exchanger design.

(3) The effectiveness-*NTU* approach simplifies the algebra involved in predicting the performance of complex flow arrangements.

8.3.4 Illustrative Examples

The following two examples show applications of the ε-*NTU* and *LMTD* methods.

(1) Given U, C_c, C_h, and terminal temperatures, determine area A.

ε-*NTU* Approach:

(a) Calculate ε and (C_{min}/C_{max}) ratio.

(b) Determine *NTU* value from proper curve.

(c) Calculate A from $A = NTU\ (C_{min}/U)$.

LMTD Approach:

(a) Calculate two parameters:

$$x = \frac{t_{co} - t_{ci}}{t_{hi} - t_{ci}}$$

$$z = \frac{t_{hi} - t_{ho}}{t_{co} - t_{ci}} = \frac{C_c}{C_h}$$

(b) Use proper curve plot to obtain $F_g = f(x,z)$.

(c) Calculate *LMTD*.

(d) Calculate q.

(e) Calculate $A = q/UF_g\ (LMTD)$.

Although both methods give a direct solution, the ε-*NTU* approach is quicker. In the following example, the ε-*NTU* approach gives a direct solution, whereas the *LMTD* method involves a trial and error solution.

(2) Given A, U, C_c, C_h, t_{hi}, and t_{ci}, determine t_{ho} *and* t_{co}.

ε-*NTU* Approach:

(a) Calculate *NTU* and (C_{min}/C_{max}).

(b) Find ε from proper flow configuration curve.

(c) Calculate q from

$$q = C_{min}\varepsilon(t_{hi} - t_{ci})$$

(d) Determine terminal temperatures from

$$q = C_c(t_{co} - t_{ci})$$
$$q = C_h(t_{hi} - t_{ho})$$

LMTD Approach:

(a) Calculate z from C_c/C_h.

(b) Assume terminal temperatures so as to evaluate first approximation of x.

(c) Obtain F_g (first approximation) from proper configuration curve.

(d) Evaluate first approximation of *LMTD*.

(e) Calculate first approximation of q from rate equation.

(f) Calculate terminal temperatures and compare with item b.

(g) Repeat for new values of terminal temperatures until satisfactory agreement is obtained.

8.3.5 Definition of Overall Fin Effectivenes

The following equations apply.

$$\eta_f = \frac{\text{Amount of heat actually dissipated from fin}}{\text{Amount dissipated if all fin surface was at root temperature}} \quad \text{(3H-110)}$$

η_{ov} = Weighted average of 100% effective prime surface and less than 100% effective fin surface

= Overall fin effectiveness

= Total surface temperature effectiveness

$$= 1-(A_f/A)(1-\eta_f) \quad \text{(3H-111)}$$

where A_f = Fin surface area (secondary surface)

A = Total heat transfer surface area (primary plus secondary)

$$\eta_f = \frac{\tanh(mL_f)}{(mL_f)}$$

for which $$m = \sqrt{\frac{hc}{kA_f}}$$

L_f = Fin length

8.3.6 Heat Exchanger Overall Coefficient of Heat Transfer

Two equations apply.

$$\frac{1}{A_h U_h} = \frac{1}{A_h \eta_{ho} h_h} + \frac{x}{A_w k} + \frac{1}{A_c \eta_{co} h_c}$$

$$= \frac{1}{A_c U_c} = \frac{1}{AU} \quad \text{(3H-112)}$$

Therefore $A_h U_h = A_c U_c = AU$ (3H-113)

In these equations $1/U$ is the overall thermal resistance, consisting of the following series components:

(1) Hot side film convection component, including the temperature ineffectiveness on the extended area of the hot side.

(2) A wall conduction component. Very often the wall resistance value is negligible and may be omitted. A_w denotes the prime surface area.

(3) Cold side film convection component, including the temperature ineffectiveness on the extended area on this side.

(4) Fouling factors to allow for service scaling or fouling on both sides may also be included. These factors are omitted from the present discussion.

Note: The value U_h in Eq. 3H-113 is based on the total heat transfer area A_h, which includes both the prime and the fin or extended area. Likewise, U_c is based on the total heat transfer area of the cold side, A_c.

8.3.7 Heat Exchanger Hydraulic Diameter and Hydraulic Radius

For this parameter:

$$r_h = \frac{\text{Cross-sectional area}}{\text{Wetted perimeter}} = \frac{A_c L}{A} \quad \text{(3H-114)}$$

where A_c = Exchanger minimum free-flow area, ft^2

A = Exchanger total heat transfer area on one side, ft^2

The hydraulic diameter, D_h, is used as the characteristic dimension in the Reynolds number of the heat exchanger.

$$D_h = 4r_h$$

8.4 Types of Heat Exchangers and Their Operating Characteristics

Both direct and indirect transfer types are discussed here.

8.4.1 Direct Transfer Types

Heat exchangers may be conveniently subdivided into a number of general classes according to the method of operation.

8.4.1.1 Counterflow

Fluids flow in a direction opposite to each other, as shown in Fig. 3H-99c.

$$\varepsilon = \frac{1-e^{-NTU\left[1-(C_{min}/C_{max})\right]}}{1-\left(\frac{(C_{min})}{(C_{max})}\right)e^{-NTU\left[1-(C_{min}/C_{max})\right]}} \qquad \text{(3H-115)}$$

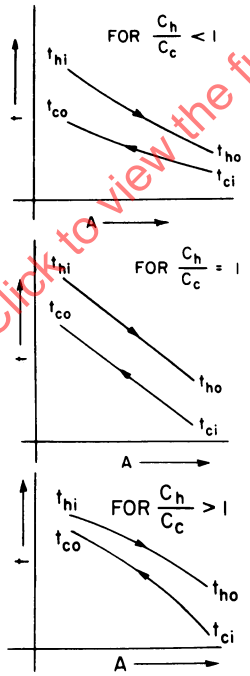

Figure 3H-99c - Example of Counterflow Temperature Changes

For a liquid-gas counterflow heat exchanger where $(C_{max} >> C_{min})$, $(C_{min}/C_{max}) \rightarrow 0$ and the effectiveness value reduces to

$$\varepsilon = 1 - e^{-NTU}$$

For a gas-to-gas heat exchanger (counterflow) where ($C_{min} \approx C_{max}$), (C_{min} / C_{max}) $\rightarrow$ 1 and the effectiveness value reduces to

$$\varepsilon = \frac{NTU}{1 + NTU} \tag{3H-116}$$

The plot of the effectiveness for increasing *NTU* values and for various capacity rate ratios is given in Fig. 3H-100.

The following generalized rules for counterflow heat exchanger operation may be formulated:

(1) The effectiveness for counterflow operation is higher than for any other type of heat exchanger; therefore, it is a useful standard of comparison.

(2) The effectiveness approaches unity as the *NTU* value becomes progressively larger in magnitude for all capacity rate ratios.

(3) The smaller the capacity rate ratio, the greater the heat exchanger effectiveness.

(4) True counterflow operation is not often utilized in practice because of header and ducting difficulties.

8.4.1.2 Parallel Flow

Fluids flow in the same direction, as shown in Fig. 3H-100a

$$\varepsilon = \frac{1 - e^{-NTU\left[1 + \left(C_{min}/C_{max}\right)\right]}}{1 + \left(C_{min}/C_{max}\right)} \tag{3H-117}$$

The effectiveness-*NTU* plot is presented in Fig. 3H-101.

For (C_{min}/C_{max}) $\rightarrow$ 0:

$$\varepsilon = 1 - e^{-NTU} \text{ (identical to Counterflow type)} \tag{3H-118}$$

For (C_{min}/C_{max}) $\rightarrow$ 1:

$$\varepsilon = \frac{1 - e^{-2\,NTU}}{2} \tag{3H-119}$$

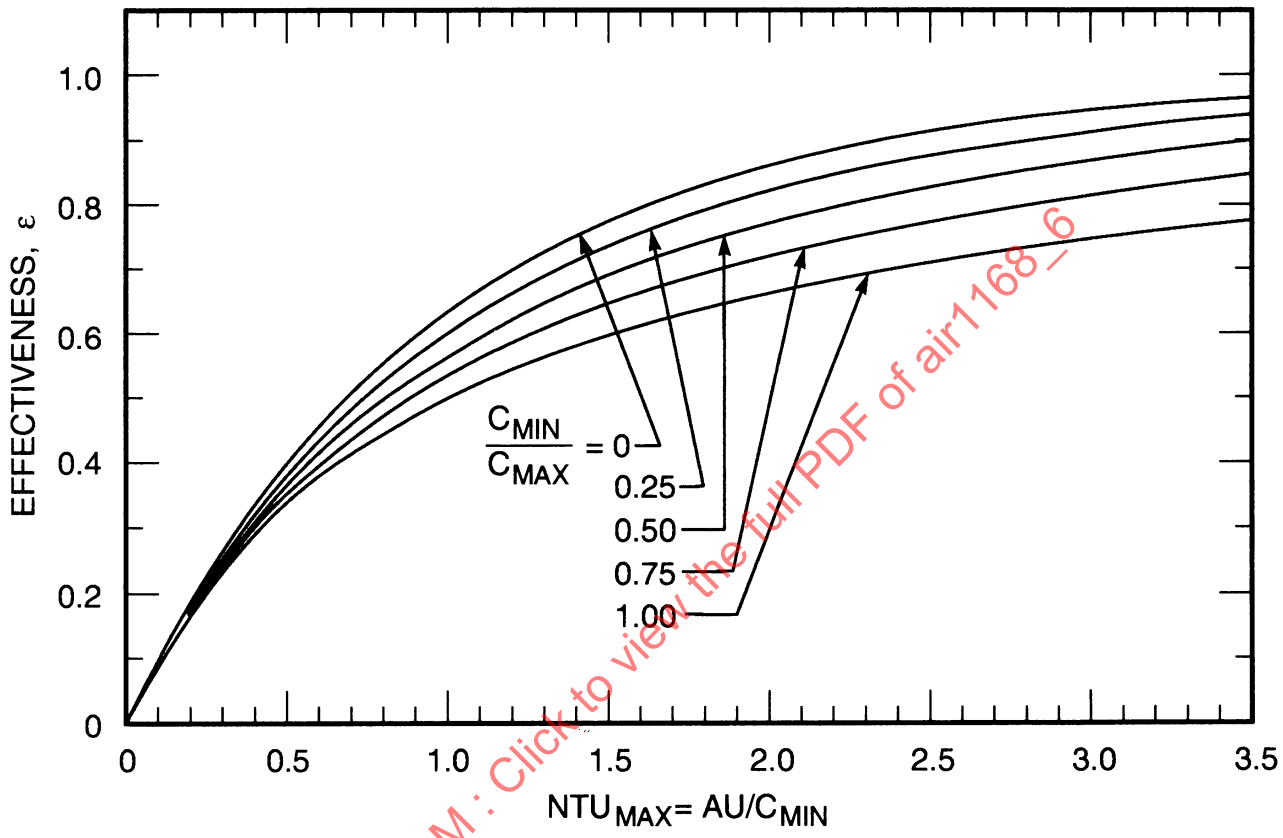

Figure 3H-100 - Effectiveness Versus *NTU* for Various Capacity Rate Ratios of Counterflow Heat Exchanger

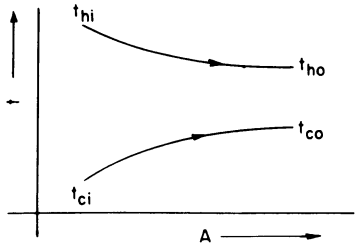

Figure 3H-100a - Example of Parallel Flow Temperature Changes

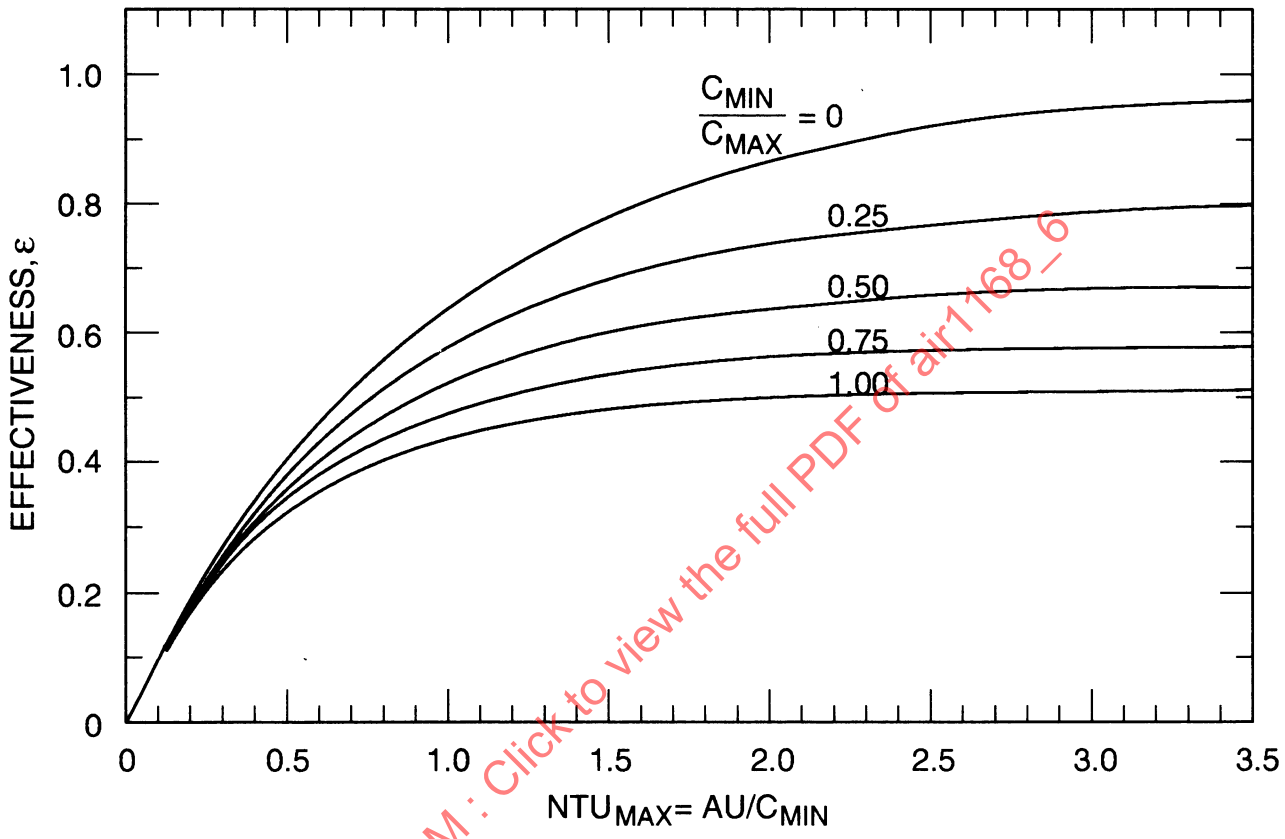

Figure 3H-101 - Effectiveness Versus *NTU* for Various Capacity Rate Ratios of Parallel Flow Heat Exchanger

The following generalized rules for parallel flow heat exchanger operation may be formulated:

(1) The effectiveness approaches unity, for large values of *NTU*, only for a capacity rate ratio = 0. For all other capacity rate ratios, the effectiveness is less than unity as the *NTU* values become infinitely large.

(2) The effectiveness of a parallel flow heat exchanger, for a capacity rate ratio = 0, is the same as that for the counterflow heat exchanger.

(3) For all capacity rate ratios greater than zero, the effectiveness of a parallel flow heat exchanger is substantially lower than that for the counterflow type.

8.4.1.3 Cross Flow Exchangers

One fluid flows at an angle (usually 90 deg) to the other fluid, as shown in Fig 3H-101a. Examples are tube banks, plate fin, and finned tubes.

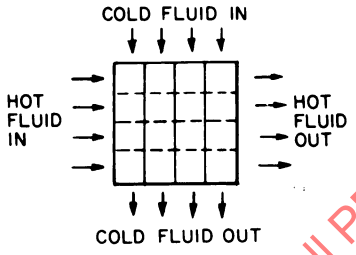

Figure 3H-101a - Typical Heat Exchange Arrangement For a Cross Flow Exchanger

The mathematical expressions for the effectiveness become complex for heat exchanger types other than counterflow and parallel flow. For the cross flow heat exchanger, the graph of Fig. 3H-102 gives the relationship of the effectiveness versus *NTU* values for various capacity rate ratios.

For cross flow heat exchangers, the effectiveness approaches unity asymptotically (similar to counterflow) as the NTU values increase. However, for all capacity rate ratios greater than zero, the effectiveness of a cross flow heat exchanger for a given *NTU* value is less than that for a counterflow heat exchanger.

Because the cross flow heat exchanger performs better than a parallel flow heat exchanger, and since the header configuration is convenient, the cross flow heat exchanger is widely utilized in the aircraft industry.

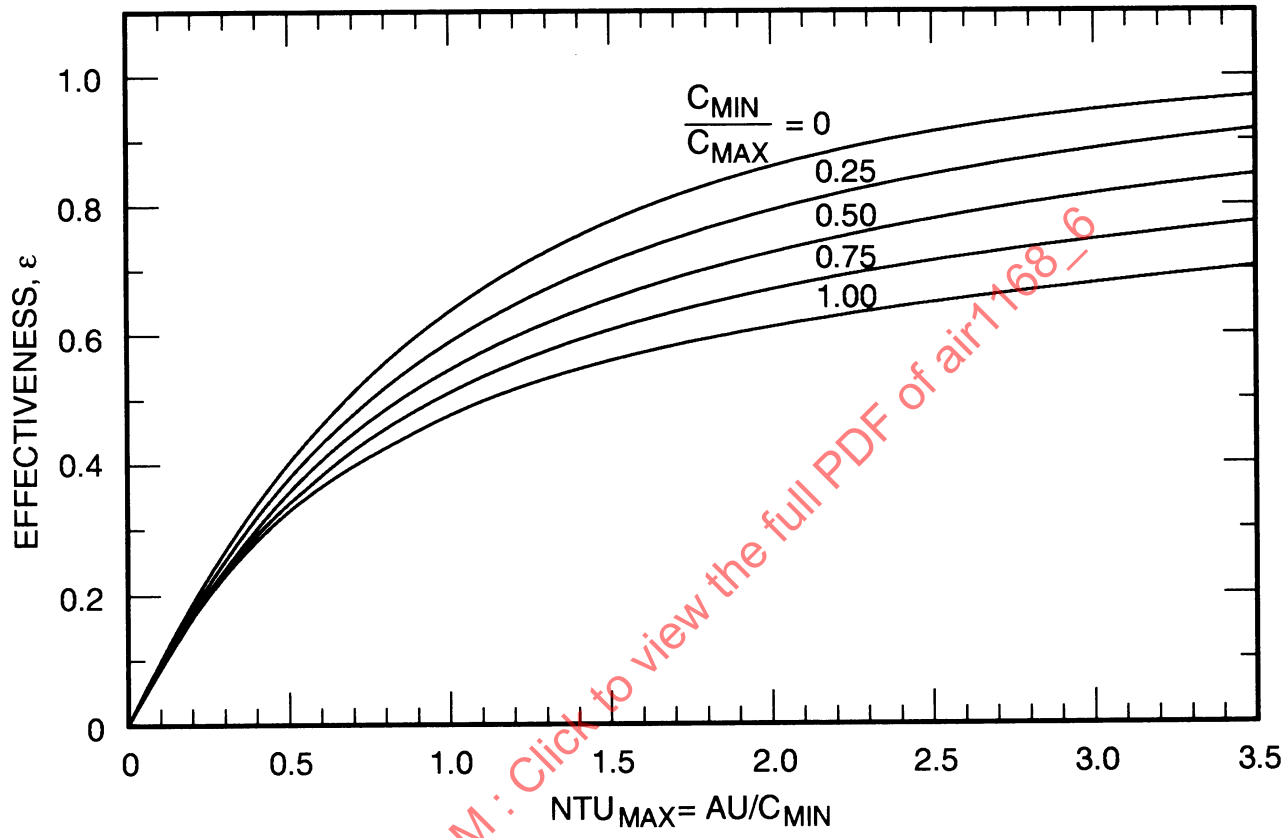

Figure 3H-102 - Effectiveness Versus *NTU* for Various Capacity Rate Ratios of Cross Flow Heat Exchanger

8.4.1.4 Condensers and Evaporators

Condensers and evaporators (also called boilers) may both be considered as special cases of the preceding types. Typical performance is plotted in Fig. 3H-102a.

Since for condensers and evaporators the fluid changing phase remains at a constant temperature throughout the exchanger, its specific heat is by definition equal to infinity. Therefore,

$$C_{max} = \infty \quad and \quad \left(\frac{C_{min}}{C_{max}} \right) = 0$$

$$\varepsilon = 1 - e^{-NTU} \qquad (3H\text{-}120)$$

Also, for condensers,

$$\varepsilon = \frac{t_{co} - t_{ci}}{t_h - t_{ci}} \tag{3H-121}$$

and for evaporators or boilers,

$$\varepsilon = \frac{t_{hi} - t_{ho}}{t_{hi} - t_c} \tag{3H-122}$$

It is evident that the performance of an evaporator or a condenser is independent of the direction of evaporating or condensing fluid flow. Therefore, from performance considerations, there is no advantage in using a counterflow heat exchanger over a cross flow heat exchanger.

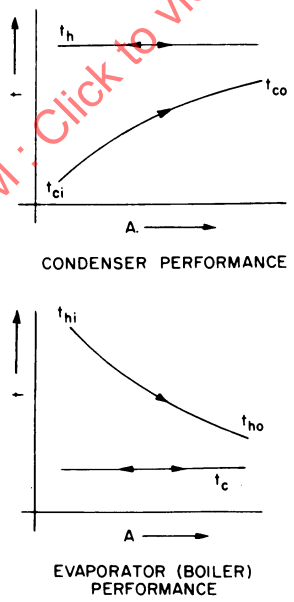

Figure 3H-102a - Example of Cross Flow Temperature Changes

8.4.1.5 Parallel Counterflow, Shell Fluid Mixed

For a parallel counterflow (1 shell pass, 2, 4, 6 ... tube passes) shell fluid mixed heat exchanger (one of the most common arrangements for shell and tube heat exchangers), the effectiveness is always less than unity, for all capacity rate ratios greater than zero, as the *NTU* value approaches infinity. Refer to Fig. 3H-102b.

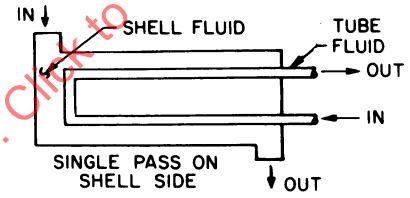

Figure 3H-102b - Heat Exchanger Arrangement for a Parallel Counterflow, Shell Fluid Mixed Heat Exchanger

As the number of passes n increases (that is, 2 shell passes, 4, 8, 12 ... tube passes; 3 shell passes, 6, 12, 18 ... tube passes), the performance of the multipass unit approaches that for a counterflow unit (achieved when n approaches infinity). Practical considerations, however, limit the number of passes to three or four.

Values of the effectiveness are shown in Fig. 3H-103 for the single pass configuration with 2, 4, 6 ... tube passes.

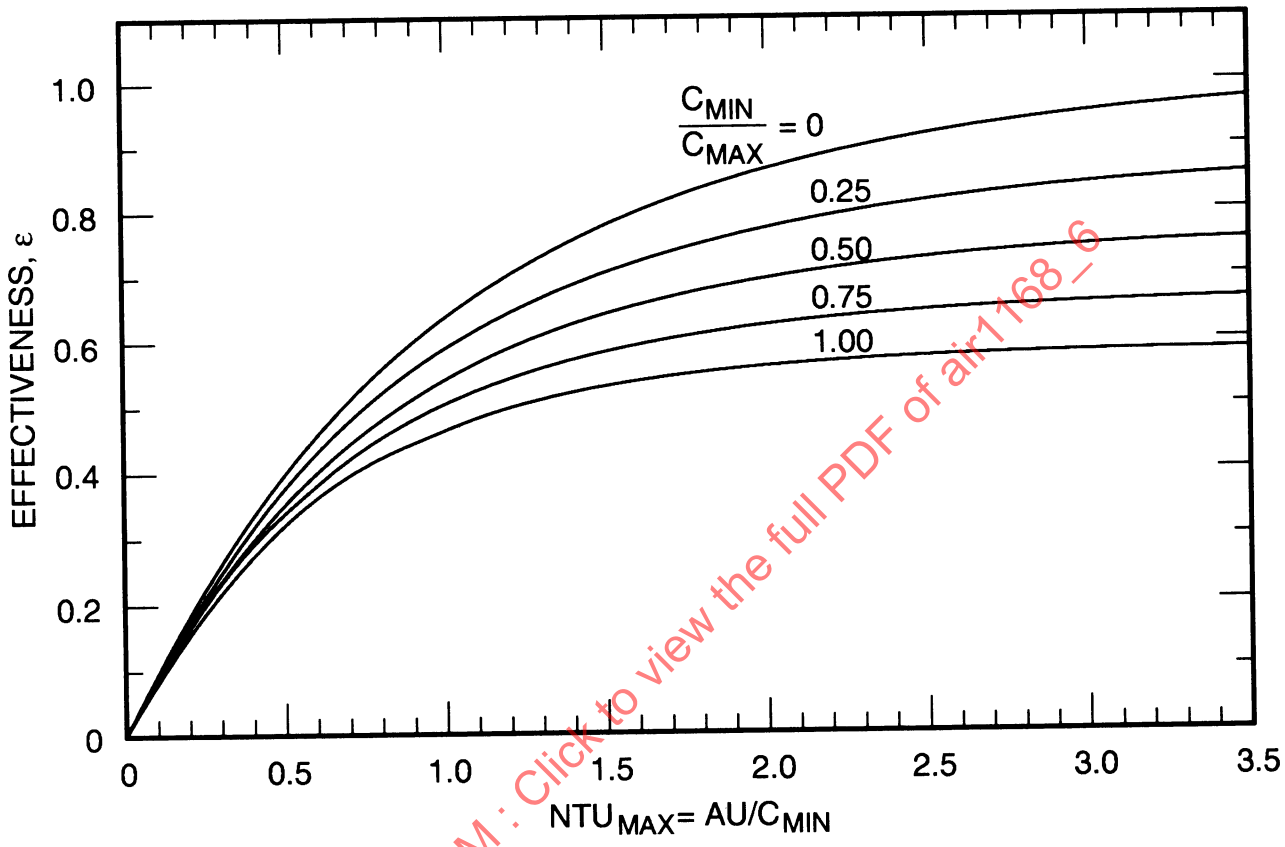

Figure 3H-103 - Effectiveness Versus NTU of Parallel Counterflow Exchanger with Shell Fluid Mixed

8.4.1.6 Summary

The relative merits and performance characteristics of the more common types of heat exchangers are compared in Fig. 3H-104. It can be seen that the poorest performance is obtained for a parallel flow configuration. In general, it must be remembered that as the capacity rate ratio approaches zero, all flow arrangements have the same performance.

For example, the capacity rate ratio is zero for condensers and evaporators. For all other values of the capacity rate ratio greater than zero, the effectiveness of the counterflow configuration is the highest. The difference in performance for the various exchangers is a maximum for capacity rate ratios of 1, as illustrated in Fig. 3H-104.

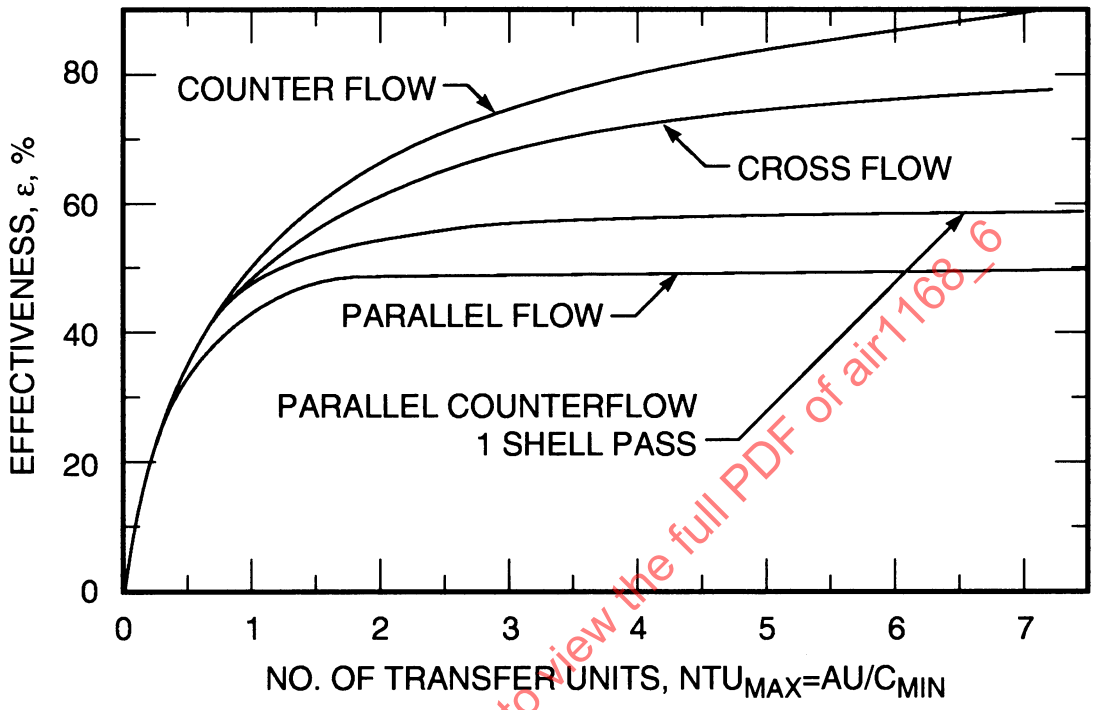

Figure 3H-104 - Exchanger Performance Effect of Flow Arrangement for $(C_{min}/C_{max}) = 1$

8.4.2 Liquid Coupled, Indirect Type Heat Exchangers

The liquid coupled heat exchanger system, defined in paragraph 8.3, introduces no additional new concepts to those already covered. Each heat exchanger may be designed separately, utilizing the effectiveness versus NTU relationships that are appropriate. The relative merits and disadvantages are discussed below.

Advantages:

(1) Less awkward heat exchanger shapes result, especially for a large density disparity between the cold and hot fluid, since the hot fluid flow area is not tied directly to the cold fluid flow area.

(2) If the cold and hot fluids are gases, and a liquid is utilized for coupling, a better and more compact arrangement may result.

Disadvantages:

(1) Greater heat transfer area is required (up to 20%).

(2) The system and its controls become more complicated with the addition of the coupling liquid.

(3) There is a lack of a universally satisfactory coupling liquid. Typical circulating fluids are water, water and ethylene glycol mixture, and liquid metals.

8.4.3 Multipass Configurations

A close approximation to counterflow performance can be achieved by multipassing on one side of a heat exchanger; that is, by multipassing a cross flow heat exchanger, as shown in Fig. 3H-104a. Usually, more than three or four passes are not warranted.

Given that ε_p = Effectiveness of each pass

n = Number of identical passes

ε = Overall effectiveness of the multipass configuration

then $\varepsilon_p = f(NTU/\text{n}, \text{basic flow configuration of the pass})$ (3H-123)

In general

$$\varepsilon = \frac{\left[\dfrac{1-(\varepsilon_p C_{min}/C_{max})}{1-\varepsilon_p}\right]^n - 1}{\left[\dfrac{1-(\varepsilon_p C_{min}/C_{max})}{1-\varepsilon_p}\right]^n - \left(\dfrac{C_{min}}{C_{max}}\right)} \quad (3H\text{-}124)$$

For the special case of $(C_{min}/C_{max}) = 1$,

$$\varepsilon = \frac{n\,\varepsilon_p}{1+(n-1)\,\varepsilon_p} \quad (3H\text{-}125)$$

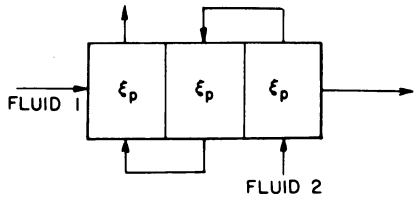

Figure 3H-104a - Heat Exchanger Arrangement for Multipass Configurations

8.5 Heat Exchanger Pressure Losses

The total pressure loss in a heat exchanger core may be divided into three parts:

(1) Entrance Pressure Losses - Due to the abrupt contraction of the fluid in going from the entrance header into the exchanger core.

(2) Core Pressure Losses - Due to friction through the core of the heat exchanger plus a pressure loss or gain due to flow acceleration or deceleration as the flow density changes through the heat exchanger. This loss or gain is usually a very small portion when compared with the friction loss.

(3) Exit Pressure Loss - Due to the abrupt expansion of the fluid in passing from the core into the exit header. There is also a pressure rise portion due to the increased area change alone without friction (static regain effect).

In addition, intermediate header losses for multipass arrangements, pressure losses in inlet and exit headers, and losses associated with connecting ducting must be added separately to the core loss.

Entrance and exit losses or gains normally provide only a small contribution to the overall pressure loss through a heat exchanger core, since the core friction term controls the magnitude of the pressure drop, owing to the large value of heat transfer surface area to free flow area. Therefore, the entrance and exit effects may usually be neglected.

The friction pressure loss through a heat exchanger core may be computed as follows:

$$\Delta p = \frac{\rho g V^2}{2g} f \frac{A}{A_c} \qquad \text{(3H-126)}$$

The Fanning friction factor f is plotted in Figs. 3H-105 through 3H-109 versus Reynolds number for various heat exchanger core arrangements.

In a liquid-to-liquid heat exchanger, accurate knowledge of the friction characteristics of heat transfer surfaces is relatively unimportant because of the low power requirements for pumping high density fluids. For gases, however, because of their low density, the friction losses assume an importance equal to that of the heat transfer characteristics.

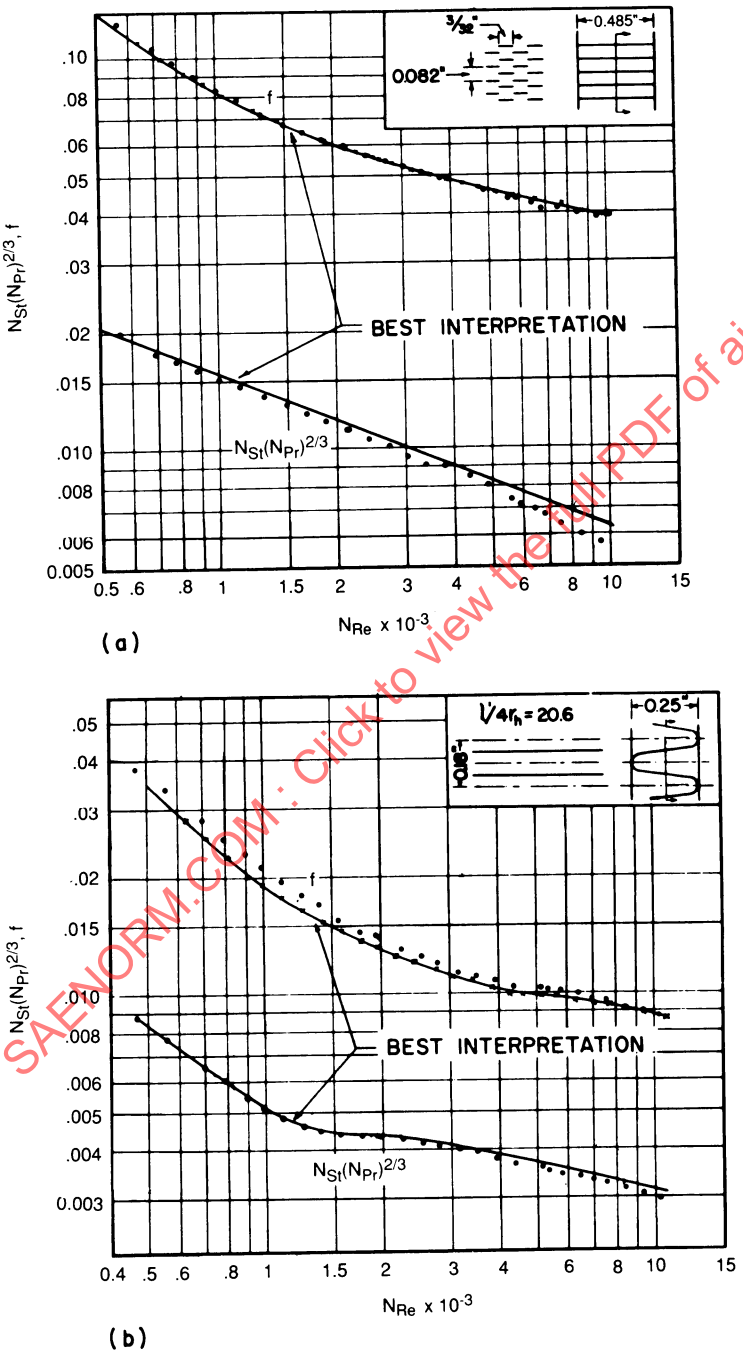

Figure 3H-105 - Plate Fins: (a) plain plate fin; (b) strip plate fin; $N_{Re} = 4r_h G/\mu$

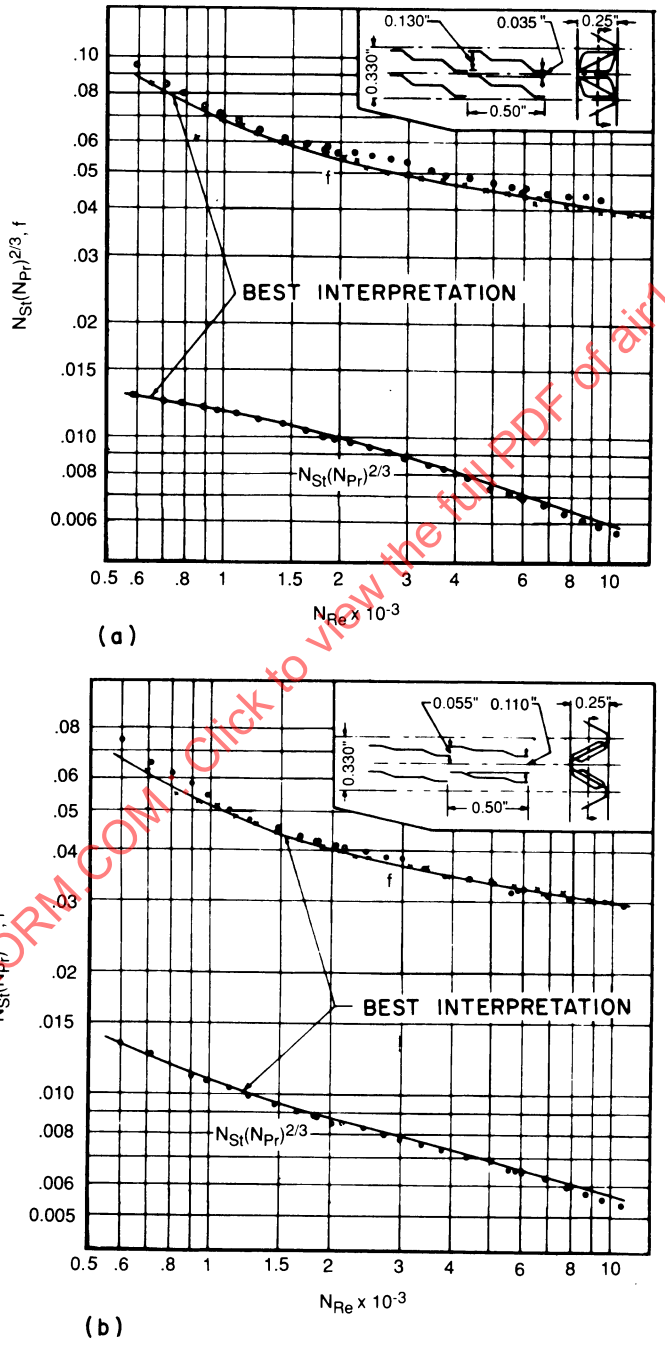

Figure 3H-106 - Louvered Plate Fins; N_{Re} =4 $r_h G/\mu$

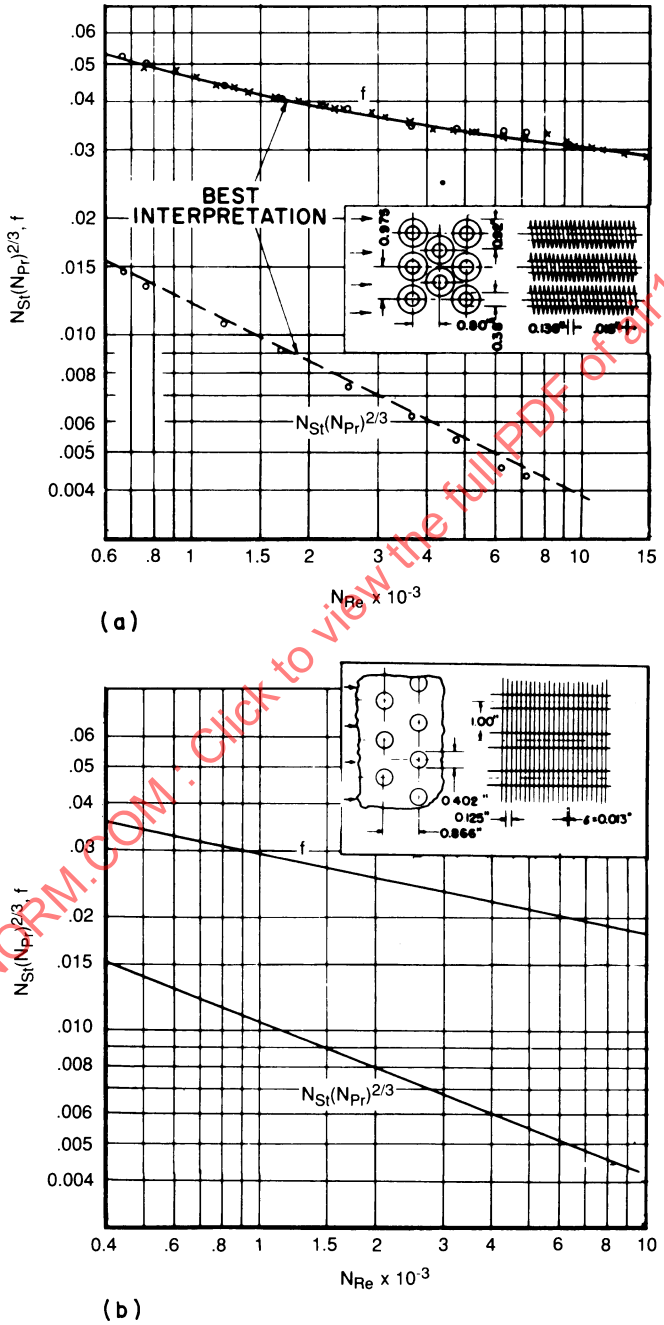

Figure 3H-107 - Finned Circular Tubes; $N_{Re} = 4r_h G/\mu$

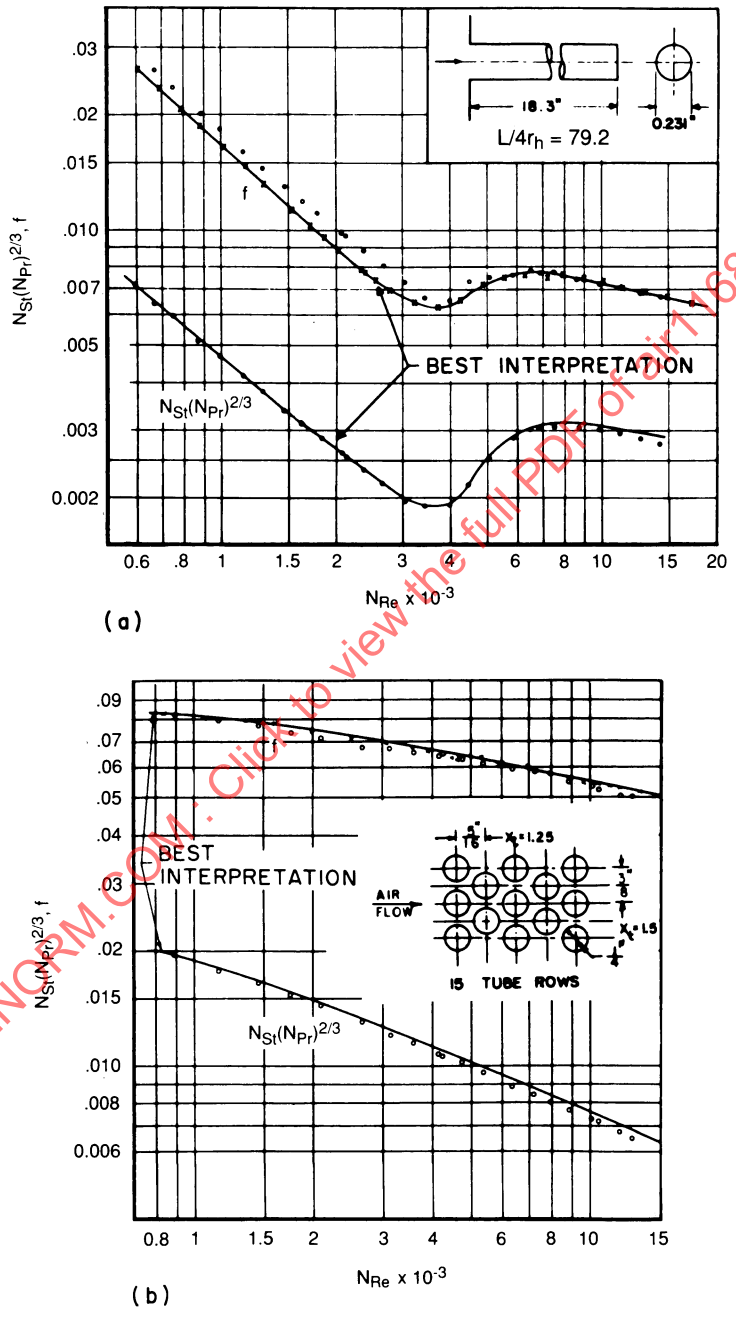

Figure 3H-108 - Tubular Surfaces: (a) flow inside circular tubes; (b) flow normal to a staggered tube bank (steady-state test data); $N_{Re} = 4r_hG/\mu$

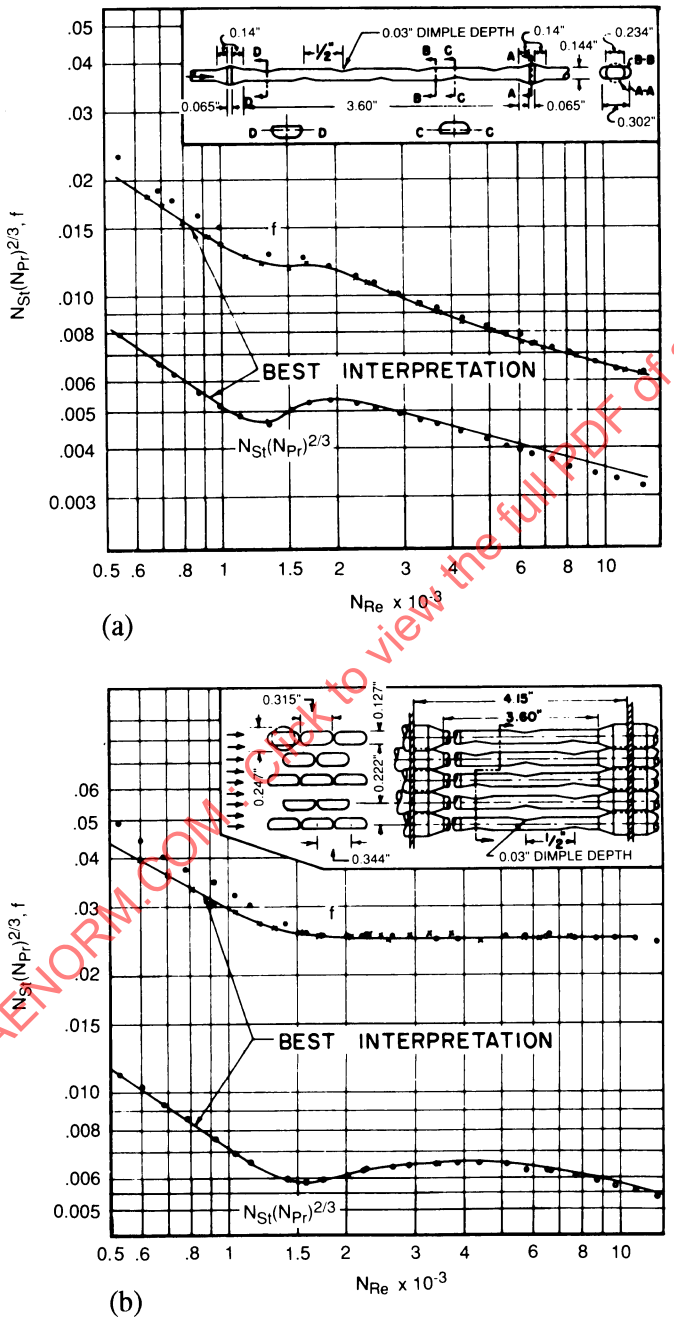

Figure 3H-109 - Dimpled Flattened Tubes; $N_{Re} = 4r_hG/\mu$

8.6 Compact Airborne Heat Exchangers

A number of different compact surface heat exchangers are being manufactured for various airborne applications. Representative samples have been selected and their characteristics are summarized below.

8.6.1 Plate-Fin Surfaces

Many fin and flow channel arrangements are possible. A plain plate-fin and a strip fin are shown in Fig. 3H-105 and a louvered fin in Fig. 3H-106.

For Fig. 3H-105(a):

Fin pitch	= 12.22/in.
b	= 0.485 in.
Fin length	= 0.094 in.
$4r_h$	= 0.01120 ft
Fin metal thickness	= 0.004 in.
β	= 340 ft^2/ft^3
A_f/A_{tot}	= 0.862

Fins are staggered symmetrically.

Note: Fin leading and trailing edges are slightly scarfed from the fin cutting operation. Friction factors may be lower with clean fins.

For Fig. 3H-105(b):

Fin pitch	= 11.1/in.
b	= 0.250 in.
$4r_h$	= 0.01012 ft
Fin metal thickness	= 0.006 in.
β	= 367 ft^2/ft^3
A_f/A_{tot}	=0.756
$1'/4r_h$	= 20.6

For the louvered plate - fin in Fig. 3H-106(a) and (b):

Fin pitch	= 6.06 /in.
b	= 0.250 in.
Louver spacing	= 0.50 in.
Fin gap	= 0.035 in.
Louver gap	= 0.130 in.
$4r_h$	= 0.01460 ft
Fin metal thickness	= 0.006 in.
β	= 256 ft^2/ft^3
A_f/A_{tot}	= 0.640

For the louvered fin in Fig. 3H-106(b):

Fin pitch	= 6.06 /in.
b	= 0.250 in.
Louver spacing	= 0.50 in.
Fin gap	= 0.110 in.
Louver gap	= 0.055 in.
$4r_h$	= 0.01460 ft
Fin metal thickness	= 0.006 in.
β	= 256 ft^2/ft^3
A_f/A_{tot}	=0.640

The major advantages of these surfaces are:

(1) They lend themselves to applications where both fluids are gases, since extended surfaces can be effectively employed on both fluid sides.

(2) A very large area compactness (heat transfer area per unit volume) is possible.

(3) Much flexibility in design is possible since the two fluid sides are independent of each other and the most suitable surface can be chosen for each of the fluids. Thus plate-fin surfaces also lend themselves to liquid/gas applications.

8.6.2 Finned Tube Surfaces

Many variations are possible; that is, circular tubes with circular spiraled fins [Fig. 3H-107(a)], circular tubes with continuous fins [Fig. 3H-107(b)], or finned flat tubes.

For Fig. 3H-107(a):

Tube OD	= 0.38 in.
Fin pitch	= 7.34 /in.
$4r_h$	= 0.0154 ft
Fin thickness (avg)	= 0.018 in.
σ	= 0.538
α	= 140 ft^2/ft^3
A_f/A_{tot}	=0.892

Fin thickness is slightly tapered.

Note: Experimental uncertainty for heat transfer results is possibly somewhat greater than the nominal ± 5% quoted for the other surfaces because of the necessity of estimating a contact resistance in the bimetal tubes.

For Fig. 3H-107(b):

Tube OD	= 0.402 in.
Fin pitch	= 8.0/in.
$4r_h$	= 0.01925 ft
Fin thickness	= 0.013 in.
σ	= 0.534
α	= 179 ft^2/ft^3
A_f/A_{tot}	=0.839

Note: Minimum free flow is in spaces transverse to flow. These data are included in this compilation because they apply to a compact surface configuration of considerable technical interest for which no data have been obtained for this type.

These surfaces lend themselves to applications where one fluid is a gas and the other is a liquid, since the external (gas side) surface area is usually many times the internal (liquid side) surface area. These surfaces usually are not as compact as the plate-fin types.

8.6.3 Tubular Surfaces

Test data for flow both inside [Fig. 3H-108(a)] and normal to the tube banks [Fig. 3H-108(b)] are presented. Dimpled flattened tube data are given in Fig. 3H-109.

For Fig. 3H-108(a):

Tube ID	= 0.231 in.
$4r_h$	= 0.01925 ft
$L\backslash 4r_h$	= 79.2

$$\frac{\text{Free flow area}}{\text{Tube}} = 0.0002908 \text{ ft}^2$$

For Fig. 3H-108(b):

Tube OD	= 0.250 in.
$4r_h$	= 0.0166 ft
σ	= 0.333
α	= 80.3 ft^2/ft^3

Note: Minimum free flow area is in spaces transverse to flow.

For Fig. 3H-109(a):

Tube ID before flattening	= 0.234 in.
Tube inside dimension perpendicular to flats	= 0.144 in.
Tube inside dimension parallel to flats	= 0.302 in.
Length of flat along tube	= 3.60 in.
Length of section from flat-to-circular-to-flat cross section	= 0.345 in.
Dimple depth	= 0.03 in.
Minimum distance between dimples	= 0.5 in.
$4r_h$	= 0.01116 ft
Minimum free flow area per tube	= 0.000169 ft^2

For Fig. 3H-109(b):

Tube OD (before flattening)	= 0.247 in.
Distance between centers parallel to flow	= 0.344 in.
Distance between centers perpendicular to flow	= 0.222 in.
Tube dimension parallel to flow	= 0.315 in.
Tube dimension perpendicular to flow	= 0.127 in.
Distance between spacing plates	= 4.15 in.
Length of flat along tube	= 3.60 in.
Dimple depth	= 0.03 in.
Minimum distance between dimples along tube	= 0.5 in.
$4r_h$	= 0.016 ft
α	= 121.9 ft^2/ft^3
σ	= 0.423

The advantages for these surfaces are:

(1) Simplest form of compact heat transfer surfaces.

(2) Dimpling tubular surfaces increases the boundary layer interruption, thus increasing the heat transfer without increasing the flow velocity.

(3) Tube banks may be utilized with a staggered or in-line tube pattern.

8.7 Heat Exchanger Design Procedure

Most manufacturers of heat exchangers have correlated and organized experimental and geometric configuration data for particular units into various forms of graphs, nomographs, tables, and simplified equations, to permit rapid computation of heat exchanger performance. The manufacturer must supply, in one form or another, data specifying the heat transfer performance, pressure losses through the particular unit, and certain configuration parameters. The basic procedure of calculating heat exchanger sizes or performance remains the same, regardless of the form of the supplied data.

A basic form for the presentation of heat exchanger design data was shown in Figs. 3H-105 through 3H-109. Both the heat transfer and pressure loss data are included as a function of the Reynolds number. The heat transfer performance is summarized by means of the Colburn parameter ($j = (N_{St}) \cdot (N_{Pr})^{2/3}$. The pressure loss data are summarized by the Fanning friction factor (f).

The calculation of a heat exchanger size to accomplish a specific application is a trial-and-error iterative procedure. First, the required heat transfer size of the heat exchanger is determined:

$$UA_{required} = NTU(C_{min}) \qquad \text{(3H-127)}$$

Secondly, a heat exchanger size is assumed, and the heat transfer size of this exchanger is computed from

$$UA_{available} = \frac{1}{(1/A_h\eta_{ho}h_h) + (1/A_c\eta_{co}h_c)} \quad \text{(3H-128)}$$

The wall conduction component has been neglected.

The data provided will enable the computation of the UA value for the particular assumed size. The value of $UA_{available}$ is compared with the value of $UA_{required}$. When the two values agree, the heat exchanger meets the required heat transfer performance.

The pressure data are then checked. If the two UA values do not agree, the heat exchanger dimensions are altered until the two values check. This trial-and-error routine converges rather rapidly, and usually four or five trials are sufficient.

8.8 References

Elaboration of the material on heat exchangers presented above can be found in Refs. 42-44.

9. REFERENCES

1. A. J. Stepanoff, Centrifugal and Axial Flow Pumps. New York: John Wiley Sons, Inc., 1948.
2. G. F. Wislicenus, Fluid Mechanics of Turbo-Machinery. New York: The McGraw-Hill Book Company Inc., 1947.
3. R. L. Daugherty and A. C. Ingersoll, Fluid Mechanics with Engineering Applications, 5th ed. New York: The McGraw-Hill Book Company Inc., 1954.
4. T. G. Hicks, Pump Selection and Application. New York: The McGraw-Hill Book Company Inc., 1957.
5. J. R. Gaddell, Fluid Flow in Practice. New York: Reinhold Publishing Corp., 1956.
6. L. S. Marks, Mechanical Engineer's Handbook. New York: The McGraw-Hill Book Company Inc., 1951.
7. A. H. Church, Centrifugal Pumps and Blowers. New York: John Wiley and Sons, Inc., 1947.
8. A. J. Stepanoff, Turbo Blowers. New York: John Wiley and Sons, Inc., 1955.
9. R. D. Madison, Fan Engineering. Buffalo, New York: Buffalo Forge Co., 1948.
10. C. Keller and L. S. Marks, Axial-Flow Fans. New York: The McGraw-Hill Book Company Inc., 1937.
11. A. H. Church, Centrifugal Pumps and Blowers. New York: John Wiley and Sons, Inc., 1947.

12. C. H. Berry, Flow and Fan. New York: Industrial Press, 1954.

13. V. M. Faires, Applied Thermodynamics. New York: The Macmillan Company, 1949.

14. D. G. Shepherd, Principles of Turbo-machinery. New York: The Macmillan Company, 1956.

15. D. G. Samaras and R. A. Tyler, "The Relative Merits of Rotary Compressors," J. Aeronaut. Sciences, Vol. 15, 1948, p. 625.

16. H. A. Sorensen, Gas Turbines. New York: The Ronald Press Company, 1951.

17. G. F. Wislicenus, Fluid Mechanics of Turbomachinery. New York: The McGraw-Hill Book Company Inc., 1947.

18. A. J. Stepanoff, Turbo-blowers. New York: John Wiley and Sons, Inc., 1955.

19. Staff of The Guggenheim Aeronautical Laboratory and The Jet Propulsion Laboratory, GALCIT, Air Technical Service Command, "Jet Propulsion," 1946.

20. K. Campbell and J. E. Talbert, "Some Advantages and Limitations of Centrifugal and Axial Aircraft Compressors," SAE J. (Trans.), Vol. 53, No. 10, October 1945.

21. Compressed Air and Gas Institute, Compressed Air Handbook. New York: The McGraw-Hill Book Company Inc., 1945.

22. S. A. Moss, C. W. Smith, and W. R. Foote, "Energy Transfer Between a Fluid and a Rotor for Pump and Turbine Machinery," ASME Trans., August 1942, p. 567.

23. G. F. Wislicenus, Fluid Mechanics of Turbomachinery. New York: The McGraw-Hill Book Company Inc., 1947.

24. S. A. Moss, C. W. Smith, and W. R. Foote, "Energy Transfer Between a Fluid and a Rotor for Pump and Turbine Machinery," ASME Trans., August 1942, p. 567.

25. D. G. Evans, "Design and Experimental Investigation of a Three Stage Multiple Re-entry Turbine," NASA Memo 1-16-59-E, 1959.

26. H. J. Wood, "Parametric Data Presentation for Radial Flow Gas Turbines," ASME paper, 1952.

27. J. T. Sinette, "Effects of Partial Admission on Performance of a Gas Turbine," NACA TN 1807, 1949.

28. D. G. Shepard, Principles of Turbomachinery. New York: The Macmillan Company, 1956.

29. J. W. Mitchell, "Design Parameters for Subsonic Air Ejectors," Tech. Report No. 40, Department of Mechanical Engineering, Stanford University, December 1958.

30. F. A. McClintock and J. H. Hood, "Aircraft Ejector Performance," J. Aeronaut. Sciences, November 1946.

31. R. Weatherston, "Mixing of Any Number of Streams in a Duct of Constant Cross-Sectional Area," J. Aeronaut. Sciences, November 1949.

32. A. J. Stepanoff, Centrifugal and Axial Flow Pumps. New York: John Wiley & Sons, 1948.

33. D. M. Considine, Handbook of Process Instruments and Control. New York: The McGraw-Hill Book Company Inc., 1958.

34. Crane Co., "Flow of Fluids through Valves, Fittings and Pipe," Tech. Paper 410, Chicago, 1957.

35. S. D. Cohn, "Performance Analysis of Butterfly Valves," Instruments, Vol. 24, No. 8, August 1951.

36. Kearfott, Technical Information for the Engineer, Servo Motors, Synchros, AC Tachometer Generators, 4th ed., 1957.

37. N. L. Morgan, "Which FHP Motor for the Job? " Product Eng., Vol. 30, Jan.19, 1959, p. 76.

38. "Selection Guide for Small Motors," Product Engineering 1954 Annual Handbook, p. H-10.

39. "Types and Uses of DC Motors and Controllers," Product Design Digest Issue, Product Engineering, Mid-October 1956, p. H-14.

40. Cook Research Laboratories, Electrohydraulic Servo Valve Report Series:

    R. E. Boyar, B. A. Johnson and L. Schmid, Part I, "A Summary of the Present State of the Art of Electrohydraulic Servo Valves," WADC TR 55-29, Part I, ASTIA No. AD 70616, April 1955.

    B. Johnson and L. Schmid, Part II, "An Investigation of a Number of Representative Electrohydraulic Servo Valves," WADC TR 55-29, Part 2, ASTIA Document No. AD97222, August 1956.

    B. Johnson, Part III, "State of the Art Summary of Electrohydraulic Servo Valves and Applications," WADC TR 55-29, Part 3, ASTIA Document No. AD 118285, April 1957.

    B. A. Johnson, L. R. Axelrod, and P. A. Weiss, Part IV, "Research on Servo Valves and Servo Systems," WADC TR 55-29, Part 4, August 1957.

41. F. D. Ezekiel and J. L. Shearer, "Pressure-Flow Characteristics of Pneumatic Valves." ASME Paper No. 56-A-104, August 1, 1956.

42. W. M. Kays and A. L. London, "Compact Heat Exchangers, A Summary of Basic Heat Transfer and Flow Friction Design Data." Palo Alto, Calif.: National Press, 1955.

43. M. Jakob, "Heat Transfer," Vol. I. New York: John Wiley and Sons, Inc., 1949.

44. W. H. McAdams, Heat Transmission. New York: The McGraw-Hill Book Company Inc., 1942.

SECTION 3J - EQUIPMENT COOLING SYSTEM DESIGN (AIRCRAFT, MISSILES)

1. INTRODUCTION

Equipment cooling system design for aircraft and missiles has, in recent years, assumed an importance equal to the equipment it must cool. Stringent reliability and performance requirements of such equipment as electronic devices, hydraulic actuators, and other control mechanisms have required effective system cooling.

In order to provide effective and efficient cooling system design, several conditions must be established. These conditions, which determine the type, size, and power usage of a cooling system, are:

(1) Type of equipment (electronic, hydraulic, mechanical).

(2) Operating temperature level.

(3) Location within aircraft or missile.

(4) Heat transfer required per unit area.

(5) Total heat transfer required.

Once these items have been determined, the designer can then turn to the selection of a cooling system consistent with the aircraft or mission envelope and geometrical requirements. An effective way of comparative evaluation of one cooling system with another is to use a penalty weight analysis, in addition to cost, maintenance, and reliability considerations.

1.1 Scope

This section describes the selection of a cooling system and the considerations necessary to design a system that will offer the lowest weight penalty to the aircraft or missile. The areas of cost, maintenance, and reliability will not be discussed. These items are entirely dependent upon the manufacturer's limitations and performance.

Since current aircraft cooling system design is based on air cycle or vapor cycle systems, these will be discussed in somewhat greater detail than some of the simpler, less effective designs. The most prominent missile equipment cooling system is one of an expendable type or one that uses ram air turbines to provide energy for operation of a cooling system. These two systems will be discussed as well as effective means of providing cooling to equipment through the use of natural convection, conduction, and radiation heat transfer paths.

In addition, specialized equipment cooling systems such as thermoelectric, hermetically sealed fluid vaporizers and condensers, and the use of fuel as a system coolant, will be described.

Much of the information included in this section is taken from Ref. 1, since it applies directly. Refs. 2 and 3 are included as additional sources of information.

1.2 Nomenclature

c_p = Dry air specific heat, Btu/lb-^oF
q = Compartment heat rejection Btu/min
L_e = Latent heat of vaporization of water, Btu/lb
M = Mach Number, dimensionless
P = Electric power input, watt (W)
p = Pressure, lb/ft^2, lb/in.^{2}
Δp_r = Ram pressure rise, lb/ft^2
SFC = Specific Fuel Consumption, lb per hr /lb thrust
t_1 = Air inlet temperature, ^oF
t_2 = Air outlet temperature, ^oF
Δt_r = Ram temperature rise, ^oR
T = Temperature, ^oR
w = Air flow rate, lb/min

Subscripts

amb = Ambient
r = Ram air
v = Vapor

2. DEFINITION OF THE VEHICLE AND ITS MISSION

The vehicle and its mission must be defined in order to properly evaluate a cooling system design. The envelopes described represent an aircraft mission, but similar envelopes can be obtained for missiles.

2.1 Vehicle Operational Envelope

The first step in the design procedure is to gather information concerning the operating pattern or envelope of the airplane. This information is needed for several reasons:

(1) To assist in locating the critical points in the airplane operating cycle.

(2) To provide background information relative to the characteristics of engine bleed air and ram air.

(3) To assist in later evaluations of the influence on vehicle performance caused by weight and drag associated with the presence of electronic equipment and its cooling provisions.

The information to be obtained should include as much of the following as is available:

(1) Mission profiles showing altitude as a function of flight duration. Each profile will be similar to the upper curve of Fig. 3J-1. Mission phase total duration is 54 minutes and is allocated as follows:

(a) Climb to 85,000 ft; 7 minutes.

(b) Mach 3.5 interception at 85,000 ft; 9 minutes.

(c) Combat at 85,000 ft; 3 minutes.

(d) Descent to 40,000 ft; 1 minute.

(e) Return at 40,000 ft and land; 34 minutes.

(2) Mission profiles showing flight Mach number as a function of flight duration, as in the lower curve of Fig. 3J-1.

(3) Mission profiles of altitude versus Mach number, as in Fig. 3J-2. These may be given directly or may be obtained by cross plotting from sets of profiles similar to the set shown in Fig. 3J-1. In most vehicles, the cooling system design point is at the vehicle maximum speed and maximum altitude.

Regulator set point is that point at which the maximum allowable bleed air pressure is attained. Flow control set point limits the bleed air flow to a desired value. Bleed air flow rate and pressure would, if not regulated, exceed the desired values at higher flight Mach numbers.

(4) A plot of fuel flow versus altitude is shown in Fig. 3J-3 for various power parameters, as follows:

Maximum power *SFC*	= 2.2
Military power *SFC*	= 0.9
Normal rated *SFC*	= 0.8
Cruise *SFC*	= 0.7

(5) A plot of thrust available as a function of altitude and power setting is useful but not essential. Such a curve is shown in Fig. 3J-4.

(6) A table of basic aircraft data, including:

(a) Flight vehicle gross weight at take-off.

(b) Flight vehicle fuel weight at take-off.

(c) Weight of basic vehicle structure and propulsion group.

(d) Total weight of flight vehicle electric powerplant, including distributing system.

(e) Flight vehicle net electric power available to all on-board equipment except electronic equipment and its cooling provisions.

(7) Specific information concerning ground operating time, pressure, humidity, temperature, and total thermal load.

(8) Availability of on-board heat sinks, such as fuel, and of expendable coolants, such as water to be evaporated.

(9) Lift-drag ratio at significant points on the performance envelope.

(10) Specific fuel consumption, lb-fuel/hr for each lb-thrust.

(11) Compartment temperatures and pressures.

(12) Available cooling air flow rates, temperatures, and pressures at flight and ground-idle conditions.

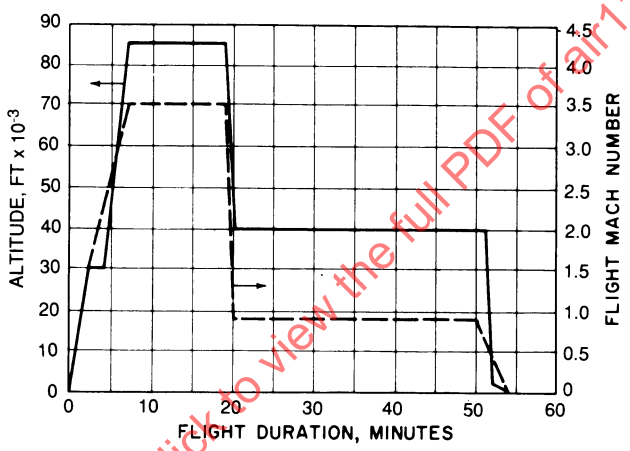

Figure 3J-1 - Hypothetical Mission Profile, Mach 3.5 Fighter-Interceptor

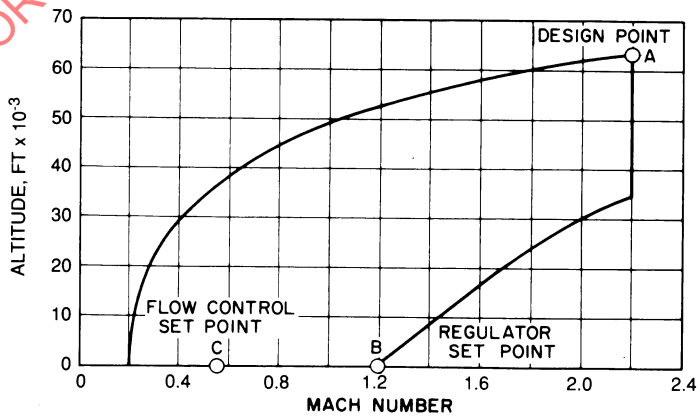

Figure 3J-2 - Flight Mission Profile, Altitude Versus Mach Number

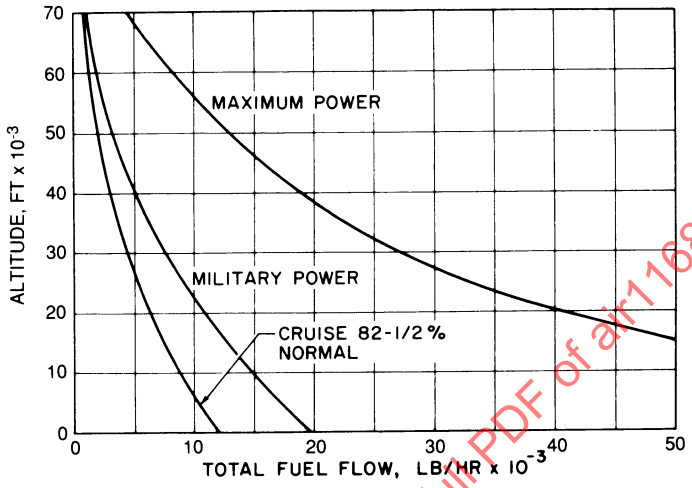

Figure 3J-3 - Fuel Flow Versus Altitude

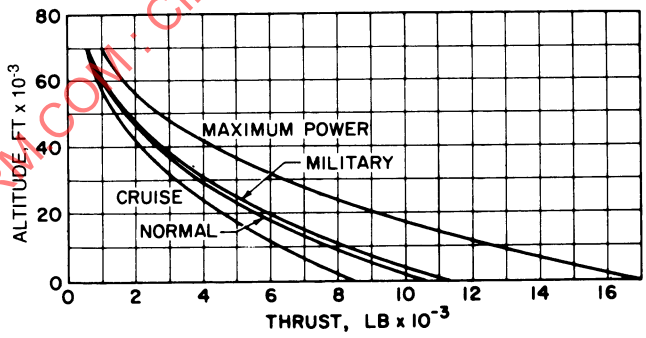

Figure 3J-4 - Thrust Versus Altitude

2.2 Ground Operation and Bench Checkout Requirements

The current applicable military specification, MIL-E-5400G, dated May 15, 1964, calls out five classes of electronic equipment. The different classes represent different ambient temperatures at sea level and different maximum altitudes for unpressurized operation, or both. A review of this specification, together with MIL-T-5422E (ASG) indicates that the envelope of bench checkout requirements is that shown in Table 3J-1.

Table 3J-1 - Test Chamber Conditions for Temperature-Altitude Test

Equipment Class	Temp, °F	Altitude ft	Time On, minutes	Time Off, minutes
1	-65.2	S.L.[1]	Cont.	
	-65.2	50,000	Cont.	
	131	S.L.	Cont.	
	68	50,000	Cont.	
	159.8	S.L.	30	15
	95	50,000	30	15
1A	-65.2	S.L.	Cont.	
	-65.2	30,000	Cont.	
	131	S.L.	Cont.	
	104	30,000	Cont.	
	159.8	S.L.	30	15
	134.7	30,000	30	15
2	-65.2	S.L.	Cont.	
	-65.2	70,000	Cont.	
	159.8	S.L.	Cont.	
	50	70,000	Cont.	
	203	S.L.	30	15
	95	70,000	30	15
3	-65.2	S.L.	Cont.	
	-65.2	100,000	Cont.	
	203	S.L.	Cont.	
	15.8	100,000	Cont.	
	257	S.L.	30	15
	69.8	100,000	30	15
	302	S.L.	10	15
	114.8	100,000	10	15
4	-65.2	S.L.	Cont.	
	-65.2	100,000	Cont.	
	257	S.L.	Cont	
	73.4	100,000	Cont.	
	302	S.L.	30	15
	120.2	100,000	30	15
	500	S.L.	10	15
	316	100,000	10	15

[1] S.L. = Sea level.

2.3 Moisture Content

The moisture content of the atmosphere varies over a very wide range, especially at low altitudes and at sea level. The design maximum value shown in Fig. 3J-5, which presents specific humidity (lb-water/lb-dry air) as a function of altitude, is described in the following paragraph, which has been adapted from MIL-STD-210, paragraph 3.4.1.

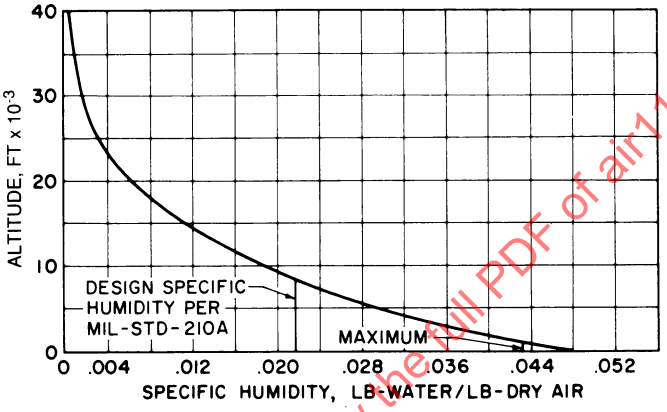

Figure 3J-5 - Specific Humidity Versus Altitude

The value of 0.022 lb-water/lb-dry air, representing a dew point temperature of 79.6 ^{o}F at sea level, is taken as the design vapor content up to the altitude where it becomes the moisture content of saturated air, whose dry bulb temperature is that given in the hot atmosphere of MIL-STD-210. At higher altitudes, up to 40,000 ft, the design vapor content is the saturation value corresponding to the altitude and hot atmosphere temperature. For all altitudes above 40,000 ft, the design vapor content is that of the specific humidity existing at the 40,000 ft level, that is, 0.0003 lb-water/lb-dry air.

These values of specific humidity are used in determining the cooling capacity of the system supplying coolant air to the electronic equipment. A value of 0.043 lb-water/lb-dry air, representing a dew point of 100 ^{o}F at sea level, is a design maximum to be considered when determining the probable condensed moisture conditions in the cooling system.

Fig. 3J-6, to be used in conjunction with Fig. 3J-5, shows dry bulb and dew point temperatures as functions of altitude, in accordance with the definitions of the previous paragraph. Note that for constant specific moisture content, the dew point temperature decreases with increasing altitude. Both figures are required for a complete analysis: Fig. 3J-5 to determine the maximum amount of water vapor to be removed, and Fig. 3J-6 to determine the temperature at which condensation will start at a particular altitude pressure.

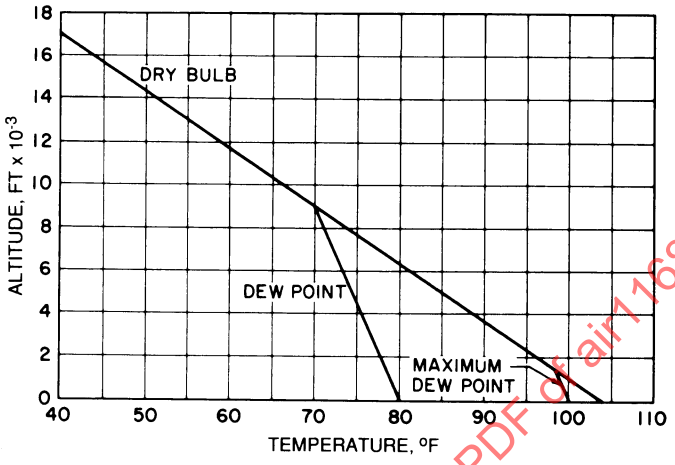

Figure 3J-6 - Dry Bulb and Dew Point Temperatures Versus Altitude

Humidity is an important consideration in the design of cooling systems, particularly if the production of essentially dry air is required. For example, removal of 0.022 lb of water requires a cooling capacity of 0.022 x 1050 = 23.1 Btu /lb-dry air. This quantity of heat removal would cool 1 lb of dry air by 96.2 °F. Herein lies the importance of defining the inlet moisture conditions.

2.4 Ram Air Characteristics

All air taken on board an airplane in flight will be at a higher temperature and pressure than the ambient air. In actual practice, the ram temperature rise will be close to the theoretical amount given by

$$\Delta t_r = 0.2M^2 T_{amb} \quad (3J\text{-}1)$$

The pressure rise for 100% efficient adiabatic compression will be

$$\Delta p_r = p_{amb}(1 + 0.2M^2)^{3.5} - p_{amb} \quad (3J\text{-}2)$$

In practice, the recoverable ram pressure rise will be 50-85% of that computed by Eq. 3J-2.

Figs. 3J-7A and 3J-7B show resulting ram temperatures and ram pressures at 100% recovery for a range of airplane speeds and altitudes, based on a MIL-STD-210 hot atmosphere. In any real problem, the temperature will be slightly lower than that shown, and the pressure will be appreciably lower than that shown.

For an actual airplane application, there may be occasionally a limit on the amount of ram air available under certain flight conditions. Also, the ram air discharge point may be located at a point on the airplane where the effective pressure is less than at the ram inlet. This pressure differential may be of assistance in forcing air through heat exchangers, and the value should be determined.

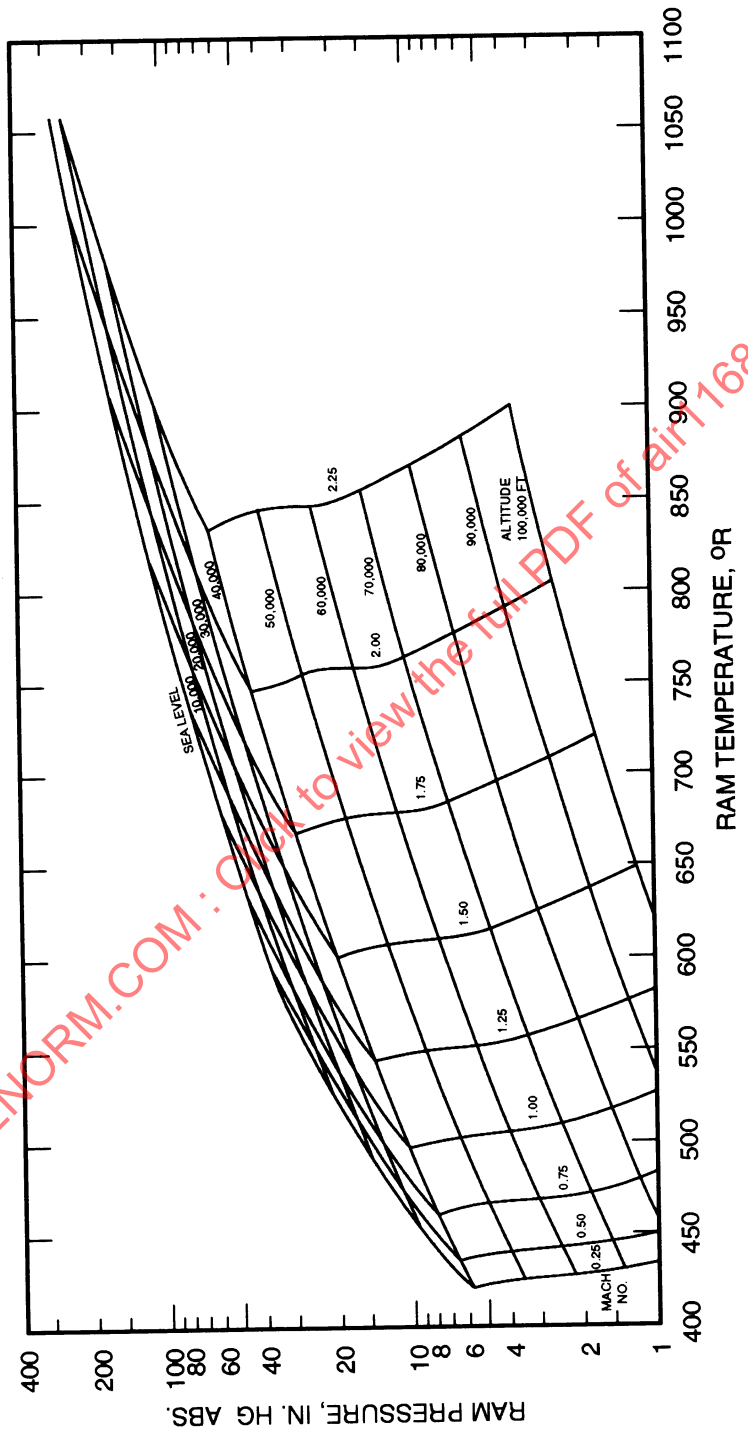

Figure 3J-7a - Maximum Ram Temperature and Pressure as Functions of Altitude and Mach Number for MIL-STD-210 Hot Atmosphere

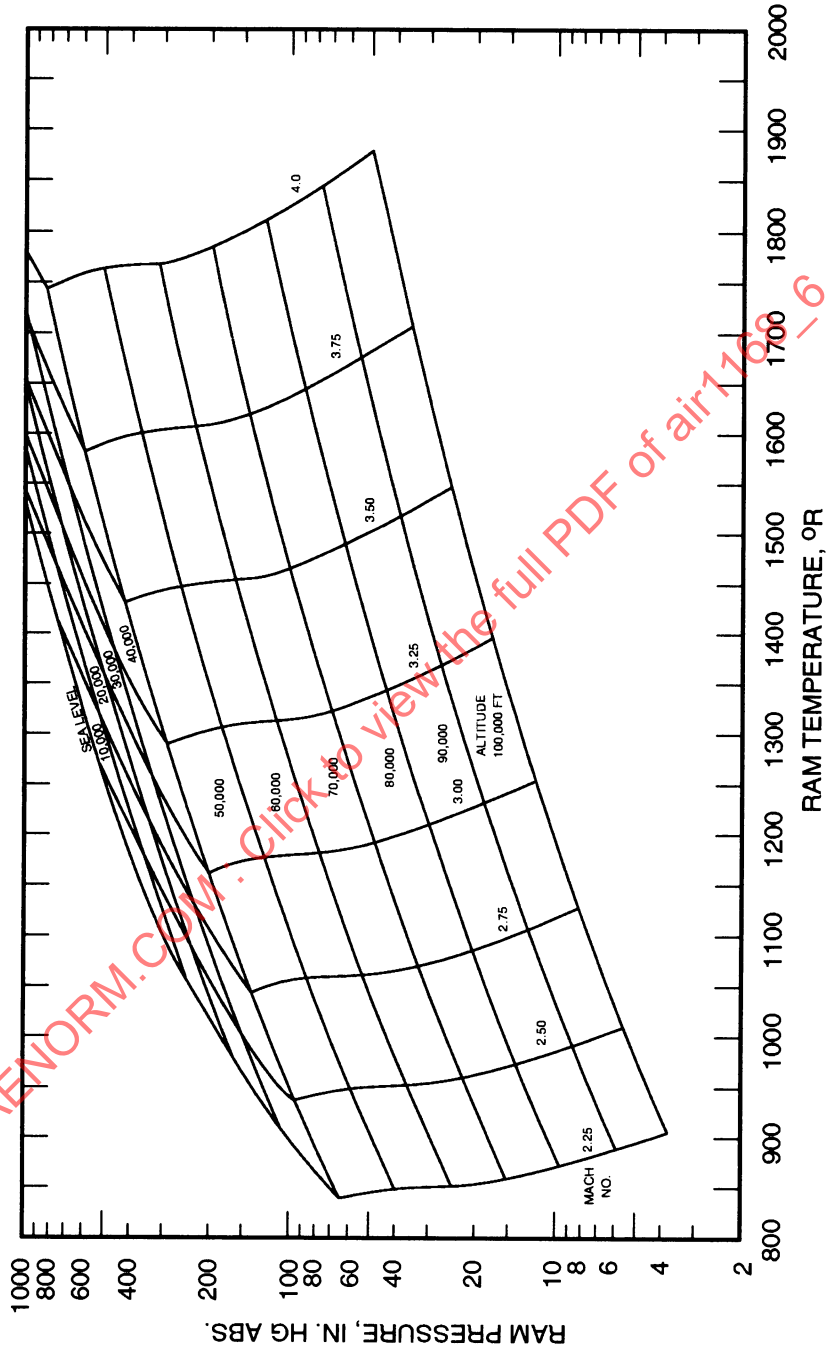

Figure 3J-7b - Maximum Ram Temperature and Pressure as Functions of Altitude and Mach Number for MIL-STD-210 Hot Atmosphere (Continuation Of Fig. 3J-7a)

2.5 Bleed Air Characteristics

Bleed air is available from the compressor of the jet engine. The three characteristics of interest are: temperature, pressure, and available flow rate. All these will vary with airplane altitude and speed; therefore, several sets of values will be needed for each mission. If ground cooling is to depend on bleed air, then the ground point characteristics must be known.

2.6 Characteristics of Other Available Power Sources

Other available power sources include: shaft power, hydraulic power, and electric power. All three are used on various transport aircraft. Combat aircraft are likely to use only electric power.

2.6.1 Shaft Power

The engine speed varies at different operating conditions (altitude, Mach number). Engine shaft power is, in some instances, extracted for use in the equipment cooling system, among other uses. Therefore, it becomes imperative that shaft power characteristics such as speed, power available, and maximum torque available be specified.

2.6.2 Hydraulic Power

In addition to operation of hydraulic machinery in the aircraft, on-board fluids (for example, oil) may be utilized in heat exchangers for fuel heating. Hence, fluid pressure, flow rate, and type of fuel should be specified.

2.6.3 Electric Power

Aircraft systems demand a type of power that can be readily and economically converted into several forms of energy: motion, heat, light, and radiation. Electricity meets these demands. Its transmission is accomplished by simple, low loss, flexible conductors that are practically unaffected by wide variations in temperature and other severe aircraft operating conditions. For these reasons, electric power for aircraft systems is widely used.

The main sources of AC power are engine - driven AC generators, which may be combined with rectifiers for DC power production. Other DC power sources are lead-acid storage batteries and self-excited, engine - driven DC generators. In addition to meeting general environmental requirements, aircraft generators are classified according to rated operating voltage, rated continuous ouput current, and operating speed.

2.6.4 Ram Air Turbine Shaft or Electric Power

Ram air turbines have been used for emergency power for aircraft or missile hydraulic and electrical controls. In many instances, where equipment requiring cooling is in a remote location, as in a wing pod, ram air turbines can provide the most effective cooling system power.

In a missile, where bleed air is not available and a large vapor cycle system is not practical, a ram air turbine can be used effectively to provide hydraulic or electric power to operate a cooling system.

2.7 System Weight Penalty Factor Evaluation Techniques[1]

The addition of a cooling system to a vehicle influences vehicle performance by the imposition of additional weight, drag, and power consumption. The additional weight is the dead weight of the cooling equipment. Additional drag results from momentum drag caused by the ram air taken on board for pressurization or cooling. Additional power consumption arises from the shaft power and bleed air requirements of the cooling system, or both. The additional drag and power consumption can be expressed in terms of extra fuel load required to maintain the same mission characteristics as a comparable airplane without a cooling system.

The effect of an electronic equipment cooling system on vehicle performance is determined analytically by formulating significant penalty parameters based on range, endurance, or rate of climb as the evaluation criterion. Two computational methods are generally in use, the Breguet method and the step-wise integration method.

The methods presented here are used primarily for aircraft. However, they can also be used for missiles whose behavior is governed by aerodynamic lift. Extremely long range missiles, which are dependent upon overcoming centripetal force and gravity rather than vehicle drag, cannot be evaluated using this method. Care must be exercised in applying to missiles the equations developed for turbojet or rocket powered airplanes.

To preserve the same structural integrity and flight characteristics, any increase in equipment weight or fuel weight must be matched by a corresponding increase in the size of the powerplant and the vehicle frame in order to provide greater thrust. This requirement of a larger engine and vehicle frame, however, is neglected.

[1] AIR1168/8 discusses air conditioning penalty factors in greater detail

Certain parameters must be given, or assumed, for the flight mission in order to make a reasonable penalty evaluation. These include the following:

(1) A typical mission profile, including data on Mach number, altitude, freestream temperature, and power setting as a function of mission duration.

(2) Engine data, including compressor pressure ratio, bleed air temperature, and specific fuel consumption as a function of altitude, power setting, and Mach number.

(3) Lift-drag ratio of the vehicle at take-off and at the beginning of each mission phase.

(4) Dead weight of the cooling system and the amount of expendable evaporants to be used during the mission.

(5) Required ram air flow, drag equivalent of bleed air extraction, drag equivalent for ram air turbine power, and/or drag equivalent of shaft power extraction for each cooling system during each of the separate mission phases.

3. DEFINITION OF THE EQUIPMENT COOLING PROBLEM

Defining the equipment cooling problem entails specification of equipment, ambient and cooling air temperatures, pressures, and moisture content. Additionally, equipment location, size, and total heat load must also be specified. The heat transfer rate per unit area is an important parameter, as is the maximum and minimum cooling air temperature allowable within a given piece of equipment.

3.1 Required Data

The second major step in the cooling system design procedure is to obtain information defining the temperature and pressure envelope under which the equipment to be cooled must operate. This information is relatively difficult to obtain, since there is less standardization in this field than in the field of aircraft operation. If actual test information on the equipment to be used is available, it should be employed.

In the case of a new aircraft, however, this will not usually be the case. The procedures described in this section provide approximate values of the data required, and the designer should seek to update this information whenever possible.